ROLES FOR THE RAD1-RAD10-SLX4, MSH2-MSH6, AND SGS1 DNA REPAIR FACTORS IN ENSURING THE EFFICIENCY AND FIDELITY OF HOMOLOGOUS RECOMBINATION IN *S. CEREVISIAE*

A Dissertation

Presented to the Faculty of the Graduate School

of Cornell University

in Partial Fulfillment of the Requirements for the Degree of

Doctor of Philosophy

by

Amy M. Lyndaker

May 2009

ROLES FOR THE RAD1-RAD10-SLX4, MSH2-MSH6, AND SGS1 DNA REPAIR FACTORS IN ENSURING THE EFFICIENCY AND FIDELITY OF HOMOLOGOUS RECOMBINATION IN *S. CEREVISIAE*

Amy M. Lyndaker, Ph.D.

Cornell University 2009

Nearly half of the human genome consists of repetitive DNA, and these sequences are a threat to genome stability because of their potential to recombine. The work presented here centers on two pathways that contribute to genome stability by ensuring the efficiency and fidelity of homologous recombination processes: 3' nonhomologous tail removal by the Rad1-Rad10-Slx4 endonuclease complex, and heteroduplex rejection by the Msh2-Msh6 mismatch recognition complex and the Sgs1 helicase.

To study the coordination of checkpoint signaling and enzymatic repair functions during repair of a single chromosomal break, mating type switching was monitored in *S. cerevisiae* strains defective for the Rad1-Rad10-Slx4 3' endonuclease complex. Mutant strains displayed *RAD9*- and *MAD2*-dependent cell cycle delays and decreased viability during mating type switching. In particular, these mutants defective for Rad1-Rad10-Slx4 exhibited a unique pattern of dead and switched daughter cells arising from the same DSB-containing cell. Thus, Rad1-Rad10-Slx4 promotes efficient repair during gene conversion events involving a single 3' nonhomologous tail, and it is proposed that the *rad1*Δ and *slx4*Δ mutant phenotypes result from inefficient repair of a lesion at the *MAT* locus that is bypassed by replication-mediated repair.

DNA mismatch repair proteins actively inhibit recombination between divergent sequences while allowing recombination between identical substrates. This

process, known as heteroduplex rejection, is thought to occur when the Msh2-Msh6 DNA mismatch recognition complex recognizes and binds to mismatches in heteroduplex DNA, and either recruits or stimulates the Sgs1 helicase to unwind inappropriate recombination intermediates. Purification of the Msh2-Msh6 complex and a soluble fragment of Sgs1, $Sgs1_{400\text{-}1268}$, in this study allowed characterization of their physical and functional interactions *in vitro*. Msh2-Msh6 and $Sgs1_{400\text{-}1268}$ physically interact as demonstrated in coimmunoprecipitation experiments, and Msh2-Msh6 appears to inhibit Sgs1-dependent unwinding of short 3' overhang substrates. Studies of the effect of Msh2-Msh6 on Sgs1 helicase activity are ongoing.

Together, this work contributes to our molecular understanding of how recombination events are both regulated and carried out, as well as how defects in these DNA repair genes contribute to a variety of disease states in humans.

BIOGRAPHICAL SKETCH

Amy Marie Hauser surprised her parents on March 14th, 1981 by entering the world a full two months earlier than her expected due date. At a tiny 3 lbs and 2 oz., Amy spent her first month of life in the hospital but eventually made it home safe and sound. When she began kindergarten at age 5 and still toddled like a toddler, Amy's parents enrolled her in dance classes to improve her muscle tone. Dancing came quite naturally to her, and it became her passion as she continued dancing for the next 15 years. After being chosen as an understudy for children's roles in the New York City Ballet's "The Sleeping Beauty" during their summer 1991 stay in Saratoga Springs, NY, Amy began her pre-professional ballet training with Patti Pugh Henderer at the Saratoga School of the Arts, which later became the Saratoga City Ballet School. Under Henderer's direction, Amy became a soloist and founding member of the Saratoga City Ballet company in 1993 at the age of 12. In the following years, Amy spent her summers training at the NYSSSA School of Ballet, the Rock School of the Pennsylvania Ballet, and the Boston Ballet School. Daily training and Friday and Saturday rehearsals were the norm for Amy throughout high school, though she also excelled in academia and played the flute in the school band. Amy graduated from Ballston Spa High School as Salutatorian of her class in 1999.

After high school, Amy attended Goucher College in Baltimore, Maryland on a full-tuition Dean's academic scholarship, where she continued to dance and perform while studying biology and chemistry. At Goucher, Amy performed in George Balanchine's Serenade, staged by Zippora Karz of the NYCB, as well as several student works. The summer after her sophomore year, Amy decided to spend the summer at Goucher doing microbiology research with Dr. Leleng To Isaacs. After an enriching experience in the lab and the frustration of trying to juggle both her dancing

and science training, Amy decided to stop dancing and to focus on science research. Amy began doing independent lab research with Dr. Lesley Brown, working to develop an *in vivo* DNA mismatch repair assay in *E. coli*. Amy was bitten by the science bug, and hasn't looked back since (except for the occasional ballet class). She spent the following summer at SUNY Upstate Medical University in Syracuse, NY studying transcriptional regulation in laboratory of Dr. Wu-Cheng Shen, where she began and completed an EMS mutagenesis, screened a yeast genomic library, and mastered tetrad dissection in a matter of 8 weeks. As if this summer of yeast genetics weren't exciting enough, Aaron Lyndaker, whom Amy had met 5 months earlier through a mutual friend, asked her to marry him! ☺

Amy returned to Goucher for her senior year while Aaron returned to Clarkson University to finish his degree in Mechanical Engineering. She continued her lab research with Dr. Brown, in addition to an independent study with Dr. Judy Levin on transcription-coupled DNA repair. Amy graduated from Goucher College in May 2003 with Honors in the Biological Sciences and a minor in Chemistry and was inducted into the Phi Beta Kappa Honors Society. After a busy year of applying and interviewing for graduate school, Amy decided to continue her scientific pursuits at Cornell University in Ithaca, NY in the Department of Molecular Biology and Genetics, graduate field of Biochemistry, Cell and Molecular Biology, where she arrived in August 2003. Amy joined the laboratory of Eric Alani in the spring of 2004 to study homologous recombination in *S. cerevisiae* using both genetic and biochemical techniques. Aaron moved to Ithaca that spring, and Amy and Aaron Lyndaker were married on October 10th, 2004 in Saratoga Springs, NY. After several amusing apartment fiascos, Amy and Aaron bought their first house in Lansing, NY in June of 2005, where they live with their two cats, Mu (μ) and Rufus.

ACKNOWLEDGMENTS

I would like to thank members of the Alani lab, past and present, for their suggestions and guidance throughout my time in the lab. Special thanks to Dr. Tamara Goldfarb for contributions to Chapter 2, particularly the experiments shown in Figures 2.2 and 2.3, and for providing the groundwork for both of the projects discussed in this dissertation. Biochemical expertise from Aaron Plys, Justin Sibert, Jennifer Surtees, and Eric Alani was greatly appreciated. I am especially grateful to Sarah Zanders and Dr. Jennifer Surtees for being thoughtful, dedicated, enthusiastic, down-to-earth scientists that I greatly admire. Thank you to Dr. Eric Alani for being an extremely supportive advisor who gave me many opportunities to meet with visiting scientists and taught me a great deal about the world of science.

Thank you to committee members Dr. Bob Weiss and Dr. Jeff Roberts, BMCB Director of Graduate Studies Dr. Volker Vogt, and Cornell R3 Group members Dr. Joe Peters and Dr. Bik Tye for thoughtful discussions, helpful suggestions, and encouragement throughout these studies.

The work presented here was supported financially by a Graduate Assistance in Areas of National Need (GAANN) fellowship, a National Institutes of Health (NIH) Training Grant, several teaching assistanceships, and two Graduate School travel awards for A.M.L. in addition to the Alani lab NIH grant GM53085.

Finally, I'd like to thank my friends and family who have been supportive and encouraging throughout my endeavors. Special thanks to Ms. Patti Pugh (Henderer) Moore for instilling in me the strength, discipline, and confidence that have helped to get me where I am today. Thank you to the Lyndakers for their caring support and for always providing a relaxing and comforting home-away-from-home. Thanks especially to my parents, Claudia and Mark Hauser, for teaching me the value of hard

work and perseverance, and for their endless love and support. Last, but not least, a special thank you to my husband, Aaron, for dealing with all the late night experiments, stressful nights before seminars, and time spent working at home, and for always reminding me to enjoy life outside of the lab, too. You're the best.

TABLE OF CONTENTS

LIST OF FIGURES

LIST OF TABLES

LIST OF ABBREVIATIONS

DSB – Double-strand break

SDSA – Synthesis-dependent strand annealing

MMR – Mismatch repair

NER – Nucleotide excision repair

SSA – Single-strand annealing

HR – Homologous recombination

HJ – Holliday junction

NHT – Nonhomologous tail

BIR – Break-induced replication

NHEJ – Nonhomologous end joining

MEPS – minimal efficient processing sequence element

HNPCC – hereditary non-polyposis colorectal cancer

CMMR-D syndrome – constitutive mismatch repair-defective syndrome

$Sgs1_{400\text{-}1268}$ – Truncated Sgs1 protein consisting of amino acids 400 to 1268 out of 1447; also contains an N-terminal HA epitope and a C-terminal hexahistidine tag.

hMsh2-Msh6 – human Msh2-Msh6

C-terminus – carboxy terminal end of the protein

N-terminus – amino terminal end of the protein

HRD domain – Helicase and RNase D domain

Ct domain – conserved carboxy-terminal domain, in reference to Sgs1 helicase

S. cerevisiae – *Saccharomyces cerevisiae*

S. pombe – *Schizosaccharomyces pombe*

E. coli – Escherichia coli

S. typhimurium – Salmonella typhimurium

ES cells – mouse embryonic stem cells

Δ - deletion

HO endonuclease – Homothallic switching endonuclease

IP - immunoprecipitation

ChIP – Chromatin immunoprecipitation

coIP – co-immunoprecipitation

FACS – Fluorescence-activated cell sorting

BND-cellulose – Benzoylated-naphthoylated DEAE cellulose

DEAE – diethylaminoethyl

HA – hemaglutinin epitope from influenza virus

SDS – Sodium dodecyl sulfate

SDS-PAGE – SDS-Polyacrylamide gel electrophoresis

PBE94 – Polybufferexchange 94 resin

Tris – Tris(hydroxymethyl)aminomethane

EDTA – Ethylenediaminetetraacetic acid

TE – Tris EDTA buffer (10 mM Tris pH 7.5, 1 mM EDTA pH 8.0)

TAE – Tris acetate EDTA buffer

TBE – Tris borate EDTA buffer

TBS – Tris-buffered saline

TBST – Tris-buffered saline plus Tween

TCA – trichloroacetic acid

YP – yeast peptone medium

YPD – yeast peptone dextrose medium

DNA – Deoxyribonucleic acid

dsDNA – double-stranded DNA

ssDNA – single-stranded DNA

oligo - oligonucleotide

RNA – Ribonucleic acid

TAP tag – Tandem affinity purification tag

His tag – Histidine tag

S - serine

kb – kilobase

bp - basepairs

nt - nucleotides

aa – amino acids

hd – helicase-dead

PCR – Polymerase chain reaction

OD – optical density

HPLC – High performance liquid chromatography

FPLC – Fast protein liquid chromatography

BSA – Bovine serum albumin, non-specific protein

ATP – Adenosine triphosphate

DTT – dithiothreitol ((*2S,3S*)-1,4-Bis-sulfanylbutane-2,3-diol)

NaCl – Sodium chloride

NaCitrate – Sodium citrate

NaAcetate – Sodium acetate

NaOH – Sodium hydroxide

$MgCl_2$ – Magnesium chloride

LiCl – Lithium chloride

KCl – Potassium chloride

Zn - Zinc

Ni NTA – Nickel nitriloacetic acid

MMS – Methylmethane sulfonate

HU – hydroxyurea

4-NQO – 4-nitroquinoline 1-oxide

UV – ultraviolet light

EGS – EthylGlycol bis(SuccinimidylSuccinate); protein-protein crosslinking agent

Ura/ura – Uracil

Trp/trp – Tryptophan

Leu/leu – Leucine

mol – moles

pmol – picomoles

M – molar (moles per liter)

mM – millimolar

nM – nanomolar

ml – milliliter

µl – microliter

mg – milligram

µg - microgram

mA – milliamps

nm – nanometers

mS – millisiemens (measure of conductivity)

cm – centimeters

Da – Daltons; grams per mole

kDa – kiloDaltons; kilograms per mole

MPa - megaPascals

U – units (1 U = the amount of enzyme that catalyzes the conversion of 1 micromole of substrate per minute)

C – Celsius

pH – potential of Hydrogen; measure of acidity or alkalinity of a solution.

hrs – hours

rpm – revolutions per minute

w/v – weight per volume

v/v – volume per volume

t – time

p – probability

n/a, NA – not applicable

TBD – To be determined

n – chromosome copy number

SEM – Standard error of the mean (standard deviation divided by square root of # of data points)

CHAPTER 1

A tale of tails: Insights into the coordination of 3' end processing during homologous recombination

Amy M. Lyndaker and Eric Alani

Department of Molecular Biology and Genetics

Cornell University

Ithaca, NY 14853-2703

This chapter is in press for publication in for the March 2009 issue of Bioessays:

Lyndaker, Amy M., and Eric Alani: A tale of tails: Insights into the coordination of 3' end processing during homologous recombination. Bioessays. 2009. Volume 31, Issue 3, Pages TBD.

Abstract

Eukaryotic genomes harbor a large number of homologous repeat sequences that are capable of recombining. Their potential to disrupt genome stability highlights the need to understand how homologous recombination processes are coordinated. The *S. cerevisiae* Rad1-Rad10 endonuclease performs an essential role in recombination between repeated sequences by processing 3' single-stranded intermediates formed during single-strand annealing and gene conversion events. Several recent studies have focused on factors involved in Rad1-Rad10-dependent removal of 3' nonhomologous tails during homologous recombination, including Msh2-Msh3, Slx4, and the newly identified Saw1 protein (Surtees and Alani 2006; Flott *et al.* 2007; Li *et al.* 2008; Lyndaker *et al.* 2008). Together, this new work provides a model for how Rad1-Rad10-dependent end processing is coordinated: Msh2-Msh3 stabilizes and prepares double-strand/single-strand junctions for Rad1-Rad10 cleavage, Saw1 recruits Rad1-Rad10 to 3' tails, and Slx4 mediates crosstalk between the DNA damage checkpoint machinery and Rad1-Rad10.

Introduction

Homologous stretches of DNA sequence scattered throughout the genome are a threat to genome stability because of their potential to recombine. It is estimated that nearly half of the human genome consists of repetitive DNA (Lander *et al.* 2001; Li *et al.* 2001), and genome rearrangements caused by recombination between repeats are known to contribute to a variety of human diseases, including many cancers (Strout *et al.* 1998; Deininger and Batzer 1999; Stenger *et al.* 2001; Kolomietz *et al.* 2002; Hedges and Deininger 2007; Mattarucchi *et al.* 2008). Repetitive sequences such as *Alu* elements are particularly susceptible to non-conservative homologous recombination via single-strand annealing (SSA), which results in the deletion of sequences located between the repeats and can mediate large-scale genome rearrangements (Pâques and Haber 1999; Symington 2002; Elliott *et al.* 2005; Hedges and Deininger 2007; VanHulle *et al.* 2007; Mattarucchi *et al.* 2008; Wang and Baumann 2008). The abundance of such repeated sequences in the human genome that are prone to mutagenic recombination underscores the need for a comprehensive understanding of the homologous recombination mechanisms that act on them.

SSA is a major recombination pathway for repairing spontaneous and induced double-strand breaks (DSBs) that arise between repeated sequences (Liang *et al.* 1998; Pâques and Haber 1999; Elliott *et al.* 2005). Recent work suggests that SSA not only creates deletions between flanking direct repeats, but also contributes to inverted repeat recombination, gene targeting, translocation formation, and chromosome fusions (VanHulle *et al.* 2007; Gao *et al.* 2008; Pannunzio *et al.* 2008; Wang and Baumann 2008). During SSA in *S. cerevisiae*, DSBs are resected 5' to 3' to reveal single-stranded homologous sequences (Figure 1.1). Following Rad52- and Rad59-dependent annealing of the homologous sequences, the 3' single-stranded DNA ends

are nonhomologous to the new flanking regions, and must be cleaved in order to complete repair of the broken strands. The Rad1-Rad10 endonuclease and Msh2-Msh3 mismatch recognition complex are required for cleaving 3' single-stranded nonhomologous tails on either side of the annealed region (Fishman-Lobell and Haber 1992; Bardwell *et al.* 1994; Ivanov and Haber 1995; Sugawara *et al.* 1997; Ciccia *et al.* 2008) and Rad59 and Srs2 have also been implicated in the 3' nonhomologous tail removal step (Pâques and Haber 1997; Sugawara *et al.* 2000). Once both 3' tails have been removed, SSA is completed by DNA synthesis initiated off of the newly cleaved 3' ends, followed by ligation (reviewed in Pâques and Haber 1999). It should be noted that if a DSB is formed within a repeated sequence, SSA may involve removal of only one 3' tail.

Rad1-Rad10 and its mammalian homolog, XPF-ERCC1, are structure-specific endonucleases that function in both nucleotide excision repair (NER) and homologous recombination (Pâques and Haber 1999; Prakash and Prakash 2000; Symington 2002; Niedernhofer *et al.* 2004; Al-Minawi *et al.* 2008; Ciccia *et al.* 2008). The significance of the role of these complexes in recombination is demonstrated by the severe developmental abnormalities in mice lacking *ERCC1,* which, unlike NER mutant phenotypes, include severe runting, reduced liver function, and death before weaning (McWhir *et al.* 1993; Weeda *et al.* 1997). A recently described human patient with ERCC1 deficiency also exhibited severe fetal development defects that are clearly distinct from NER-related phenotypes (Jaspers *et al.* 2007). In yeast, the absence of Rad1-Rad10 leads to cell death or plasmid loss (depending on the assay) during recombination by SSA due to lack of repair, since 3' nonhomologous tail removal is an essential step in SSA (Fishman-Lobell and Haber 1992; Sugawara *et al.* 1997). Several recent papers have highlighted factors involved in Rad1-Rad10-dependent 3' nonhomologous tail removal during homologous recombination in *S. cerevisiae*

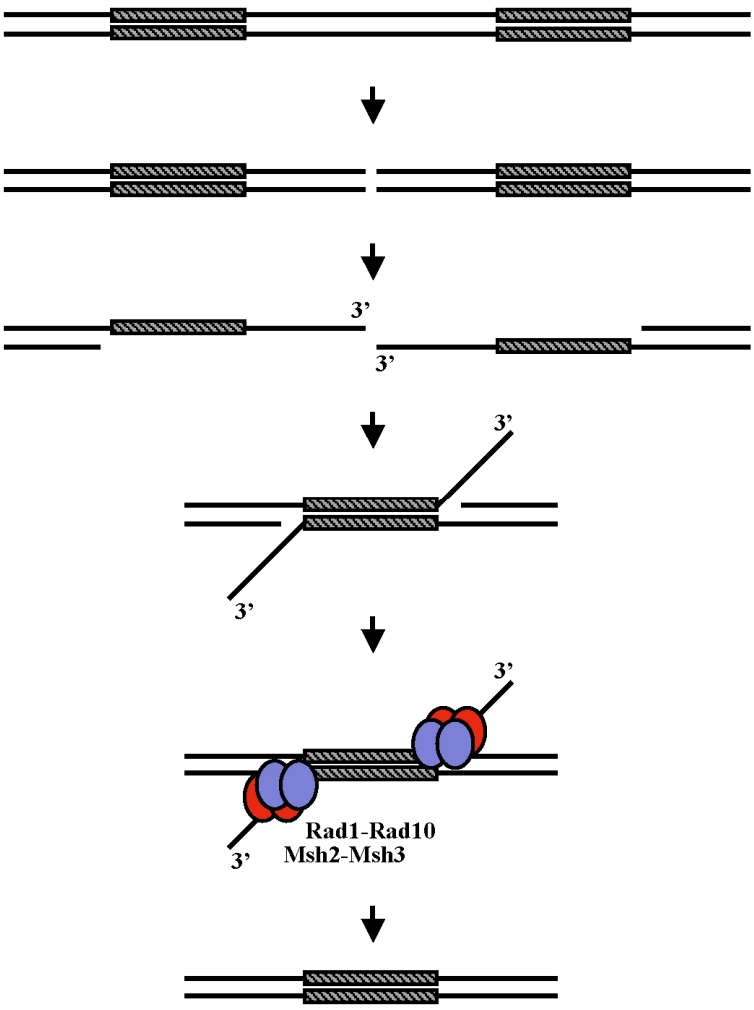

Figure 1.1. Single-strand annealing mechanism of double-strand break (DSB) repair between repeated sequences. DSBs that arise between repeated sequences are resected by 5' to 3' exonuclease activity, and the single-stranded DNA is annealed at regions of homology. Pairing of these sequences reveals 3' nonhomologous tails on either side of the intermediate that are cleaved off in a Rad1-Rad10- and Msh2-Msh3-dependent manner. Removal of the 3' nonhomologous ends allows initiation of repair synthesis to produce final recombinant products.

(Surtees and Alani 2006; Flott *et al.* 2007; Li *et al.* 2008; Lyndaker *et al.* 2008), and it is these non-NER functions of Rad1-Rad10 that are reviewed here. The role of Rad1-Rad10 in nucleotide excision repair has been reviewed elsewhere (Prakash and Prakash 2000; Ciccia *et al.* 2008).

Homologous recombination by gene conversion also involves the removal of 3' nonhomologous tails. Most mitotic gene conversion events are thought to occur by a synthesis-dependent strand annealing mechanism (Figure 1.2; Pâques and Haber 1999; Symington 2002; Ira *et al.* 2006). During such gene conversion events, the DSB is resected 5' to 3', and one of the 3' ends undergoes Rad51-mediated strand invasion into a duplex region of DNA containing a homologous sequence (Figure 1.2A). DNA synthesis initiating from the 3' invading strand allows for copying of DNA sequence from the donor template, and unwinding of the invading strand from the donor template allows it to anneal back to its native locus. The non-invading strand is then able to be repaired using the invading strand as a template (reviewed in Pâques and Haber 1999; Symington 2002).

Rad1-Rad10-dependent nonhomologous tail removal during gene conversion can occur during the strand invasion step as well as after annealing, depending on whether one or both 3' ends contain nonhomology with respect to the donor locus. If both sides of a DSB are nonhomologous to the donor (Figure 1.2B), the invading strand contains a 3' nonhomologous tail that must be removed in order to prime repair synthesis off of the donor. When nonhomologous sequence resides on only one side of a DSB (Figure 1.2A), the 3' end of the break that shares homology with the donor sequence performs the strand invasion step, and there is thus no barrier to initiate new DNA synthesis on the invading strand.

Figure 1.2. Synthesis-dependent strand annealing mechanism of gene conversion involving the removal of either one (A) or two (B) 3' nonhomologous tails. A. After DSB formation and 5' to 3' resection, one 3' end invades a donor locus containing a homologous sequence. DNA synthesis is primed from this invading 3' end and copies the donor sequence, and unwinding of this strand allows it to reanneal to its native locus. When the newly repaired strand differs in sequence from the original sequence, a 3' nonhomologous tail remains at the non-invading strand. Removal of this 3' tail involves Rad1-Rad10 and Slx4, but not Msh2-Msh3. 3' nonhomologous tail removal allows for completion of repair by gene conversion. B. If nonhomologous sequence flanks both sides of a DSB, the 3' invading strand must also be processed in order for strand invasion to be productive. 3' nonhomologous tail removal on the invading strand requires both the Rad1-Rad10 and Msh2-Msh3 complexes, and presumably Slx4. After 3' tail removal, gene conversion proceeds via synthesis-dependent strand annealing as described in A.

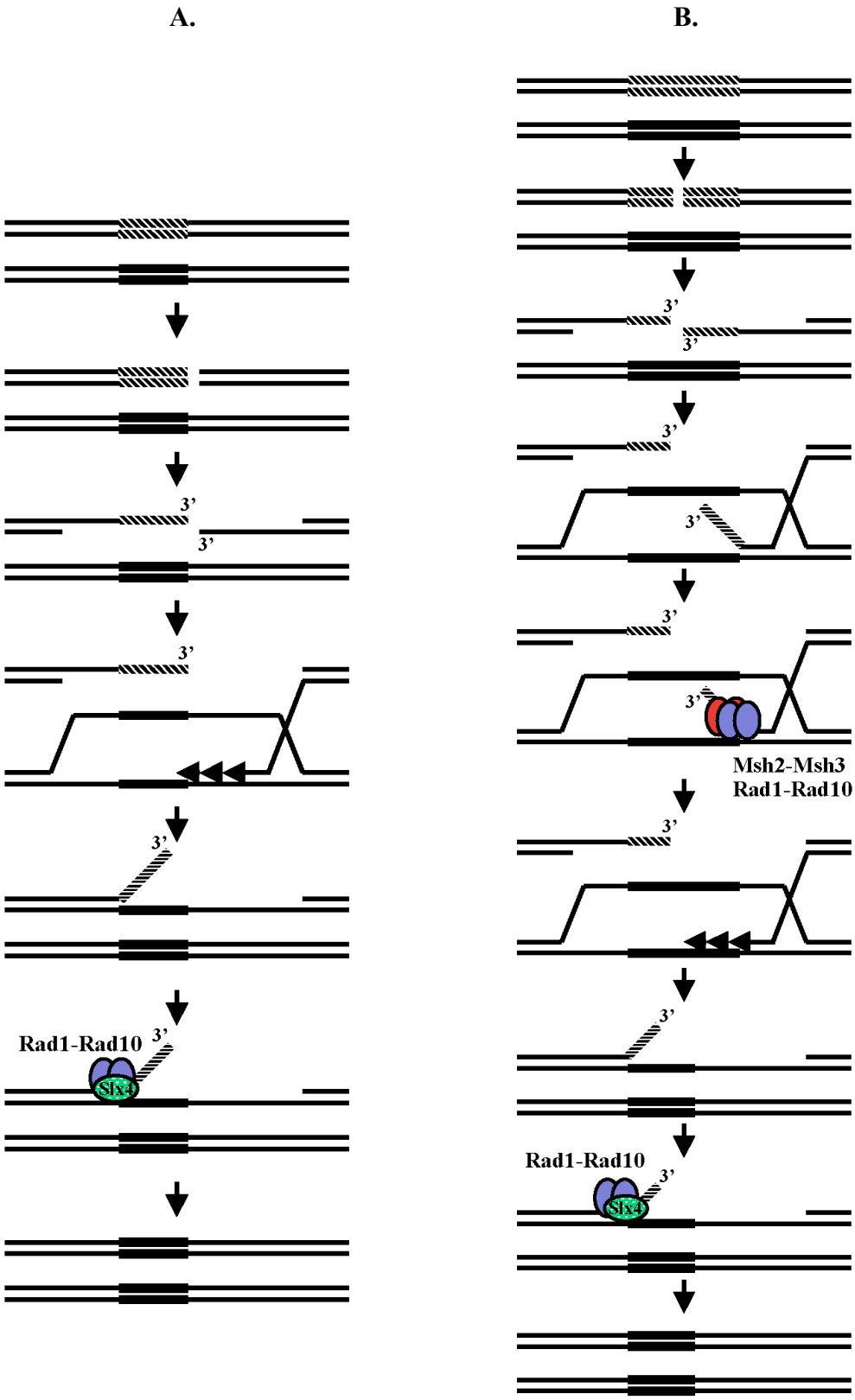
A.
B.
3'
3'
3'
3'
3'
Rad1-Rad10
3'
SIX4
3'
3'
3'
3'
3'
Msh2-Msh3
Rad1-Rad10
3'
3'
Rad1-Rad10
3'
SIX4

Differential requirements for Rad1-Rad10-dependent 3' nonhomologous tail removal during gene conversion

The requirement for Rad1-Rad10 during gene conversion depends on both the number and length of nonhomologous tails. Rad1-Rad10 is critical for gene conversion when both ends of a DSB contain 30 or more nucleotides of nonhomologous sequence (Pâques and Haber 1997; Sugawara *et al.* 1997; Colaiácovo *et al.* 1999; Lyndaker *et al.* 2008), but DSB repair is more subtly reduced in *rad1*Δ mutants when only one nonhomologous tail is present (Colaiácovo *et al.* 1999; Holmes and Haber 1999; Lyndaker *et al.* 2008). The differential requirement for Rad1-Rad10 during gene conversion when one or two ends of a DSB contain nonhomology has been ascribed to the structural nature of the DNA junctions. The initial invasion of 3' single-stranded DNA into a homologous duplex is proposed to create an unstable paranemic joint, which might be a better substrate for Rad1-Rad10 (Sugawara *et al.* 1997). In contrast, when nonhomologous sequence is only on one side of a DSB, the homologous 3' end can perform strand invasion, leaving the nonhomologous tail on the second, non-invading end (Figure 1.2A). The sequence adjacent to this nonhomologous 3' end would likely form a stable plectonemic joint, since the rest of the strand can fully base pair. It is possible that Rad1-Rad10 is minimally required when only one nonhomologous tail is present because plectonemic joints are not ideal substrates for Rad1-Rad10, and/or Rad1-Rad10 is only one of a host of other factors that process these types of structures.

When 3' nonhomologous tails are only 10 nucleotides in length, gene conversion remains efficient in the absence of *RAD1, MSH2,* or *MSH3,* and the short 3' tails are removed by the proofreading 3' to 5' exonuclease activity of Polymerase δ (Pâques and Haber 1997). A second Rad1-Rad10- and Msh2-Msh3-independent

pathway of 3' nonhomologous tail removal is proposed to exist (Ivanov and Haber 1995; Pâques and Haber 1997; Holmes and Haber 1999; Lyndaker *et al.* 2008), though the inefficiency of this proposed pathway suggests that Rad1-Rad10-dependent end processing is preferred. There is no evidence that known factors play a role in this backup pathway of nonhomologous tail removal, as neither Mus81-Mms4 nor the proofreading activities of Pol δ and Pol ε appear to contribute (Pâques and Haber 1997; Lyndaker *et al.* 2008). Replication of partially repaired recombination intermediates might also bypass the requirement for 3' nonhomologous tail removal (Kang and Symington 2000; Lyndaker *et al.* 2008).

Msh2-Msh3 facilitates Rad1-Rad10-dependent 3' nonhomologous tail removal

The Msh2-Msh3 DNA mismatch recognition complex functions in Rad1-Rad10-dependent 3' end processing during homologous recombination (Figures 1.1, 1.2B; (Saparbaev *et al.* 1996; Pâques and Haber 1997; Sugawara *et al.* 1997; Colaiácovo *et al.* 1999; Evans *et al.* 2000). Msh2-Msh3 specifically recognizes insertion/deletion loops of up to 17 base pairs in DNA mismatch repair (Habraken *et al.* 1996; Sia *et al.* 1997; Jensen *et al.* 2005). During homologous recombination, Msh2-Msh3 is proposed to act in the recognition and stabilization of 3' tails at the junction of double-stranded and single-stranded DNA to aid in either the recruitment or cleavage activity of Rad1-Rad10 (Sugawara *et al.* 1997; Bertrand *et al.* 1998; Studamire *et al.* 1999; Langston and Symington 2005). A similar mechanism involving Msh2-Msh3 and Rad1-Rad10 also functions to remove large loops during meiosis (Kirkpatrick and Petes 1997; Kearney *et al.* 2001; Jensen *et al.* 2005). Consistent with its role in 3' tail removal, an *in vitro* DNA binding study showed that purified Msh2-Msh3 binds specifically to branched DNA substrates containing 3'

single-stranded ends, with an affinity comparable to that of its binding to +8 mismatch loops (Surtees and Alani 2006). Msh2-Msh3 appears to bind asymmetrically around double-strand/single-strand junctions, and binding opens the conformation of the junction slightly, potentially to facilitate Rad1-Rad10-dependent cleavage of 3' tails (Surtees and Alani 2006).

Msh2 physically interacts with both Rad1 and Rad10 independently of other mismatch repair factors (Bertrand *et al.* 1998), and no other mismatch repair factors are required for Rad1-Rad10-dependent 3' end processing besides Msh2-Msh3 (Saparbaev *et al.* 1996; Sugawara *et al.* 1997; Langston and Symington 2005). The role of Msh2-Msh3 in nonhomologous tail removal during recombination can be distinguished from its role in DNA mismatch repair, since mutations have been isolated in *MSH2* that disrupt mismatch repair but are functional for recombination (Studamire *et al.* 1999). Msh2 localizes rapidly to DSBs flanked by nonhomologous sequence on chromosomal and plasmid substrates (Evans *et al.* 2000; Goldfarb and Alani 2004; Lyndaker *et al.* 2008), and Msh2 and Msh3 have been reported to physically interact with subunits of the single-strand binding protein RPA (Gavin *et al.* 2002; Gavin *et al.* 2006; Krogan *et al.* 2006). Together these data support a very early role for the Msh2-Msh3 complex in 3' nonhomologous tail removal that might aid in 3' tail recognition.

Rad1-Rad10-dependent 3' end processing does not always require Msh2-Msh3. During SSA, the requirement for Msh2-Msh3 depends upon the length of the annealed region. Strains lacking *MSH2* or *MSH3* are defective in SSA when the annealed region is only 205 bp, but show only a small reduction in repair relative to wild-type when the annealed region is more than 1 kb (Sugawara *et al.* 1997). Decreased dependence on Msh2-Msh3 is also observed with larger loop sizes during Rad1-Rad10-dependent meiotic loop repair (Kearney *et al.* 2001). Despite a predicted

role and clear localization of Msh2 to DSBs, Msh2-Msh3 is also dispensable for gene conversion during mating type switching, where Rad1-Rad10 plays a significant role (Lyndaker *et al.* 2008). Only when nonhomologous sequence is inserted on the invading strand does the role of Msh2-Msh3 in Rad1-Rad10-dependent 3' nonhomologous tail removal become apparent (Lyndaker *et al.* 2008). Altogether, these results support the idea that Msh2-Msh3 plays a role in stabilizing 3' tail intermediates in preparation for Rad1-Rad10-dependent cleavage. Recent work has shown differential roles, with respect to repeat size, for the Rad59 and Rad52 strand annealing factors in SSA. More specifically, Rad59 plays a greater role in SSA involving short repeats (Pannunzio *et al.* 2008). It will be interesting to see whether the requirement for Msh2-Msh3 in 3' nonhomologous tail removal correlates with Rad59 dependence, or whether its role depends only on the stability of the annealed DNA intermediate.

Slx4 is a critical component of the Rad1-Rad10 3' tail removal pathway

Recent work by Flott *et al*. (2007) identified Slx4 as an essential component of the Rad1-Rad10 3' nonhomologous tail removal pathway. Slx4 was initially characterized as a subunit of the Slx1-Slx4 endonuclease, deletion of which is synthetically lethal with *sgs1*Δ (Mullen *et al.* 2001). Slx1-Slx4 is a 5' flap endonuclease, of which Slx1 is thought to be the catalytic subunit (Fricke and Brill 2003). In addition to its function as a heterodimer with Slx1, Slx4 appears to have at least two other separate functions, one involving Rad1-Rad10, and another that is independent of both Slx1 and Rad1-Rad10 and promotes cellular resistance to MMS (Ito *et al.* 2001; Roberts *et al.* 2006; Flott *et al.* 2007; Li *et al.* 2008). A screen for mutants defective in SSA recently found that *slx4*Δ mutants are blocked at the 3' tail

removal step of SSA (Li *et al.* 2008), and Slx4 was found to play an important role during mating type switching in the same pathway as the Rad1-Rad10 complex (Lyndaker *et al.* 2008). Additionally, the Flott *et al.* study found that at least three residues on Slx4 are directly phosphorylated by the Mec1 and Tel1 checkpoint kinases, and that this phosphorylation is essential for the SSA functions of Slx4 but not for resistance to MMS or viability in *sgs1*Δ mutants (Flott and Rouse 2005; Flott *et al.* 2007).

These new findings support a model in which Slx4 is acted upon directly by the checkpoint machinery in response to DSBs to recruit or activate Rad1-Rad10 and promote 3' nonhomologous tail removal. The DNA damage response is thought to be activated during SSA because of the relatively slow kinetics of repair and the extensive resection required. Since phosphorylation of Slx4 is absolutely essential for 3' nonhomologous tail removal during SSA but is dispensable for its other functions (Flott *et al.* 2007), this phosphorylation is likely to provide the specificity to channel Slx4 to its recombination function.

While gene conversion involving a single 3' nonhomologous tail does not require checkpoint activation, recent work has shown that *rad1*Δ and *slx4*Δ mutants exhibit *RAD9*- and *MAD2*-dependent checkpoint activation during mating type switching, a single-nonhomology gene conversion event (Lyndaker *et al.* 2008). It is possible that the recruitment or activity of Rad1-Rad10-Slx4 is required to turn off the DNA damage checkpoint by signaling that repair is proceeding normally.

Slx4 is not required for checkpoint activation, but provides a crucial link between DNA damage sensing and activation of DNA repair. Slx4, but not its endonuclease partner Slx1, is required for the repair of alkylation damage (Flott and Rouse 2005). In addition to SSA, Slx4 is phosphorylated in a Mec1/Tel1-dependent manner in response to a variety of DNA-damaging agents, including MMS,

camptothecin, hydroxyurea, ionizing radiation, and the UV mimetic 4-NQO, and is required for efficient DNA repair throughout the cell cycle (Flott and Rouse 2005). Thus, it appears that Slx4 plays a critical role in the response to many types of DNA damage, and the strict requirement for its checkpoint-dependent phosphorylation in 3' nonhomologous tail removal provides a beautiful example of how DNA damage sensed by the checkpoint machinery directly promotes DNA repair.

Saw1 is a component of the Rad1-Rad10 end-processing machinery

The *SAW1* (*YAL027W*) gene was recently identified in a microarray-based screen for mutants defective in SSA (Li *et al.* 2008). Saw1, for single-strand annealing weakened 1, physically interacts with Rad1-Rad10, Msh2-Msh3, and Rad52 (Gavin *et al.* 2002; Krogan *et al.* 2006; Li *et al.* 2008), all of which function in SSA, and like *slx4*Δ mutants, *saw1*Δ mutants are defective specifically in 3' nonhomologous tail removal (Li *et al.* 2008). Li *et al.* found that the Rad1 protein fails to localize to SSA intermediates in *saw1*Δ mutants, and *saw1*Δ18-24 mutants, whose mutant Saw1 protein fails interact with Rad1 but still interacts with Msh2 and Rad52, are completely defective in SSA (2008). These new findings provide strong evidence that Saw1 recruits Rad1-Rad10 to recombination intermediates containing Rad52.

Rad14 is thought to target Rad1-Rad10 to its substrates during NER (Guzder *et al.* 1996; Prakash and Prakash 2000; Guzder *et al.* 2006), but it has been unclear how Rad1-Rad10 is targeted to 3' tails during recombination, especially since Msh2-Msh3 is dispensable for some gene conversion and SSA events. In human cell-free extracts, Rad52 and the Rad1-Rad10 homolog XPF-ERCC1 stably associate through interaction of XPF with the N-terminus of Rad52 (Motycka *et al.* 2004). This physical interaction stimulates the endonuclease activity of XPF-ERCC1 and attenuates the

strand annealing activity of Rad52, both of which promote the removal of 3' tails from recombination intermediates (Motycka *et al.* 2004). Though an equivalent interaction between Rad1-Rad10 and Rad52 has not been observed, it appears that Saw1 provides this physical interaction in *S. cerevisiae* (Li *et al.* 2008). These new findings reveal how Saw1, and potentially Slx4, may recruit and regulate Rad1-Rad10 and 3' nonhomologous tail removal during homologous recombination.

Conclusions: A comprehensive model for Rad1-Rad10-dependent 3' nonhomologous tail removal during SSA

The new findings reviewed here provide a more comprehensive understanding of how Rad1-Rad10-dependent 3' end processing is coordinated during homologous recombination. As shown in Figure 1.3, resection of DSBs during SSA creates 3' single-stranded tails that are coated by the RPA single-stranded DNA binding protein. The extensive single-stranded DNA activates the DNA damage response, which promotes phosphorylation of Slx4 by the Mec1 and Tel1 checkpoint kinases. Once resection has revealed regions of homology, the Rad52 strand annealing protein anneals the homologous sequences, creating 3' nonhomologous tails on either side of the intermediate. When the length of homology is limited and creates an unstable paranemic intermediate, Msh2-Msh3 stabilizes the junction and slightly opens it to create a more suitable substrate for Rad1-Rad10 cleavage. Saw1 recruits Rad1-Rad10 to Rad52-containing annealed sequences at double-strand/single-strand junctions bound by Msh2-Msh3. Phosphorylated Slx4 binds to Rad1-Rad10, but does not appear to interact with Rad52, Saw1, or Msh2-Msh3. The result of these physical interactions is the positioning of Rad1-Rad10 at the double-strand/single-strand

Figure 1.3. Model for coordination of 3' nonhomologous tail removal factors during single-strand annealing. Following DSB formation, 5' to 3' resection creates single-stranded DNA that is coated by RPA. This process also signals to the Mec1 and Tel1 checkpoint kinases which, once activated, phosphorylate Slx4. The Rad52 strand annealing protein facilitates pairing of the homologous sequences, displacing RPA from the annealed regions. The Msh2-Msh3 complex recognizes the junction of double-stranded and 3' single-stranded DNA, potentially interacting with RPA, and opens the DNA junction slightly to create a better substrate for Rad1-Rad10 cleavage. The Saw1 protein recruits Rad1-Rad10 endonuclease to the junction of Rad52- and Msh2-Msh3-containing DNA, and association of Rad1-Rad10 with phosphorylated Slx4 allows it to cleave the DNA near the double-strand/single-strand junction, freeing the 3' nonhomologous tail.

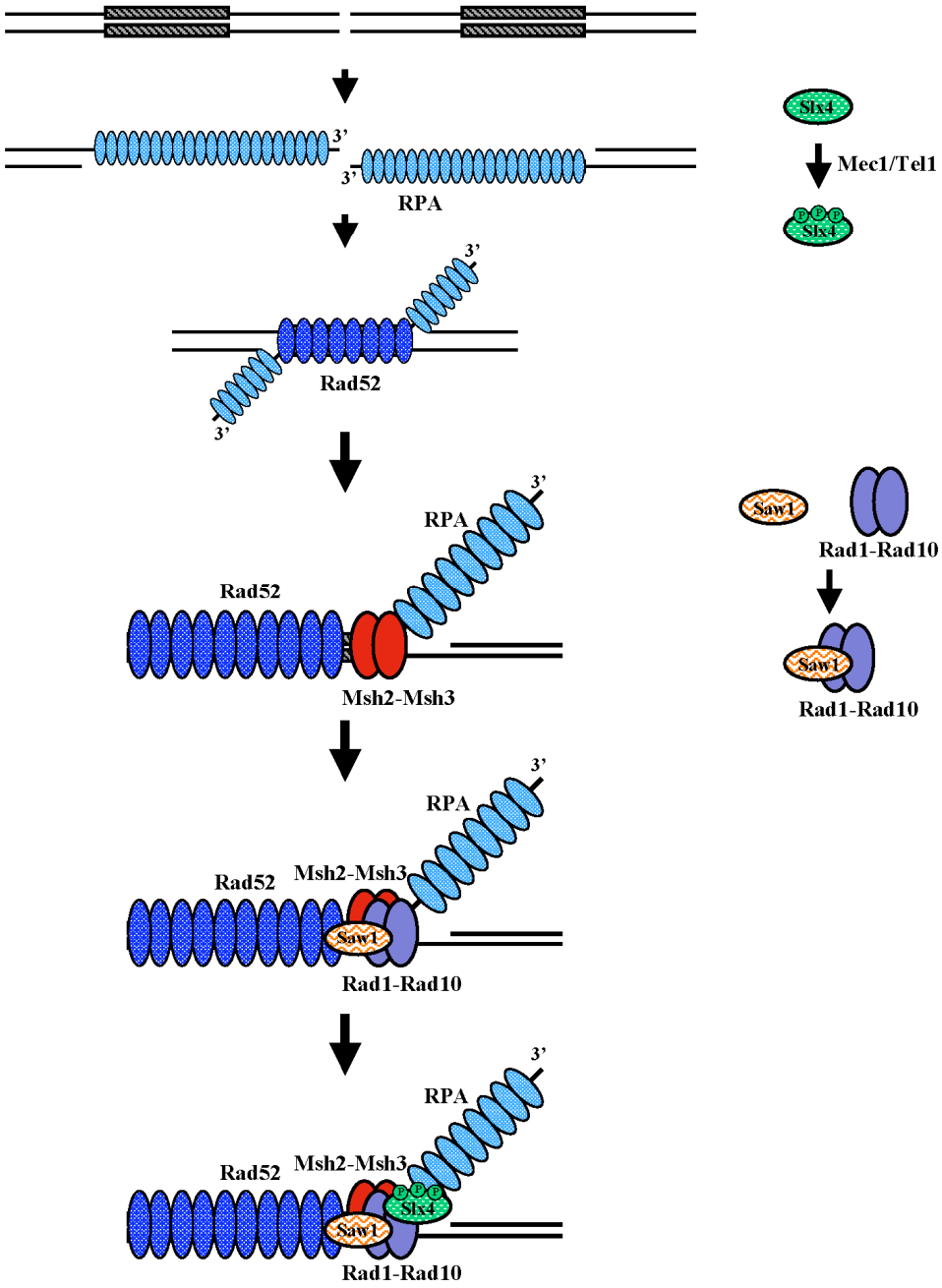
3'
3'
RPA
3'
Rad52
3'
3'
RPA
Rad52
Msh2-Msh3
3'
RPA
Rad52
Msh2-Msh3
Saw1
Rad1-Rad10
3'
RPA
Rad52
Msh2-Msh3
Slx4
Saw1
Rad1-Rad10
Slx4
Mec1/Tel1
Slx4
Saw1
Rad1-Rad10
Saw1
Rad1-Rad10

junction between Saw1 and Slx4. Rad1-Rad10 cleaves the strand near the junction, removing the 3' nonhomologous tail and providing a free 3' hydroxyl for extension by DNA polymerases. Though this model is drawn for SSA, it is also applicable to gene conversion, with the differences being the additional presence of Rad51 and differential requirements for Rad1-Rad10-Slx4 and Msh2-Msh3 for one versus two 3' nonhomologous tails.

It is not clear whether these physically interacting factors arrive at recombination intermediates in a sequential fashion, or whether a stable complex of Saw1-Msh2-Msh3-Rad1-Rad10-Slx4 exists *in vivo* and is simply recruited to Rad52-containing DNA, perhaps in response to Slx4 phosphorylation by Mec1/Tel1. It is striking that *saw1*Δ and *slx4*Δ mutants exhibit opposing phenotypes with regard to rDNA stability (Li *et al.* 2008), so additional work is needed to understand the distinct functions of Slx4 and Saw1 in recombination and how they relate to coordination of Rad1-Rad10 3' tail cleavage. It will be interesting to identify the critical function of Slx4 in this process, whether it is primarily to transmit a repair signal from the DNA damage checkpoint or whether there are additional roles in recruiting, positioning, or activating the endonuclease activity of Rad1-Rad10. While the findings reviewed here provide a clearer picture of how Rad1-Rad10 identifies and cleaves its substrates during recombination, many questions still remain. What is the physical activity of Saw1? How does Slx4 arrive at junctions containing 3' tails? What is the function of phosphorylated Slx4? Why is Msh2-Msh3 essential in some cases and dispensable for others? Addressing these questions will edge us closer to understanding the link between DNA damage recognition, checkpoint signaling, and efficient DNA repair.

Acknowledgments

We thank members of the Alani lab for helpful comments on the manuscript. A.M.L and E.A. were supported by National Institutes of Health grant GM53085.

REFERENCES

Al-Minawi, A. Z., N. Saleh-Gohari and T. Helleday (2008). "The ERCC1/XPF endonuclease is required for efficient single-strand annealing and gene conversion in mammalian cells." Nucl. Acids Res. **36**(1): 1-9.

Bardwell, A., L. Bardwell, A. Tomkinson and E. Friedberg (1994). "Specific cleavage of model recombination and repair intermediates by the yeast Rad1-Rad10 DNA endonuclease." Science **265**(5181): 2082-5.

Bertrand, P., D. X. Tishkoff, N. Filosi*, et al.* (1998). "Physical interaction between components of DNA mismatch repair and nucleotide excision repair." Proc. Natl. Acad. Sci. USA **95**: 14278-83.

Ciccia, A., N. McDonald and S. C. West (2008). "Structural and functional relationships of the XPF/MUS81 family of proteins." Annu. Rev. Biochem. **77**(1): 259-87.

Colaiácovo, M. P., F. Pâques and J. E. Haber (1999). "Removal of one nonhomologous DNA end during gene conversion by a *RAD1*- and *MSH2*-independent pathway." Genetics **151**: 1409-23.

Deininger, P. L. and M. A. Batzer (1999). "*Alu* repeats and human disease." Mol. Genet. Metab. **67**(3): 183-93.

Elliott, B., C. Richardson and M. Jasin (2005). "Chromosomal translocation mechanisms at intronic *Alu* elements in mammalian cells." Mol. Cell **17**(6): 885-94.

Evans, E., N. Sugawara, J. E. Haber and E. Alani (2000). "The *Saccharomyces cerevisiae* Msh2 mismatch repair protein localizes to recombination intermediates *in vivo*." Mol. Cell **5**: 189-99.

Fishman-Lobell, J. and J. Haber (1992). "Removal of nonhomologous DNA ends in double-strand break recombination: the role of the yeast ultraviolet repair gene *RAD1*." Science **258**(5081): 480-4.

Flott, S., C. Alabert, G. W. Toh*, et al.* (2007). "Phosphorylation of Slx4 by Mec1 and Tel1 regulates the single-strand annealing mode of DNA repair in budding yeast." Mol. Cell. Biol. **27**(18): 6433-45.

Flott, S. and J. Rouse (2005). "Slx4 becomes phosphorylated after DNA damage in a Mec1/Tel1-dependent manner and is required for repair of DNA alkylation damage." Biochem. J. **391**(2): 325-33.

Fricke, W. M. and S. J. Brill (2003). "Slx1-Slx4 is a second structure-specific endonuclease functionally redundant with Sgs1-Top3." Genes Dev. **17**: 1768-78.

Gao, G., C. McMahon, J. Chen and Y. S. Rong (2008). "A powerful method combining homologous recombination and site-specific recombination for targeted mutagenesis in Drosophila." Proc. Natl. Acad. Sci. USA **105**(37): 13999-14004.

Gavin, A.-C., P. Aloy, P. Grandi*, et al.* (2006). "Proteome survey reveals modularity of the yeast cell machinery." Nature **440**(7084): 631-6.

Gavin, A.-C., M. Bosche, R. Krause*, et al.* (2002). "Functional organization of the yeast proteome by systematic analysis of protein complexes." Nature **415**: 141-7.

Goldfarb, T. and E. Alani (2004). Chromatin immunoprecipitation to investigate protein-DNA interactions during genetic recombination. Genetic recombination: Reviews and protocols. A. S. Waldman. Totowa, NJ, Humana Press Inc. **262:** 223-37.

Guzder, S. N., C. H. Sommers, L. Prakash and S. Prakash (2006). "Complex formation with damage recognition protein Rad14 is essential for *Saccharomyces cerevisiae* Rad1-Rad10 nuclease to perform its function in nucleotide excision repair *in vivo*." Mol. Cell. Biol. **26**(3): 1135-41.

Guzder, S. N., P. Sung, L. Prakash and S. Prakash (1996). "Nucleotide excision repair in yeast is mediated by sequential assembly of repair factors and not by a pre-assembled repairosome." J. Biol. Chem. **271**(15): 8903-10.

Habraken, Y., P. Sung, L. Prakash and S. Prakash (1996). "Binding of insertion/deletion DNA mismatches by the heterodimer of yeast mismatch repair proteins MSH2 and MSH3." Curr. Biol. **6**(9): 1185-7.

Hedges, D. J. and P. L. Deininger (2007). "Inviting instability: Transposable elements, double-strand breaks, and the maintenance of genome integrity." Mut. Res. **616**(1-2): 46-59.

Holmes, A. M. and J. E. Haber (1999). "Double-strand break repair in yeast requires both leading and lagging strand DNA polymerases." Cell **96**: 415-24.

Ira, G., D. Satory and J. E. Haber (2006). "Conservative inheritance of newly synthesized DNA in double-strand break-induced gene conversion." Mol. Cell. Biol. **26**(24): 9424-9.

Ito, T., T. Chiba, R. Ozawa*, et al.* (2001). "A comprehensive two-hybrid analysis to explore the yeast protein interactome." Proc. Natl. Acad. Sci. USA **98**(8): 4569-74.

Ivanov, E. and J. Haber (1995). "*RAD1* and *RAD10*, but not other excision repair genes, are required for double-strand break-induced recombination in *Saccharomyces cerevisiae*." Mol. Cell. Biol. **15**(4): 2245-51.

Jaspers, N. G. J., A. Raams, M. C. Silengo*, et al.* (2007). "First reported patient with human *ERCC1* deficiency has cerebro-oculo-facio-skeletal syndrome with a mild defect in nucleotide excision repair and severe developmental failure." Am. J. Hum. Genet. **80**(3): 457-66.

Jensen, L. E., P. A. Jauert and D. T. Kirkpatrick (2005). "The large loop repair and mismatch repair pathways of *Saccharomyces cerevisiae* act on distinct substrates during meiosis." Genetics **170**(3): 1033-43.

Kang, L. E. and L. S. Symington (2000). "Aberrant double-strand break repair in *rad51* mutants of *Saccharomyces cerevisiae*." Mol. Cell. Biol. **20**(24): 9162-72.

Kearney, H. M., D. T. Kirkpatrick, J. L. Gerton and T. D. Petes (2001). "Meiotic recombination involving heterozygous large insertions in *Saccharomyces*

cerevisiae: Formation and repair of large, unpaired DNA loops." Genetics **158**(4): 1457-76.

Kirkpatrick, D. T. and T. D. Petes (1997). "Repair of DNA loops involves DNA-mismatch and nucleotide-excision repair proteins." Nature **387**: 929-31.

Kolomietz, E., S. M. Meyn, A. Pandita and J. A. Squire (2002). "The role of *Alu* repeat clusters as mediators of recurrent chromosomal aberrations in tumors." Gen. Chrom. Canc. **35**: 97-112.

Krogan, N. J., G. Cagney, H. Yu*, et al.* (2006). "Global landscape of protein complexes in the yeast *Saccharomyces cerevisiae*." Nature **440**(7084): 637-43.

Lander, E., L. Linton, B. Birren*, et al.* (2001). "Initial sequencing and analysis of the human genome." Nature **409**(6822): 860-921.

Langston, L. D. and L. S. Symington (2005). "Opposing roles for DNA structure-specific proteins Rad1, Msh2, Msh3, Sgs1 in yeast gene targeting." EMBO J. **24**: 2214-23.

Li, F., J. Dong, X. Pan*, et al.* (2008). "Microarray-based genetic screen defines *SAW1*, a gene required for Rad1/Rad10-dependent processing of recombination intermediates." Mol. Cell **30**(3): 325-35.

Li, W.-H., Z. Gu, H. Wang and A. Nekrutenko (2001). "Evolutionary analyses of the human genome." Nature **409**: 847-9.

Liang, F., M. Han, P. J. Romanienko and M. Jasin (1998). "Homology-directed repair is a major double-strand break repair pathway in mammalian cells." Proc. Natl. Acad. Sci. USA **95**: 5172-7.

Lyndaker, A. M., T. Goldfarb and E. Alani (2008). "Mutants defective in Rad1-Rad10-Slx4 exhibit a unique pattern of viability during mating type switching in *Saccharomyces cerevisiae*." Genetics **179**(4): 1807-21.

Mattarucchi, E., V. Guerini, A. Rambaldi*, et al.* (2008). "Microhomologies and interspersed repeat elements at genomic breakpoints in chronic myeloid leukemia." Gen. Chrom. Canc. **47**(7): 625-32.

McWhir, J., J. Selfridge, D. J. Harrison*, et al.* (1993). "Mice with DNA repair gene (*ERCC-1*) deficiency have elevated levels of p53, liver nuclear abnormalities and die before weaning." Nat. Genet. **5**(3): 217-24.

Motycka, T. A., T. Bessho, S. M. Post*, et al.* (2004). "Physical and functional interaction between the XPF/ERCC1 endonuclease and hRad52." J. Biol. Chem. **279**(14): 13634-9.

Mullen, J. R., V. Kaliraman, S. S. Ibrahim and S. J. Brill (2001). "Requirement for three novel protein complexes in the absence of the Sgs1 DNA helicase in *Saccharomyces cerevisiae*." Genetics **157**: 103-18.

Niedernhofer, L. J., H. Odijk, M. Budzowska*, et al.* (2004). "The structure-specific endonuclease Ercc1-Xpf is required to resolve DNA interstrand cross-link-induced double-strand breaks." Mol. Cell. Biol. **24**(13): 5776-87.

Pannunzio, N. R., G. M. Manthey and A. M. Bailis (2008). "RAD59 is required for efficient repair of simultaneous double-strand breaks resulting in translocations in *Saccharomyces cerevisiae*." DNA Repair **7**(5): 788-800.

Pâques, F. and J. E. Haber (1997). "Two pathways for removal of nonhomologous DNA ends during double-strand break repair in *Saccharomyces cerevisiae*." Mol. Cell. Biol. **17**(11): 6765-71.

Pâques, F. and J. E. Haber (1999). "Multiple pathways of recombination induced by double-strand breaks in *Saccharomyces cerevisiae*." Microbiol. Mol. Biol. Rev. **63**(2): 349-404.

Prakash, S. and L. Prakash (2000). "Nucleotide excision repair in yeast." Mut. Res. **451**(1-2): 13-24.

Roberts, T. M., M. S. Kobor, S. A. Bastin-Shanower*, et al.* (2006). "Slx4 regulates DNA damage checkpoint-dependent phosphorylation of the BRCT domain protein Rtt107/Esc4." Mol. Biol. Cell **17**(1): 539-48.

Saparbaev, M., L. Prakash and S. Prakash (1996). "Requirement of mismatch repair genes *MSH2* and *MSH3* in the *RAD1-RAD10* pathway of mitotic recombination in *Saccharomyces cerevisiae*." Genetics **142**(3): 727-36.

Sia, E. A., R. J. Kokoska, M. Dominska*, et al.* (1997). "Microsatellite instability in yeast: Dependence on repeat unit size and DNA mismatch repair genes." Mol. Cell. Biol. **17**(5): 2851-8.

Stenger, J. E., K. S. Lobachev, D. Gordenin*, et al.* (2001). "Biased distribution of inverted and direct *Alu*s in the human genome: Implications for insertion, exclusion, and genome stability." Genome Res. **11**(1): 12-27.

Strout, M. P., G. Marcucci, C. D. Bloomfield and M. A. Caligiuri (1998). "The partial tandem duplication of ALL1 (MLL) is consistently generated by *Alu*-mediated homologous recombination in acute myeloid leukemia." Proc. Natl. Acad. Sci. USA **95**(5): 2390-5.

Studamire, B., G. Price, N. Sugawara*, et al.* (1999). "Separation-of-function mutations in *Saccharomyces cerevisiae MSH2* that confer mismatch repair defects but do not affect nonhomologous-tail removal during recombination." Mol. Cell. Biol. **19**(11): 7558-67.

Sugawara, N., G. Ira and J. E. Haber (2000). "DNA length dependence of the single-strand annealing pathway and the role of *Saccharomyces cerevisiae* RAD59 in double-strand break repair." Mol. Cell. Biol. **20**(14): 5300-9.

Sugawara, N., F. Pâques, M. Colaiacovo and J. E. Haber (1997). "Role of *Saccharomyces cerevisiae* Msh2 and Msh3 repair proteins in double-strand break-induced recombination." Proc. Natl. Acad. Sci. USA **94**: 9214-9.

Surtees, J. A. and E. Alani (2006). "Mismatch repair factor MSH2-MSH3 binds and alters the conformation of branched DNA structures predicted to form during genetic recombination." J. Mol. Biol. **360**(3): 523-6.

Symington, L. S. (2002). "Role of *RAD52* epistasis group genes of homologous recombination and double-strand break repair." Microbiol. Mol. Biol. Rev. **66**(4): 630-70.

VanHulle, K., F. J. Lemoine, V. Narayanan*, et al.* (2007). "Inverted DNA repeats channel repair of distant double-strand breaks into chromatid fusions and chromosomal rearrangements." Mol. Cell. Biol. **27**(7): 2601-14.

Wang, X. and P. Baumann (2008). "Chromosome fusions following telomere loss are mediated by single-strand annealing." Mol. Cell **31**(4): 463-73.

Weeda, G., I. Donker, J. de Wit*, et al.* (1997). "Disruption of mouse *ERCC1* results in a novel repair syndrome with growth failure, nuclear abnormalities and senescence." Curr. Biol. **7**(6): 427-39.

CHAPTER 2

Mutants defective in Rad1-Rad10-Slx4 exhibit a unique pattern of viability during mating type switching in *S. cerevisiae*

Amy M. Lyndaker, Tamara Goldfarb[1], and Eric Alani

Department of Molecular Biology and Genetics

Cornell University

Ithaca, NY 14853-2703

[1]Current address:

Center for Cancer Research, National Cancer Institute, Bethesda, Maryland

This chapter was originally published in the August 2008 issue of Genetics:

Lyndaker, Amy M., Tamara Goldfarb, and Eric Alani. 2008: Mutants defective in Rad1-Rad10-Slx4 exhibit a unique pattern of viability during mating type switching in *S. cerevisiae*. Genetics. 2008. Volume 179, Issue 4, Pages 1807-21.

Abstract

Efficient repair of DNA double-strand breaks (DSBs) requires the coordination of checkpoint signaling and enzymatic repair functions. To study these processes during gene conversion at a single chromosomal break, we monitored mating type switching in *S. cerevisiae* strains defective in the Rad1-Rad10-Slx4 complex. Rad1-Rad10 is a structure-specific endonuclease that removes 3' nonhomologous single-stranded ends that are generated during many recombination events. Slx4 is a known target of the DNA damage response that forms a complex with Rad1-Rad10 and is critical for 3' end processing during repair of DSBs by single-strand annealing. We found that mutants lacking an intact Rad1-Rad10-Slx4 complex displayed *RAD9*- and *MAD2*-dependent cell cycle delays and decreased viability during mating type switching. In particular, these mutants exhibited a unique pattern of dead and switched daughter cells arising from the same DSB-containing cell. Furthermore, we observed that mutations in post-replicative lesion bypass factors (*mms2*Δ, *mph1*Δ) resulted in decreased viability during mating type switching, and conferred shorter cell cycle delays in *rad1*Δ mutants. We conclude that Rad1-Rad10-Slx4 promotes efficient repair during gene conversion events involving a single 3' nonhomologous tail, and propose that the *rad1*Δ and *slx4*Δ mutant phenotypes result from inefficient repair of a lesion at the *MAT* locus that is bypassed by replication-mediated repair.

Introduction

In the baker's yeast *Saccharomyces cerevisiae,* spontaneous and induced DNA double-strand breaks (DSBs) are primarily repaired by homologous recombination (reviewed in Pâques and Haber 1999). In the initial steps of repair, DSBs are acted upon by a 5' to 3' exonuclease activity to yield two 3' single-stranded ends. These ends interact with RPA, Rad51, Rad52, Rad54, Rad55, and Rad57 to allow strand invasion into a homologous double-stranded donor sequence. DNA synthesis initiating from the 3' invading end results in copying of DNA sequence from the donor locus, and recombination is completed either by resolution of a Holliday junction intermediate or by synthesis-dependent strand annealing (SDSA). Homologous recombination can also occur by non-conservative mechanisms including single-strand annealing (SSA) and break-induced replication (BIR). During SSA, a DSB located between repeated sequences is processed by 5' to 3' exonuclease activity and the 3' single-stranded ends anneal at homologous sequences, resulting in deletion of the intervening sequence. In BIR, strand invasion of one 3' end into a homologous sequence is followed by replication that continues along the chromosome arm (reviewed in Pâques and Haber 1999).

Mating type switching in *S. cerevisiae* is a unidirectional gene conversion event in which a DSB created at the *MAT* locus is repaired using one of two silent mating type cassettes, *HMR***a** or *HML***α** (reviewed in Haber 1998). This programmed recombination event is initiated by HO endonuclease cleavage within *MAT*, and donor preference is such that cells preferentially repair the DSB using the donor sequence of the opposite mating type (Wu and Haber 1995; Wu and Haber 1996; Wu *et al.* 1997; Haber 1998). Crossovers, which would lead to intrachromosomal deletions, are rarely associated with mating type switching (Klar and Strathern 1984), and mating type

switching is thought to occur by a SDSA mechanism (McGill *et al.* 1989; Haber 1998; Pâques and Haber 1999; Ira *et al.* 2006).

The HO cleavage site at the *MAT* locus is located at the junction between homologous and nonhomologous sequence with respect to the donor cassette. Strand invasion is thought to be initiated by the 3' tail that is homologous to the donor sequence, leaving the second 3' end as a nonhomologous tail following annealing of the repaired invading strand (Figure 2.1A). Thus, a single 3' nonhomologous tail must be removed to complete repair. Previous genetic studies have shown that 3' nonhomologous tail removal depends on the activity of the Rad1-Rad10 endonuclease, as well as the Msh2-Msh3 DNA mismatch recognition complex (Fishman-Lobell and Haber 1992; Ivanov and Haber 1995; Saparbaev *et al.* 1996; Kirkpatrick and Petes 1997; Sugawara *et al.* 1997).

Rad1-Rad10 is a structure-specific endonuclease that cleaves DNA at the junction of double-stranded and 3' single-stranded DNA, and has been characterized in its role during nucleotide excision repair (NER) as well as in the removal of 3' nonhomologous tails and blocked 3' termini, including Top1-associated DNA (Sung *et al.* 1993; Bardwell *et al.* 1994; Vance and Wilson 2002; Guzder *et al.* 2004). The importance of Rad1-Rad10 for its non-NER DNA processing functions is highlighted by the fact that mice lacking the mammalian homolog of Rad1-Rad10, ERCC1-XPF, exhibit features of premature aging including very reduced lifespan (20-38 days), severe runting, and abnormalities of the liver, skin, kidney, and spleen, while mice lacking other NER factors develop normally and have a normal lifespan (McWhir *et al.* 1993; Weeda *et al.* 1997).

In plasmid-based studies, both Rad1-Rad10 and Msh2-Msh3 are required for recombinational repair when two 3' nonhomologous tails are present (Sugawara *et al.* 1997; Colaiácovo *et al.* 1999). Repair events involving only one nonhomologous end

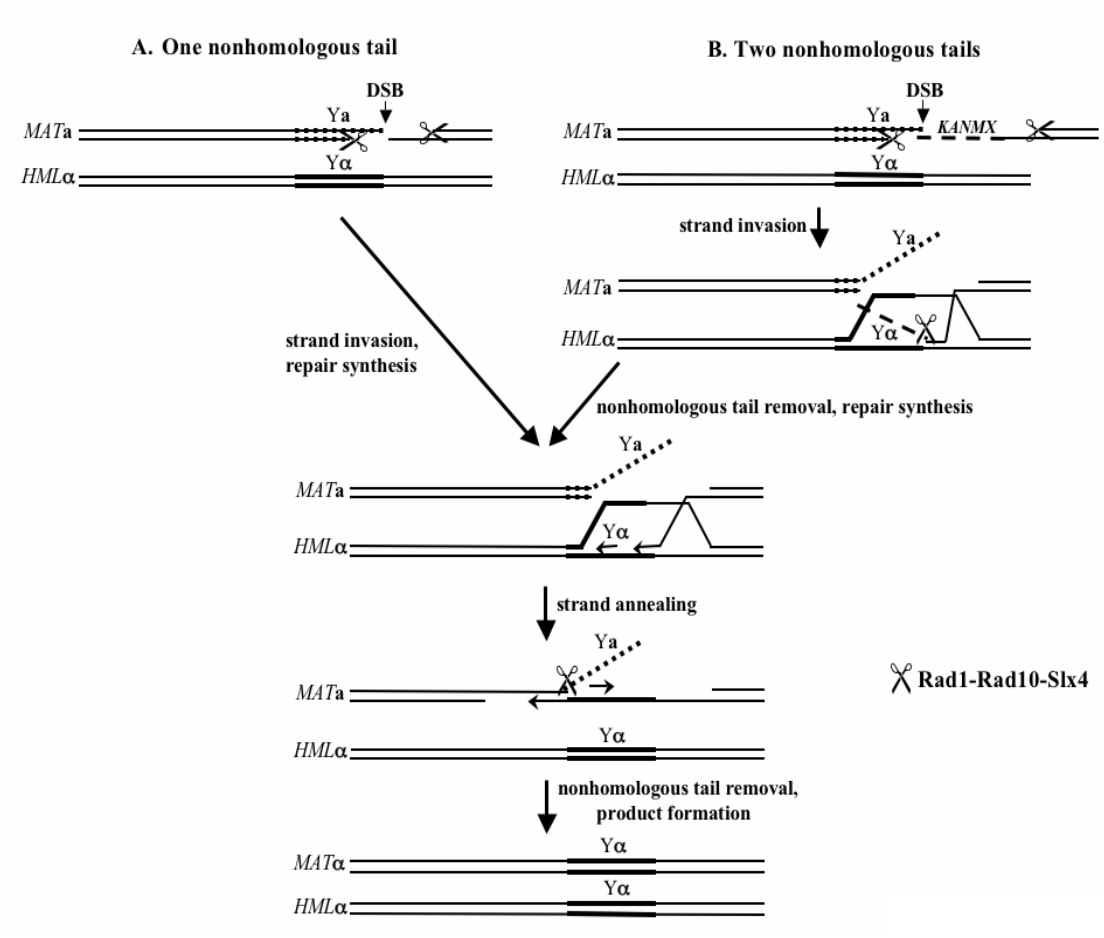

Figure 2.1. Synthesis-dependent strand annealing model for mating type switching in *Saccharomyces cerevisiae* (adapted from Pâques and Haber 1999). A. Only the *MAT***a** and *HML***α** loci are shown. Mating type switching is initiated by a DSB formed by HO endonuclease at the *MAT***a** locus near the Y/Z1 junction. This is followed by 5' to 3' resection to create 3' single-stranded ends, and the 3' end with homology to the *HML***α** donor sequence initiates strand invasion and primes DNA synthesis off of the donor template. Strand displacement from the donor sequence followed by annealing onto the broken chromosome results in the formation of a 3' single-stranded nonhomologous tail that must be excised prior to the subsequent DNA synthesis and ligation steps. Rad1-Rad10-Slx4 is hypothesized to act in 3' nonhomologous tail removal at this step. B. Mating type switching involving two nonhomologous ends due to insertion of *KANMX* sequence on the distal side of the break. A 3' nonhomologous tail removal step is required to allow priming of DNA synthesis off of the invading strand. Repair then proceeds as above.

are also hypothesized to require Rad1-Rad10 and Msh2-Msh3, though a second, less efficient pathway involving the 3' to 5' proofreading activity of DNA Polymerase δ has been shown to remove 3' ssDNA less than 30 nucleotides long (Pâques and Haber 1997; Colaiácovo *et al.* 1999). The Haber lab previously reported that mating type switching in G1-arrested cells is significantly less efficient in *rad1*Δ mutants, but stated no further defects (Holmes and Haber 1999).

Rad1-Rad10 and Msh2-Msh3 are also required during SSA, which involves two nonhomologous tails. The requirement for Msh2-Msh3 depends on the length of the annealed region; annealed regions greater than 1 kb in length are repaired independently of Msh2-Msh3. Thus, Msh2-Msh3 is thought act by binding and stabilizing the double-strand/single-strand junctions to promote Rad1-Rad10-dependent cleavage of 3' ends (Sugawara *et al.* 1997; Pâques and Haber 1999). Consistent with this, *in vitro* biochemical studies have shown that purified Msh2-Msh3 binds specifically to double-strand/single-strand junctions and opens up the junction, possibly providing a more suitable substrate for Rad1-Rad10 cleavage (Surtees and Alani 2006). Recent work from Flott *et al.* (2007) has also implicated the Slx4 protein in Rad1-Rad10-dependent 3' nonhomologous tail removal. The authors found that Slx4 forms a complex with Rad1-Rad10 that is mutually exclusive of the interaction with its endonuclease partner, Slx1. Slx4 was found to be required for Rad1-dependent DSB repair by single-strand annealing, presumably at the 3' nonhomologous tail removal step (Flott *et al.* 2007).

A single unrepaired DSB is sufficient to trigger G2/M cell cycle arrest in *S. cerevisiae* (Sandell and Zakian 1993). Arrest at the G2/M transition can be elicited by the DNA damage or spindle checkpoints. While cell cycle checkpoints are not normally activated during mating type switching, the DNA damage response is activated in strains lacking both donor sequences which are thus unable to repair the

DSB by gene conversion (Pellicioli *et al.* 1999; Pellicioli *et al.* 2001; Lee *et al.* 2003). Activation of the DNA damage checkpoint has also been shown to occur during DSB repair at *MAT* when the donor locus is on a separate chromosome, most likely because the repair process takes longer to occur (Vaze *et al.* 2002). A role for the spindle checkpoint during mating type switching has not been reported.

In this study, we used a variety of techniques to examine the importance of the Rad1-Rad10-Slx4 complex in 3' nonhomologous tail removal during mating type switching. We show that mutants defective in the Rad1-Rad10-Slx4 complex exhibited a *RAD9*-dependent, partially *MAD2*-dependent cell cycle arrest and decreased cell survival during mating type switching. A third of *rad1*Δ and *slx4*Δ cells induced for mating type switching showed a unique viability profile during pedigree analysis, with one switched and one dead daughter cell arising from the same DSB-induced cell. We hypothesize that this phenotype arises from replication bypass of an inefficiently repaired DNA lesion at *MAT*. This work indicates that the Rad1-Rad10-Slx4 complex promotes the efficient repair of DSBs involving a single 3' nonhomologous tail intermediate.

Materials and Methods

Strains and plasmids. All strains used in this study are shown in Table 2.1. Parental strains EAY745 (*MAT***a** to *MAT*$\boldsymbol{\alpha}$), EAY 744 (*MAT***a** to *MAT***a**), and EAY742 (*donorless*) were created by single-step gene replacement with *Sph*I- and *Pvu*II-digested pEAI118 to integrate *MSH2-HA*$_4$*::LEU2* at the endogenous *MSH2* locus in JKM161, JKM160, or JKM139, respectively, kindly provided by J. Haber. Insertion of the HA_4 epitope into Msh2 did not disrupt gene function (Goldfarb and Alani 2004). All strains contain *HO* endonuclease gene under control of the galactose-

inducible *GAL10* promoter to allow for inducible mating type switching. To create the parental strain EAY1042 used in the double non-homology experiments (Figure 2.1; Appendix, Supplementary Figure 2.6; Table 2.1), EAY745 was transformed with a PCR-generated fragment containing 57 bp of Y**a** sequence proximal to the *MAT* HO cut site, 1428 bp of *KANMX* sequence (Wach *et al.* 1994), and 52 bp of sequence distal to the HO cut site. Integration of the *KANMX*-containing fragment (*MAT***a***::KANMX4)* was confirmed by both PCR and Southern blot analysis. Yeast were transformed with the appropriate DNA fragments using the lithium acetate method (Gietz and Schiestl 1991), and integrations were confirmed by PCR followed by phenotype testing.

Media and culture conditions. For time course experiments, dilutions of stationary phase cultures were made in yeast-peptone (Difco) medium pH 6.8 containing 2% (w/v) lactate and grown at 30° C until mid-log phase (1-2 x 10^7 cells/ml). Cultures were induced with galactose (US Biological) to 2% (w/v) final concentration and samples were collected at relevant time points. *HO* expression was suppressed after 30 minutes by the addition of glucose (US Biological) to 2% (w/v) final concentration. To maintain a consistent number of cells at each time point throughout the time course, individual samples were diluted to the same cell density as the time zero sample.

Cell survival assays. Asynchronous cultures were grown to mid-log phase and induced with galactose for 30 minutes. Uninduced controls were diluted similarly with water. Both induced and uninduced cultures were diluted 2,500-fold and plated in triplicate on YPD plates immediately following the addition of glucose to the media. After growth for 3 days at 30º C, percent survival was calculated as the

Table 2.1. Strains used in this study. All strains used in this study are derived from JKM161, JKM160, and JKM139, kindly provided by J. Haber. Gene disruptions and mutant alleles were made by transforming *S. cerevisiae* strains with restriction-digested plasmids for *rad1*Δ*, msh2*Δ*, msh3*Δ*, rad51*Δ, and *pol3-01* as listed above. All other disruptions were made by integrative transformation of PCR products generated by amplification of *KANMX* sequences either from plasmid pFA6-KanMX4 (Wach *et al.* 1994) or genomic DNA from the *Saccharomyces* Genome Deletion Project knockout strains (http://www-sequence.stanford.edu/group/yeast_deletion_project/deletions3.html). See Materials and Methods for details.

	Name	Genotype	Strain notes and deletion constructs
*MAT***a** to *MAT***α**	EAY745	wild-type	Derived from JKM161 (Δ*ho, HML***α***, MAT***a**, Δ*hmr::ADE1, ade1-100, leu2-3,112, lys5, trp1::hisG, ura3-52, ade3::GAL10::HO*)
	EAY853	*rad1*Δ	pWS1510 (*rad1*Δ*::URA3,* E. Friedberg)
	EAY969	*msh2*Δ	pEAI99 (*msh2*Δ*::TRP1,* this lab)
	EAY854	*msh3*Δ	pEAI88 (*msh3*Δ*::hisG-URA3-hisG,* this lab)
	EAY2087	*slx4*Δ	*slx4*Δ*::KANMX*
	EAY1788	*pol3-01*	YIpAM26 (*pol3-01::URA3,* from A. Sugino)
	EAY1332	*mus81*Δ	*mus81*Δ*::KANMX*
	EAY1730	*rad9*Δ	*rad9*Δ*::KANMX*
	EAY1968	*mad2*Δ	*mad2*Δ*::KANMX*
	EAY1562	*mms2*Δ	*mms2*Δ*::KANMX*
	EAY1778	*mph1*Δ	*mph1*Δ*::KANMX*
	EAY2125	*rad1*Δ*rad10*Δ	*rad10*Δ*::KANMX,* see above
	EAY2090	*rad1*Δ*slx4*Δ	see above
	EAY1803	*rad1*Δ*pol3-01*	see above
	EAY797	*rad1*Δ*mus81*Δ	see above
	EAY1726	*rad1*Δ*rad9*Δ	see above
	EAY1973	*rad1*Δ*mad2*Δ	see above
	EAY1725	*rad1*Δ*mms2*Δ	see above
	EAY1776	*rad1*Δ*mph1*Δ	see above
*MAT***a** to *MAT***a**	EAY744	wild-type	Derived from JKM160 *(*Δ*ho,* Δ*hml::ADE1, MAT***a***, HMR***a***, ade1-100, leu2-3,112, lys5, trp1::hisG, ura3-52, ade3::GAL10::HO*)
	EAY1356	*rad1*Δ	pWS1510 (*rad1*Δ*::URA3,* E. Friedberg)
	EAY2084	*slx4*Δ	*slx4*Δ*::KANMX*
*MAT***a**::*KANMX* to *MAT***α**	EAY1042	wild-type	Derived from JKM161, see Materials and Methods
	EAY1115	*rad1*Δ	pWS1510 (*rad1*Δ*::URA3,* E. Friedberg)
	EAY1040	*msh2*Δ	pEAI99 (*msh2*Δ*::TRP1*)
	EAY1118	*msh3*Δ	pEAI88 (*msh3*Δ*::hisG-URA3-hisG*)
	EAY1407	*rad51*Δ	pJH683 (*rad51*Δ*::URA3*, from J. Haber)
donorless	EAY742	wild-type	Derived from JKM139 (Δ*ho,* Δ*hml::ADE1, MAT***a**, Δ*hmr::ADE1, ade1-100, leu2-3,112, lys5, trp1::hisG, ura3-52, ade3::GAL10::HO*)

number of colonies arising from induced relative to uninduced cultures. At least four independent cultures were used for each strain (Table 2.2). Results are shown as the mean ± SEM, and were statistically analyzed using an unpaired two-tailed Student's T-test (http://www.physics.csbsju.edu/stats/t-test_bulk_form.html; see Results).

Mating type switching assay. To determine mating types, individual colonies from cell survival assays (20-40 per replicate) were crossed with *arg4 MAT***a** and *MAT***α** tester strains (EAY759 and EAY760; from N. Sugawara, Haber laboratory) and replica plated onto synthetic complete plates (Rose *et al.* 1990) lacking both arginine and lysine to select for diploids. The percentage of switched cells was determined for each cell survival experiment, and is shown in Table 2.2 as the mean ± SEM.

Southern blot analysis. Chromosomal DNA was isolated during time course experiments as described (Holmes and Haber 1999; Goldfarb and Alani 2004) following a 30-minute galactose induction. DNA was then digested with *Sty*I (New England Biolabs) for single nonhomology strains or *Ava*II, *Ban*I, and *Blp*I (New England Biolabs) for double nonhomology strains, and electrophoresed on 1% TAE-agarose gels with 1x TAE buffer. Southern blot transfer and hybridizations were performed essentially as described by the manufacturer (Amersham) using the Church and Gilbert method (1984).

All probes used for Southern blot analysis were amplified by PCR using EAY745 yeast genomic DNA and [^{32}P]-labeled using the NEBlot kit (New England Biolabs) according to the manufacturer's description. To probe *MAT*-specific bands, we radiolabeled a 638 bp PCR product beginning 67 bp downstream of the *MAT Z2* region using pJH364 forward and reverse primers (5'ACGAATTGGCTATACGGGAC and 5'GTCCAATCTGTGCACAATGAAG,

respectively, from the Haber lab). Efficient DSB formation was detected 30 minutes after galactose induction by Southern blot analysis (Figure 2.2). To visualize mating type switching in double nonhomology strains, probes were produced from a 277 bp PCR product amplified using primers AO585 (5'CTTAGCATCATTCTTTGTTCTTAT) and AO586 (5'CAAGAAGGCGAATAAGATAAAGA). Loading control probes for blots of the double nonhomology strains were created by amplifying a 235 bp PCR product with primers AO583 (5'CTCGTATTGGAGAAATAAGTTTTCGT) and AO584 (5'GGTAGAGTCTTATTGGCAAGATAG) (Appendix, Supplementary Fig. 2.6). Y**a**-specific probes (Appendix, Supplementary Fig. 2.7) were created by labeling a 539 bp PCR fragment made using primers AO1425 (5'GGACAACATGGATGATATTTGTAGTATGGCGG) and AO1049 (5'CTGTTGCGGAAAGCTGAAAC), both located within Y**a**. Blots were visualized using the Phosphor Imaging system and quantified using the ImageQuant program (Molecular Dynamics). Quantification of repair efficiency in Figure 2.2C was done as described previously (Wang *et al.* 2004), with product bands set relative to the first HO cut band and normalized relative to the *MAT* distal band in each lane. Y**a** loss was quantified by setting the Y**a** proximal band in each lane relative to the value at t = 0 (Appendix, Supplementary Fig. 2.7).

Chromatin immunoprecipitation. Samples from time course experiments were chromatin immunoprecipitated as described previously (Goldfarb and Alani 2004). Msh2-HA_4 was immunoprecipitated from yeast cell extracts using the 12CA5 monoclonal antibody, and expression of Msh2p-HA_4 was confirmed by Western blot (Goldfarb and Alani 2004; 2005). All strains used in the ChIP experiments contain a deletion of the *HMR***a** donor so that the *MAT***a** locus could be specifically amplified by

PCR. PCR reactions, electrophoresis conditions, and quantification were similar to those described in Evans *et al.* (2000), but with different primer sets. To detect sequences proximal to the DSB, a 267 bp fragment containing the Y**a** sequence was amplified from immunoprecipitated and input chromosomal DNA using AO1048 (5'TCACCCCAAGCACGGGCATT) and AO1049 (5'CTGTTGCGGAAAGCTGAAAC), which are adjacent to the HO recognition site (Figure 2.3). Samples were run on 1.5% TAE-agarose gels and bands were quantified relative to the maximal signal using Scion Image (Scion Corporation). Since the input signal decreases during mating type switching as the Y**a** sequence is removed, the data are presented as the amount of chromatin immunoprecipitated Y**a** PCR product detected after *HO* induction relative to that at t = 0. A 163 bp *CRY1* control band was also amplified from the chromosomal input DNA using primers AO1106 (5'CGCCAGAGTTACTGGTGGTATGAAGG) and AO1107 (5'GGAGTCTTGGTTCTAGTACCACCGG). The PCR signal was quantified within the linear range of detection, and ChIP was specific to both the epitope tag and formaldehyde crosslinking (Goldfarb and Alani 2004).

FACS analysis. Cells were collected at various times after HO induction as described above. Aliquots of cells were pelleted at the relevant time points, fixed in 70% ethanol, and stored at 4º C for up to 7 days. Cell samples were resuspended in 50 mM NaCitrate pH 7.4, sonicated briefly, and treated 1 hr with RNase A at 37º C, followed by a 1 hr treatment with Proteinase K at 37º C. DNA was stained with 1 nM final concentration of Sytox Green (Invitrogen), and samples were analyzed at the Cornell University Biomedical Sciences Flow Cytometry Core Laboratory (Ithaca, NY). Percentage of cells in G1, S, or G2/M phases was determined by gating according to 1n and 2*1n DNA content. A representative FACS profile for wild-type cells at t = 0

is shown in Figure 2.4B, with vertical gates for G1, S, and G2/M phases. Values shown in Figure 2.4A reflect the mean of three or more samples per time point ± SEM.

Pedigree analysis. Cells were induced for HO cleavage at *MAT* as described above. Following addition of glucose to the medium at t = 0.5 hrs, 15 µl of culture was dropped down the center of a YPD plate and single, unbudded cells were separated at one cm intervals under the light microscope using a microdissection needle. Cells were visualized beginning at t = 0.5 hrs, incubated at 30° C between manipulations, and monitored every 20-30 minutes until daughter cells were able to be separated from each other (t = ~4-10 hrs). Cells that did not complete cell division within 10 hours were not scored. The length of time required for completion of cell division is reported in Table 2.4 as the mean of all cells in each category ± SEM. Plates were incubated for 3 days at 30° C, and colonies were tested for mating type as described above. Cells were categorized by viability and mating type as shown in Table 2.3. Pairs of daughter cells scored as both unswitched were not included because we cannot rule out the failure to form a DSB in these cells. The number of cells present in dead cell clusters was also recorded, and is visualized in Supplementary Figure 2.8B (See Appendix). Photographs of representative cells (Appendix, Supplementary Figure 2.8) were taken under the light microscope using a Fuji FinePix S5000 digital camera.

Results

Decreased mating type switching in the absence of the Rad1-Rad10-Slx4 complex. Rad1-Rad10 and Msh2-Msh3 are proposed to act during mating type switching in steps involving the removal of a single 3' nonhomologous tail on the non-invading strand as depicted in Figure 2.1 (Holmes and Haber 1999; Pâques and Haber 1999, Figure 1). Previous work examining the role of Rad1-Rad10 during gene conversion primarily utilized plasmid-based assays in which DNA sequence on one or both sides of a DSB site contained nonhomologous sequence with respect to a donor sequence, also present on the plasmid (Sugawara *et al.* 1997; Colaiácovo *et al.* 1999). To examine the coordination of repair and checkpoint signaling factors during gene conversion on the chromosome, we analyzed roles for Rad1-Rad10-Slx4 and Msh2-Msh3 in mating type switching in *S. cerevisiae,* which is hypothesized to involve removal of a single 3' nonhomologous tail following the annealing step of SDSA (Figure 2.1A; Haber 1998; Pâques and Haber 1999; Ira *et al.* 2006).

Mating type switching was induced in *MAT***a** strains expressing HO endonuclease from the galactose-inducible *GAL10* promoter (Materials and Methods). As shown in Table 2.2, cell viability following DSB induction was high in wild-type (76% ± 3) but reduced in *rad1*Δ (59% ± 2; $p < 0.01$, Student's T-test) and *rad1*Δ*rad10*Δ double mutants (63% ± 1; data not shown). The decrease in cell viability was specific to strains induced for *MAT***a** to *MAT*α switching; no significant decrease was observed in strains induced for completely homologous switching (*MAT***a** to *MAT***a**) that does not involve 3' nonhomologous tails (Table 2.2). In addition, the percentage of surviving cells that had switched mating type was reduced in *rad1*Δ strains relative to wild-type (71% ± 3 vs. 86% ± 3, $p < 0.01$). This decrease in gene conversion may be due to an increase in repair of the break by nonhomologous

end joining to yield *MAT***a** cells, or could be indicative of aberrant repair or more disruptive NHEJ that disrupts the *MAT* locus and yields an "**a**-like faker" phenotype, since cells lacking a functional *MAT* locus phenocopy *MAT***a** by default (Strathern *et al.* 1981).

Recently, Flott *et al.* (2007) reported that the Slx4 protein forms a complex with Rad1-Rad10, and is critical for its 3' nonhomologous tail removal activity during repair by single-strand annealing (SSA). As predicted from this work, Slx4 also functions with Rad1-Rad10 in mating type switching. *slx4*Δ and *rad1*Δ*slx4*Δ mutants showed viability (57% ± 3 and 54% ± 2, respectively) and switching phenotypes (68% ± 4 and 69% ± 4, respectively) similar to *rad1*Δ strains (Table 2.2). In contrast, *msh2*Δ and *msh3*Δ strains displayed only a subtle decrease in viability (68% ± 4), and the percentage of switched cells was similar to wild-type (Table 2.2). Thus, Msh2-Msh3 appears nearly dispensable for nonhomologous tail removal during mating type switching, where the 3' tail is on the non-invading strand.

We hypothesized that the gene conversion observed in the absence of Rad1-Rad10-Slx4 could be facilitated by the action of redundant nucleases that remove the 3' Y**a** nonhomologous tail. However, disruption of Mus81-Mms4 or the Polymerase δ 3' to 5' proofreading activity did not have a significant effect on the viability of *rad1*Δ mutants following mating type switching (Table 2.2). Since mating type switching can occur in *rad1*Δ mutants, albeit less efficiently, it is likely that unknown nucleases or multiple redundant nucleases are able to remove 3' nonhomologous tails when Rad1-Rad10-Slx4 is absent. A recent study identified Saw1, a protein that interacts with Rad1-Rad10 and is thought to recruit Rad1-Rad10 to recombination intermediates (Li *et al.* 2008). It is possible that Saw1 may recruit other nucleases as well, allowing for completion of mating type switching in the absence of Rad1-Rad10-Slx4.

Table 2.2. Viability and mating type switching efficiency of wild-type and mutant strains. Percent cell survival (induced/uninduced) was determined by examining the viability of cells plated after a 30 minute induction of *HO* expression. Surviving cells were assayed to determine the percentage that had switched mating type from *MAT***a** to *MAT*α as described in the Materials and Methods. Data are presented as the mean ± SEM of at least 4 independent experiments. Asterisks indicate values significantly different from wild-type with $p < 0.01$, Students T-test. For one nonhomologous end (standard mating type switching), nonhomologous sequence (Y**a**) is present on only the proximal side of the DSB. For two homologous ends, strains were induced for *MAT***a** to *MAT***a** switching; thus, % switched is not applicable (n/a). For two nonhomologous ends, the indicated strains contain nonhomologous sequences on both sides of the DSB due to insertion of *KANMX* on the distal side of the break (see Figure 2.1B).

	% Survival	% Switched
One nonhomologous end (*MAT***a** to *MAT***α**)		
wild-type	76.1 ± 3.1	85.7 ± 2.7
*rad1*Δ	58.6 ± 2.1*	70.6 ± 2.8*
*slx4*Δ	57.1 ± 2.5*	67.6 ± 3.9*
*rad1*Δ*slx4*Δ	54.4 ± 2.2*	69.3 ± 4.3*
*msh2*Δ	67.6 ± 4.0	80.6 ± 2.5
*msh3*Δ	67.9 ± 2.0	81.5 ± 3.0
*mus81*Δ	72.6 ± 1.7	88.7 ± 5.9
pol3-01	65.1 ± 5.1	83.2 ± 3.4
*rad1*Δ*mus81*Δ	56.1 ± 3.8*	74.5 ± 7.5
*rad1*Δ*pol3-01*	55.6 ± 5.2*	70.6 ± 3.8*
*rad9*Δ	75.1 ± 3.1	82.5 ± 2.6
*rad1*Δ*rad9*Δ	56.3 ± 2.7*	74.7 ± 3.3
Two homologous ends (*MAT***a** to *MAT***a**)		
wild-type	99.7 ± 2.2	n/a
*rad1*Δ	95.3 ± 4.5	n/a
*slx4*Δ	93.8 ± 4.3	n/a
Two nonhomologous ends (*MAT***a**::*KANMX* to *MAT***α**)		
wild-type	62.7 ± 3.7	72.8 ± 7.4
*rad1*Δ	26.8 ± 1.2*	0.8 ± 0.8*
*msh2*Δ	23.5 ± 2.9*	9.8 ± 2.3*
*msh3*Δ	29.9 ± 1.7*	10.0 ± 3.1*
*rad51*Δ	25.2 ± 2.7*	0.0 ± 0.0*

Southern blot analysis was used to examine product formation in wild-type and *rad1*Δ strains during mating type switching (Figure 2.2). Efficient DSB formation was observed at the *MAT* locus within 30 minutes of induction in all strains and products were detectable by one hour post-induction in wild-type, consistent with previous studies (White and Haber 1990; Colaiácovo *et al.* 1999). *rad1*Δ mutants displayed a ~10% reduction in product formation relative to wild-type. This result is much more subtle than that seen in an analysis of *MAT***α** *to MAT***a** switching in G1-arrested *rad1*Δ cells (Holmes and Haber 1999), but is consistent with the viability data presented above. The defects exhibited by mutants lacking Rad1-Rad10-Slx4 are more apparent in the pedigree, FACS, and chromatin immunoprecipitation studies described below, and may indicate that, while *MAT***α** product formation appears to be only mildly reduced in *rad1*Δ mutants, the gene conversion at *MAT* might be associated with BIR, aberrant recombination, or disrupted signaling.

Previous studies have shown a strict requirement for both Rad1-Rad10 and Msh2-Msh3 when both sides of a DSB contain nonhomologous sequence (Sugawara *et al.* 1997; Colaiácovo *et al.* 1999). In repair of such breaks, a 3' nonhomologous tail must be removed during the strand invasion step in order for repair DNA synthesis to proceed, in addition to 3' nonhomologous removal at the later synthesis-dependent annealing step (Figure 2.1B). To confirm that Rad1-Rad10 and Msh2-Msh3 are required for removing 3' nonhomologous tails on the invading strand during chromosomal mating type switching, we inserted the *KANMX* sequence on the distal side of the HO cut site at the *MAT* locus (Figure 2.1B). In wild-type strains containing the *KANMX* insertion, gene conversion was delayed but completed with little loss of viability (Table 2.2; Appendix, Supplemental Fig. 2.6). Consistent with previous studies, we found that both Rad1-Rad10 and Msh2-Msh3 complexes were required for gene conversion involving two 3' nonhomologous tails. No gene conversion product

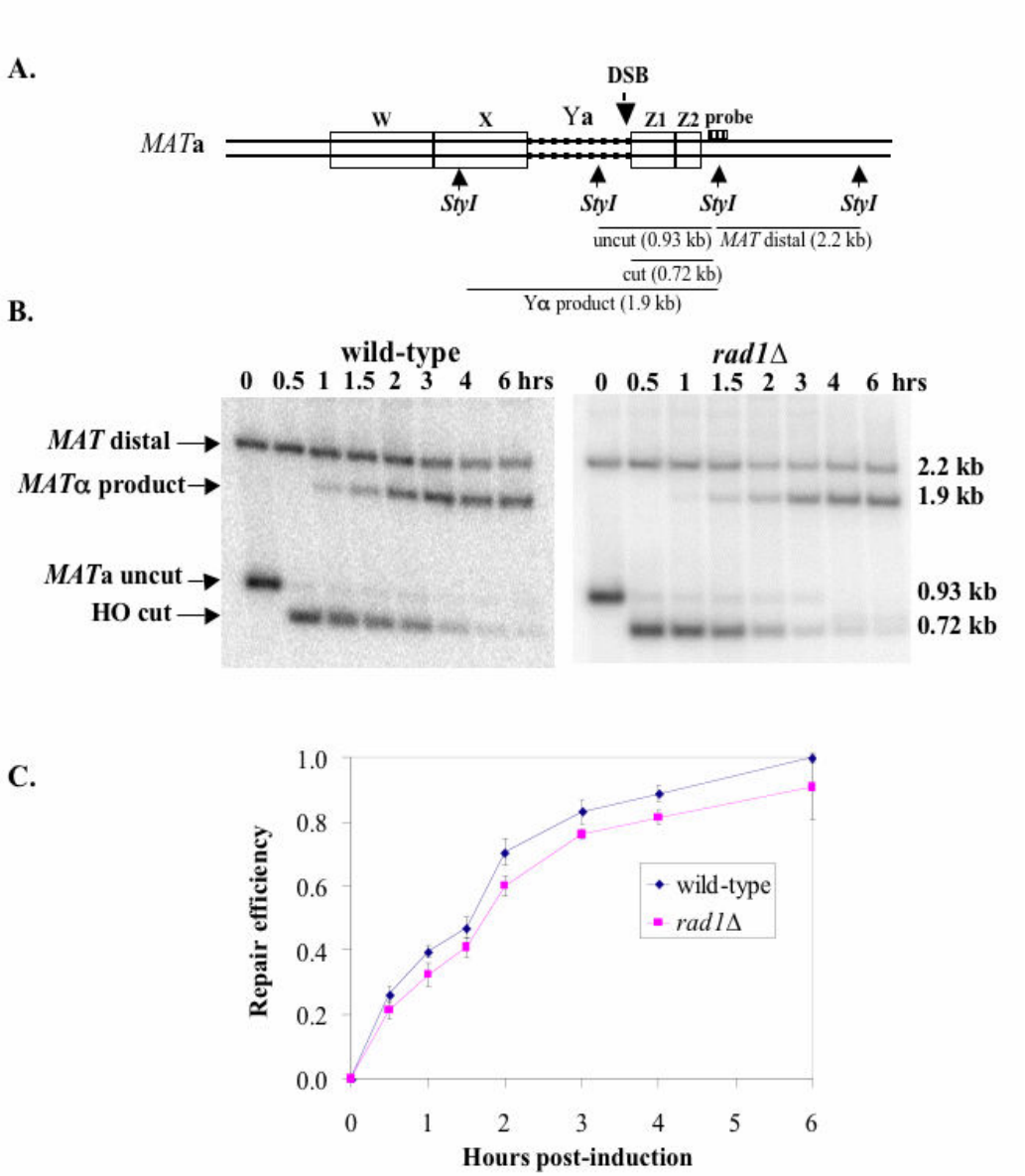

Figure 2.2. Southern blot analysis of mating type switching in wild-type and *rad1*Δ strains. A. Diagram of the *MAT* locus showing the restriction sites used for Southern blot analysis, expected fragment lengths, and location of the probes used for detection of mating type switching. B. Analysis of digested DNA for wild-type and *rad1*Δ mutants induced for mating type switching. Experiments were performed at least three times, with representative time courses shown. C. Quantification of repair efficiency as described in Materials and Methods. Experiments in this figure were performed by both A. M. Lyndaker and T. Goldfarb.

was detected by Southern blot in *rad1*Δ and *msh3*Δ mutants (Appendix, Supplementary Fig. 2.6), and the viability and switching efficiency of *rad1*Δ mutants was comparable to that of *rad51*Δ mutants completely defective in gene conversion, as shown in Table 2.2 (Sugawara *et al.* 1995). While the viability of *msh2*Δ and *msh3*Δ strains was equivalent to that of *rad1*Δ mutants, both *msh* mutants exhibited a greater percentage of switched cells (10%; Table 2.2), consistent with the idea that Msh2-Msh3 plays a supporting role that may be less critical than the role of Rad1-Rad10. The residual viability in *rad1*Δ*, msh2*Δ*, msh3*Δ, and *rad51*Δ strains is likely due to nonhomologous end-joining, as seen in strains completely lacking donor sequences (Moore and Haber 1996).

Prolonged Msh2 localization to the DSB in *rad1*Δ mutants. Because Rad1-Rad10 is predicted to remove 3' nonhomologous tails on the non-invading strand following the annealing step (Fig. 2.1), we reasoned that *rad1*Δ mutants would exhibit a delay in removal of the 3' Y**a** sequence. Using Y**a**-specific probes, we were unable to detect a difference in the loss of Y**a** between wild-type and *rad1*Δ strains (Supplementary Fig. 2.7). Detection of any delay is confounded by the fact that the initial resection of the break should lead to loss of the 5' strand of Y**a** with similar kinetics in both strains. Thus, we additionally performed chromatin immunoprecipitation using HA-tagged Msh2, α-HA antibody, and PCR primers located within the Y**a** sequence as described previously (Goldfarb and Alani 2004). Our lab previously showed that the Msh2 protein localizes rapidly to DSBs (Evans *et al.* 2000).

As shown in Fig. 2.3, Msh2 localized immediately to the *MAT* locus following DSB formation, peaked at one hour post-induction, and then decreased, consistent with the kinetics of product formation shown in Figure 2.2 and a role for Msh2-Msh3 in DSB repair. A similar pattern was seen using primers specific to the X-Y**a**

junction; however, peak levels were achieved at a slightly later time point (1.5 hrs, data not shown). While the input signal is lost over time due to conversion to *MAT***α**, the input signal at the unrelated *CRY1* locus was constant throughout the time course.

In *rad1*Δ mutants, Msh2 localized to *MAT* following DSB formation, but in contrast to wild-type, Msh2 remained near the break for approximately 3 hours (Fig. 2.3). We observed a similar Msh2 localization pattern for *donorless* mutants unable to complete mating type switching, where the 3' ends are thought to be stable despite a complete inability to perform homologous repair (Vaze *et al.* 2002; Aylon *et al.* 2003). Msh2 localization was also prolonged at the X-Y**a** junction in *rad1*Δ compared to wild-type (data not shown). Thus, while we were unable to detect a delay in loss of the Y**a** sequence in *rad1*Δ mutants, the prolonged presence of Msh2 at the break during mating type switching suggests that at least a subset of *rad1*Δ mutants contain recombination intermediates at later time points.

rad1*Δ mutants induced for mating type switching exhibit G2/M arrest.** The above observations encouraged us to examine the cell cycle progression of *rad1*Δ mutants during mating type switching. Mutants lacking both donor sequences have previously been shown to exhibit a prolonged G2/M cell cycle delay due to an inability to repair the DSB by homologous recombination (Toczyski *et al.* 1997; Lee *et al.* 1998). We used FACS analysis to measure the DNA content of wild-type, *rad1*Δ, and *donorless* mutants following DSB induction. As shown in Figure 2.4, wild-type strains showed little variation in the percentage of cells in G1, S, or G2/M phase during the course of mating type switching. Consistent with the known arrest phenotype, the majority of cells from a strain lacking both *HMLα** and *HMR***a** sequences (*donorless*) were present in G2/M phase at 4 hrs (83.5% ± 1.5) and 6 hrs post-induction (71.8% ± 3.9). *rad1*Δ strains showed a significant increase in the percentage of G2/M cells at 2 hrs (58.3%

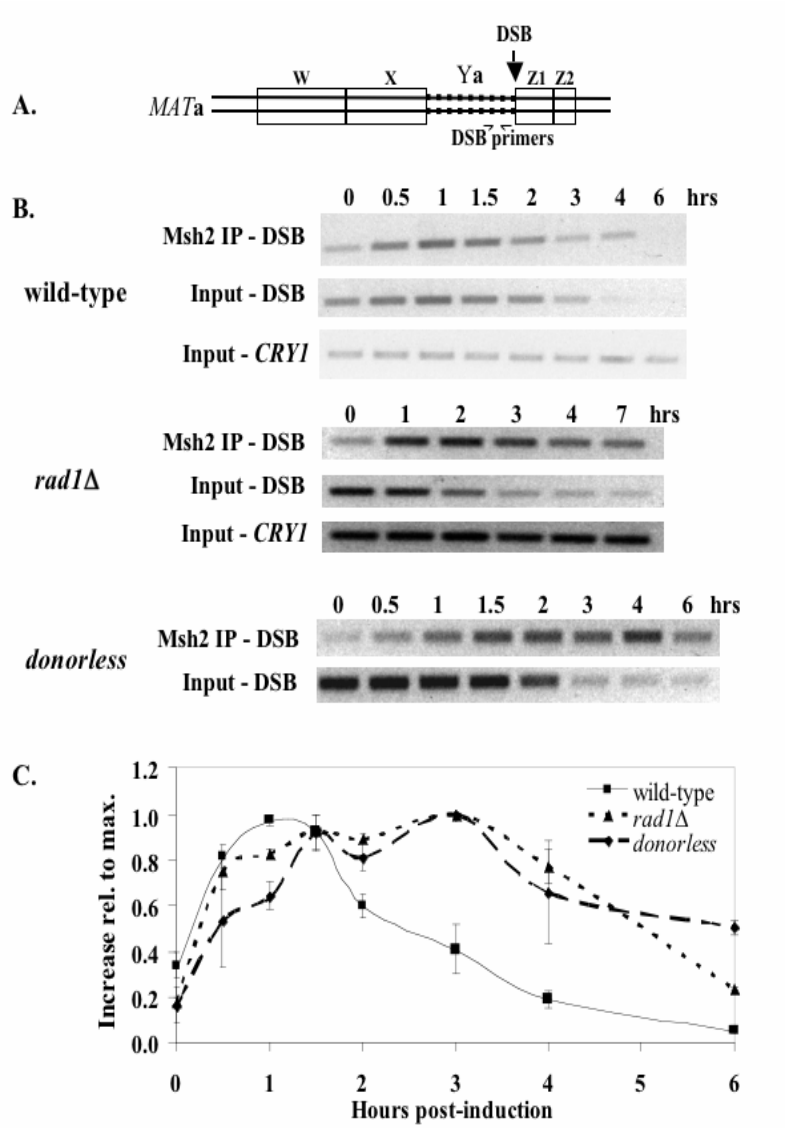

Figure 2.3. Msh2 localization to the DSB in wild-type, *rad1*Δ, and *donorless* mutants. A. Location of primers used for semi-quantitative PCR following Msh2 chromatin immunoprecipitation. B. Chromatin immunoprecipitation and PCR detection of Msh2 localization to *MAT* during mating type switching in wild-type, *rad1*Δ, and *donorless* mutants. Since the Y**a** sequence is removed during mating type switching, the input signal is also shown using primers to an unrelated locus (*CRY1)*. C. For each time point, the Msh2 ChIP signal was set relative to the t = 0 signal, with the maximum signal for each time course set as 1.0 to compare relative the timing of Msh2 localization. Each data point represents the mean of 3-4 experiments ± SEM. This experiment was performed by T. Goldfarb.

± 4.0) and 4 hrs post-induction (65.1% ± 1.6) relative to wild-type (41.9% ± 1.5 and 30.1% ± 3.3, respectively; $p < 0.01$), but returned to wild-type levels by 6 hrs, suggesting that the absence of Rad1-Rad10 leads to a G2/M arrest that is both shorter and earlier than observed in *donorless* mutants. This is consistent with gene conversion occurring in *rad1*Δ mutants, though inefficiently, in contrast to *donorless* mutants which can only survive by nonhomologous end joining (Moore and Haber 1996).

Mutants lacking Rad1-Rad10-Slx4 show unique viability profiles in pedigree analysis following mating type switching. To further analyze the viability and cell cycle phenotypes seen in *rad1*Δ and *slx4*Δ mutants during mating type switching, we performed pedigree experiments in which single, unbudded (G1) cells were isolated after DSB formation and monitored through the cell cycle. Daughter cells were separated following the first cell division (Materials and Methods). Cells that grew into colonies were subsequently assayed for mating type. As shown in Table 2.3, 96% of wild-type cells yielded two viable daughter cells that had both switched mating type. In contrast, only 38% of *rad1*Δ mutants formed two switched colonies, and of the remaining cells, 32% formed one switched colony and one dead cell cluster and 28% formed two dead cell clusters. *slx4*Δ and *rad1*Δ*slx4*Δ strains exhibited phenotypes similar to *rad1*Δ mutants (Table 2.3). No such decrease in viability was seen in these strains in the absence of the DSB, nor in *rad1*Δ strains induced for completely homologous *MAT***a** to *MAT***a** switching (Table 2.3B; data not shown). The "one switched, one dead" category is particularly intriguing, since repair and death arise from the same induced cell, and it is unique to cells undergoing gene conversion. Thus, the effect of the *rad1*Δ and *slx4*Δ mutations on mating type switching is much

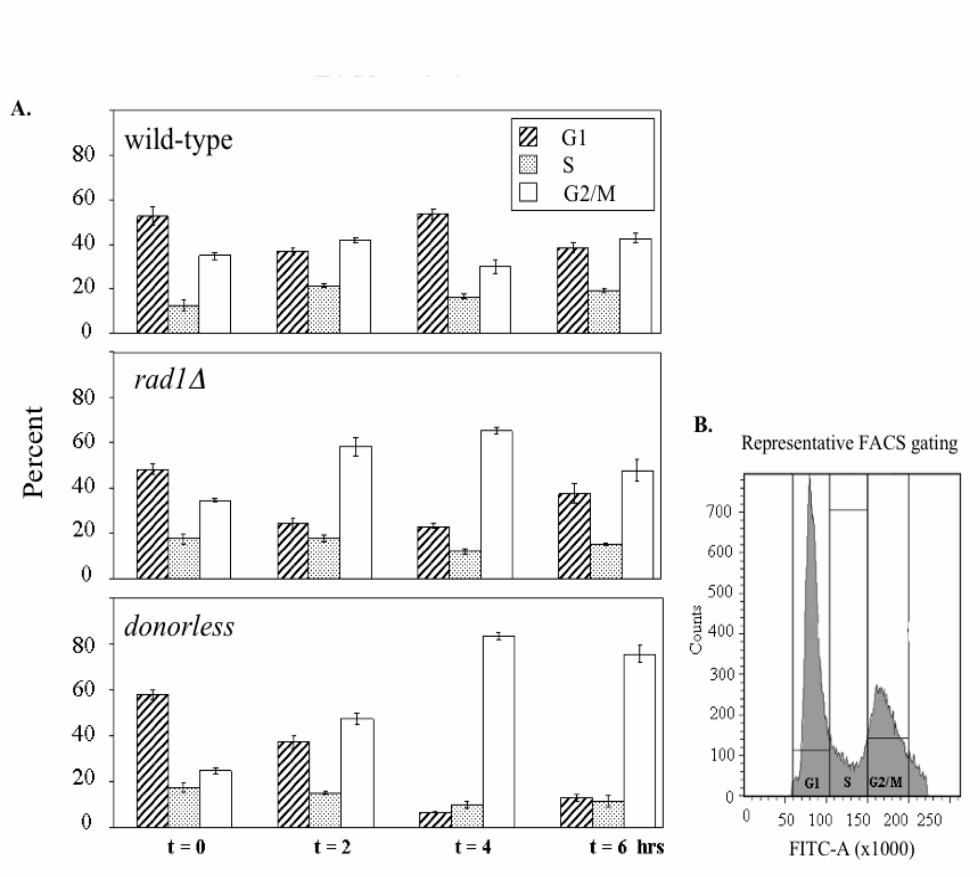

Figure 2.4. FACS analysis of cells undergoing mating type switching. A. Bar graphs of the percentage of cells in either G1, S, or G2/M phases of the cell cycle at 0, 2, 4, and 6 hours following induction of mating type switching in wild-type, *rad1*Δ, and *donorless* strains (average of at least three experiments ± SEM). See Materials and Methods for details. The increase in the percentage of G2/M cells in *rad1*Δ mutants relative to wild-type is statistically significant ($p < 0.01$ at t =2 and t = 4 hrs, Student's T-test). B. Representative FACS profile for wild-type cells at t = 0, with vertical gates separating the 1n (G1) and 2n (G2/M) DNA content.

Table 2.3. Pedigree analysis of wild-type and mutants (A) induced for mating type switching or (B) mock-induced. Following induction of mating type switching in liquid culture, single cells were separated on YPD medium under the light microscope using a microdissection needle. Cells were monitored at regular intervals, and daughter cells were separated apart after completion of the first cell division. Cells that formed colonies were tested for mating type as described in Materials and Methods. The number of cells (N) tested for each strain is shown. For cells induced for mating type switching, "% other" includes pairs of daughter cells scored as "one unswitched and one dead" or "one unswitched and one switched." Pairs of daughter cells scored as both unswitched were not included because we cannot rule out the failure to form a DSB in these cells. For the uninduced experiments, viability is shown for cells mock-induced with water.

A. Induced	2 switched	1 switched, 1 dead	2 dead	other	N
wild-type	96%	4%	0%	0%	81
donorless	0%	0%	96%	4%	51
*rad1*Δ	38%	32%	28%	2%	97
*slx4*Δ	51%	33%	12%	4%	49
*rad1*Δ*slx4*Δ	29%	44%	19%	8%	59
*msh2*Δ	78%	7%	11%	4%	81
*rad9*Δ	82%	12%	6%	0%	90
*mad2*Δ	84%	10%	4%	2%	49
*rad1*Δ*rad9*Δ	20%	41%	39%	0%	102
*rad1*Δ*mad2*Δ	33%	43%	15%	8%	60
*mms2*Δ	79%	7%	12%	2%	58
*mph1*Δ	69%	16%	10%	5%	70
*rad1*Δ*mms2*Δ	19%	54%	26%	1%	99
*rad1*Δ*mph1*Δ	28%	38%	30%	3%	81

B. Uninduced	2 alive	1 alive, 1 dead	2 dead	N
wild-type	99%	0%	1%	91
donorless	100%	0%	0%	41
*rad1*Δ	98%	2%	0%	119
*slx4*Δ	94%	3%	3%	36
*rad1*Δ*slx4*Δ	94%	5%	2%	62
*msh2*Δ	84%	9%	7%	76
*rad9*Δ	98%	0%	2%	51
*mad2*Δ	100%	0%	0%	26
*rad1*Δ*rad9*Δ	89%	3%	8%	72
*rad1*Δ*mad2*Δ	91%	2%	8%	53
*mms2*Δ	90%	7%	3%	71
*mph1*Δ	100%	0%	0%	52
*rad1*Δ*mms2*Δ	87%	9%	4%	92
*rad1*Δ*mph1*Δ	96%	3%	1%	75

more severe than was apparent in liquid culture assays, where asynchronous cells were induced for mating type switching and the fate of daughter cells could not be assessed. We also measured the length of the first cell division following DSB induction during the pedigree experiments. As shown in Table 2.4, completion of cell division was delayed by three hours in *rad1*Δ mutants compared to wild-type ($p < 0.01$, Student's T-test), consistent with the FACS analysis presented above (Figure 2.4). Strains lacking donor sequences exhibited an even longer delay (10 ± 0.2 hours to complete division compared to 4.5 ± 0.1 hours in wild-type; Table 2.4). During this extended period, *rad1*Δ and *donorless* cells displayed a large-budded morphology suggestive of G2/M arrest (Appendix, Supplementary Fig. 2.8A).

After completion of the first cell division, approximately 45% of *rad1*Δ cells failed to form colonies in the pedigree analysis (the dead cells from both the "two dead" and "one switched, one dead" categories), but divided several times before forming dead cell clusters (average of 8 ± 1 cells; Appendix, Supplementary Fig. 2.8B). This phenotype is consistent with the phenomenon of break adaptation, in which cells exit the cell cycle arrest despite the continued presence of unrepaired DNA, and differs from the death seen in cells undergoing DSB repair that fail to exit a G2/M arrest (Toczyski *et al.* 1997; Lee *et al.* 1998; Pellicioli *et al.* 2001; Lee *et al.* 2003). This adaptation phenotype is consistent with a significant proportion of *rad1*Δ cells induced for mating type switching being unable to complete repair of the break. Inviable cells from *donorless* strains exhibited a more severe phenotype following checkpoint exit and died with one large-budded cell or two cells (adaptation for only one cycle) as documented previously (Lee *et al.* 1998), most likely due to the presence of more extensive DNA damage due to prolonged 5' to 3' resection.

Consistent with the cell survival assays described above, *msh2*Δ and *msh3*Δ mutations had little effect on viability during mating type switching in pedigree

experiments. Viability was reduced equally in both the induced and uninduced states, with ~80% of *msh2*Δ cells forming two viable colonies, ~10% forming one alive and one dead cell cluster, and ~10% with two inviable cells (Table 2.3). Thus, the absence of *MSH2* confers a general decrease in viability that appears unrelated to the formation of an HO-induced DSB. A more subtle decrease in viability (5%) was observed for strains lacking *SLX4*.

G2/M delay in *rad1*Δ mutants is dependent upon both the DNA damage response and the spindle checkpoint. To test whether the cell division delay observed in *rad1*Δ mutants was mediated by the DNA damage checkpoint, we measured cell viability and cell cycle duration in *rad1*Δ mutants defective for the Rad9-dependent DNA damage response. *rad1*Δ*rad9*Δ double mutants exhibited cell cycle lengths comparable to wild-type and *rad9*Δ mutant cells (~5 hours, Table 2.4), in contrast to ~8 hours for *rad1*Δ mutants. Thus, the G2/M cell cycle arrest exhibited by *rad1*Δ mutants is dependent upon *RAD9*, presumably via Rad9-mediated activation of the DNA damage response (Harrison and Haber 2006). Elimination of the arrest had very little effect on the viability of *rad1*Δ mutants (Tables 2.2 and 2.3), pointing to an inability of the DNA damage response to promote repair.

Slx4 forms a complex with Rad1-Rad10 that is critical for 3' nonhomologous tail removal during repair by single-strand annealing (Flott *et al.* 2007). As shown in Table 2.3, *slx4*Δ and *rad1*Δ*slx4*Δ mutants exhibited significantly shorter cell cycle delays than *rad1*Δ single mutants (1 hr vs. 2 hrs for "two switched," and 2 hrs vs. 3.5 hrs for "one switched, one dead"). It is not surprising that the absence of Slx4 reduces the delay, since Slx4 is a known target of the Mec1 and Tel1 checkpoint kinases, requires checkpoint-dependent phosphorylation for Rad1-dependent SSA, and has

Table 2.4. Average length of cell cycle in cells undergoing mating type switching. Cell cycle duration was determined during pedigree analysis (see Table 2.3 and Materials and Methods), and is shown as the mean length of time required for division (hrs) ± SEM. "n/a" denotes categories containing less than 10% of cells, and thus cell cycle lengths are not reported. * Denotes statistical significance from wild-type with $p < 0.01$; values were compared to wild-type "uninduced" or "two switched" as appropriate.

	Average time required for cell division (hrs)			
	uninduced	**two switched**	**one switched, one dead**	**two dead**
wild-type	4.5 ± 0.2	4.5 ± 0.1	n/a	n/a
donorless	4.9 ± 0.2	n/a	n/a	10 ± 0.2*
*rad1*Δ	4.7 ± 0.2	7.0 ± 0.3*	8.4 ± 0.3*	8.2 ± 0.4*
*slx4*Δ	4.7 ± 0.1	5.8 ± 0.2*	7.0 ± 0.4*	8.6 ± 0.4*
*rad1*Δ*slx4*Δ	4.5 ± 0.1	5.5 ± 0.4*	6.8 ± 0.4*	9.0 ± 0.4*
*msh2*Δ	4.3 ± 0.1	5.6 ± 0.1*	n/a	6.5 ± 0.3*
*rad9*Δ	4.9 ± 0.1	4.5 ± 0.1	4.8 ± 0.2	n/a
*mad2*Δ	4.9 ± 0.2	4.9 ± 0.2	4.2 ± 0.3	n/a
*rad1*Δ*rad9*Δ	5.2 ± 0.1*	4.8 ± 0.2	4.8 ± 0.1	5.3 ± 0.1
*rad1*Δ*mad2*Δ	5.5 ± 0.2*	5.6 ± 0.3*	6.7 ± 0.3*	6.3 ± 0.2*
*mms2*Δ	4.5 ± 0.1	5.1 ± 0.1*	n/a	6.1 ± 0.5*
*mph1*Δ	4.5 ± 0.1	4.7 ± 0.1	5.9 ± 0.6*	6.5 ± 0.8*
*rad1*Δ*mms2*Δ	4.5 ± 0.1	5.8 ± 0.3*	6.4 ± 0.1*	6.3 ± 0.1*
*rad1*Δ*mph1*Δ	5.3 ± 0.1*	6.2 ± 0.3*	8.1 ± 0.3*	8.3 ± 0.3*

been shown to regulate checkpoint-dependent processes (Flott and Rouse 2005; Roberts *et al.* 2006; Flott *et al.* 2007). The fact that *slx4*Δ mutants exhibit *rad1*Δ-like phenotypes, but with shorter cell cycle delays, is additional evidence that Slx4 provides a link between the 3' end-processing machinery and the DNA damage checkpoint.

Several studies have suggested a link between the DNA damage response and the spindle checkpoint (Aylon and Kupiec 2003; Kim and Burke 2008). We hypothesized that the cell death in *rad1*Δ mutants was due to aberrant repair involving gross chromosomal changes which might activate the spindle checkpoint, and thus tested whether the G2/M arrest in these mutants required *MAD2*. As shown in Tables 2.3 and 2.4, *mad2*Δ mutants induced for mating type switching had only slightly decreased viability and displayed cell cycle lengths similar to wild-type. However, *rad1*Δ*mad2*Δ double mutants exhibited reduced cell cycle delays relative to *rad1*Δ mutants (Table 2.4). Cells in the "two dead" and "one switched, one dead" pedigree categories took ~6.5 hours to divide in *rad1*Δ*mad2*Δ mutants, compared to ~8 hours in *rad1*Δ single mutants ($p < 0.015$). Interestingly, *rad1*Δ mutants that formed two switched colonies exhibited arrests that appeared fully *MAD2*-dependent, unlike the partially *MAD2*-dependent arrests described above (Table 2.4). These results suggest that although gene conversion occurs without loss of viability for cells in the "two switched" class, repair is inefficient and disruptive to the assembly or function of the mitotic spindle. The variety of arrest phenotypes in *rad1*Δ mutants further distinguishes the pedigree viability categories from each other, and suggests that different defects or modes of repair operate in these subsets of cells.

Unique viability pattern in pedigree analysis is consistent with replication-mediated repair. Approximately one third of *rad1*Δ mutant cells divided to form

both one switched and one dead colony in the pedigree analysis (Table 2.3). We hypothesized that these cells may complete gene conversion by replicating partially-repaired intermediates containing one intact switched strand, and one unrepaired strand (Figure 2.5; Kang and Symington 2000). To test such a model, we examined whether post-replicative lesion bypass repair pathways were involved in completing gene conversion during mating type switching. We focused on *MMS2*- and *MPH1*-dependent repair pathways, mutations in which cause defects in the error-free bypass pathways involving fork reversal and recombinational replication restart, respectively (Torres-Ramos *et al.* 2002; Schürer *et al.* 2004; Watts 2006). Both *mms2*Δ and *mph1*Δ mutants displayed decreased viability in the wild-type background during mating type switching. As shown in Table 2.3, the percentage of cells in the "two switched" category for pedigree analysis was reduced to 79% in *mms2*Δ and 69% in *mph1*Δ mutants compared to 96% in wild-type. *mms2*Δ mutants also displayed a slight reduction in viability in the absence of the DSB (Table 2.3), but viability was further decreased for cells induced for switching. Both of these mutants had an increased proportion of cells in both the "one switched, one dead" and "two dead" categories, indicating that replicative lesion bypass pathways play a role in the completion of gene conversion during mating type switching.

To test whether the error-free lesion bypass pathways are responsible for repair in the absence of Rad1-Rad10-Slx4, we analyzed both *rad1*Δ*mms2*Δ and *rad1*Δ *mph1*Δ double mutants in pedigree experiments. *rad1*Δ*mms2*Δ double mutants exhibited a decrease in the percentage of "two switched" cells from 38% to 19%, and this decrease was directly correlated with an increase in the "one switched, one dead" category; however, no change in the percentage of "two dead" cells was seen for either *rad1*Δ*mms2*Δ or *rad1*Δ*mph1*Δ relative to *rad1*Δ single mutants, suggesting that death

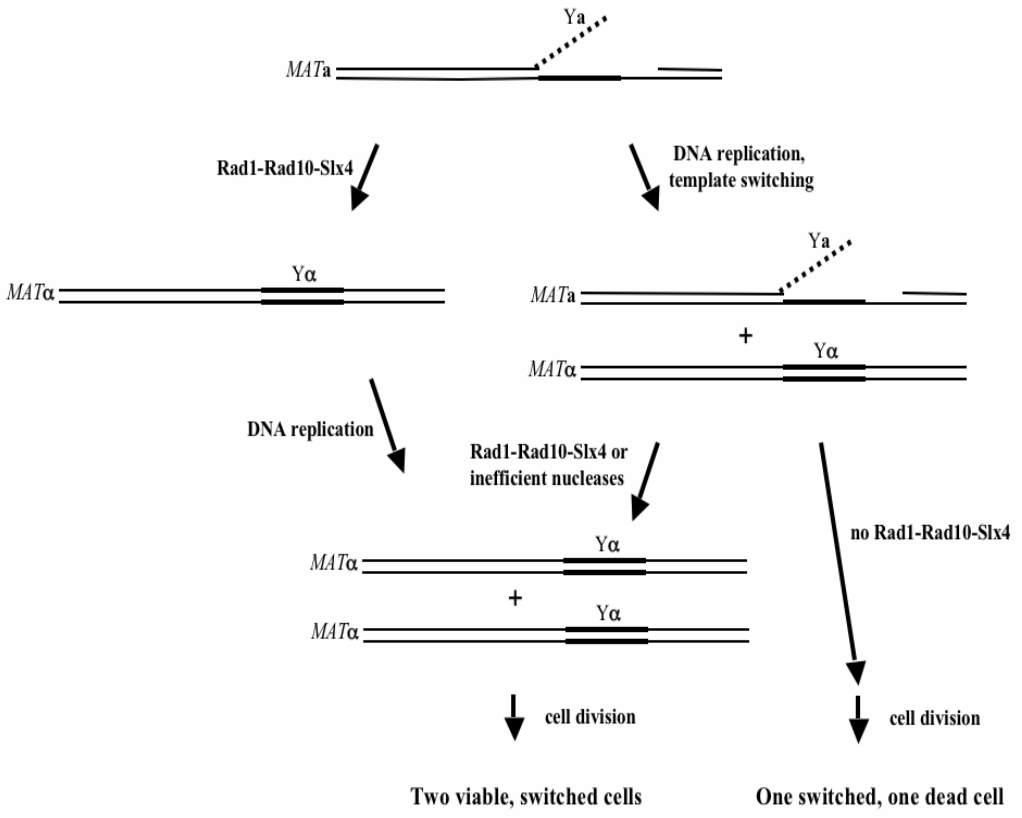

Figure 2.5. Model for mating type switching facilitated by DNA replication. We propose that mating type switching can be mediated by ongoing DNA replication. DSB formation, 5' to 3' resection, strand invasion, synthesis, and repair of the invading strand occur as shown in Figure 2.1 and predicted by SDSA models. The partially-repaired recombination intermediate shown at the top of the figure containing a single-stranded break can then be acted on by either the DNA replication machinery or the Rad1-Rad10-Slx4 complex. In the presence of Rad1-Rad10-Slx4, the 3' Y**a** nonhomologous tail is removed efficiently, either prior to, during, or following DNA replication, and once DNA replication has been completed, the cell can divide to produce two viable cells of the switched mating type. In the absence of Rad1-Rad10-Slx4, mating type switching products are produced largely by replication of the partially-repaired recombination intermediate to yield either one switched and one dead daughter cell, or, after the action of inefficient nucleases, two viable switched daughters.

of these cells occurs by a separate mechanism. The *mph1*Δ mutation appeared roughly epistatic to *rad1*Δ in this assay, with very little decrease in viability relative to *rad1*Δ.

The *mms2*Δ mutation reduced the length of cell cycle delay in *rad1*Δ mutants, from 2 hrs to 1 hr for the "two switched" cells and from 3.5 to 2 hrs for the "one switched, one dead" and "two dead" categories (Table 2.4). *rad1*Δ*mph1*Δ double mutants exhibited a similar decrease in length of arrest for "two switched" cells, but not for dying cells. Thus, it is tempting to speculate that checkpoint signaling in *rad1*Δ mutants might be initiated or enhanced by the collision of a replication fork with recombination intermediates (see Discussion). Together, the above phenotypes suggest a role for post-replicative lesion bypass repair in the completion of gene conversion during mating type switching.

Discussion

In this study, we investigated the requirements for the Rad1-Rad10, Slx4, and Msh2-Msh3 factors in 3' nonhomologous tail removal during gene conversion at the chromosomal *MAT* locus. Rad1-Rad10 and Msh2-Msh3 have been proposed to act during mating type switching in steps involving the removal of a single 3' nonhomologous tail on the non-invading strand, primarily based on their roles in 3' nonhomologous tail removal during single-strand annealing and in plasmid-based assays (Haber 1998; Pâques and Haber 1999; Figure 2.1). As described above, mating type switching in *rad1*Δ mutants led to a checkpoint-dependent G2/M cell cycle delay and decreased viability. In the absence of functional Rad1-Rad10-Slx4, cells displayed a unique viability profile consistent with a model in which gene conversion can be facilitated by replication of partially-repaired recombination intermediates.

Msh2-Msh3, however, played only a subtle role in such repair, in contrast to its critical role in DSB repair involving two 3' nonhomologous tails.

Previous work in the Symington lab proposed that replication of partially-repaired recombination intermediates might bypass the requirement for Rad1-Rad10-dependent 3' nonhomologous tail removal in a plasmid retention assay (Kang and Symington 2000). We extend this model to explain the unique viability pattern observed in *rad1*Δ and *slx4*Δ mutants in pedigree experiments, where a third of cells divide to produce both repaired (switched) and dead daughter cells (Table 2.3, Figure 2.5). In this model, mutants lacking Rad1-Rad10-Slx4 initiate repair normally, but encounter difficulty after annealing of the repaired invading strand back to the *MAT* locus. In the absence of 3' nonhomologous tail removal activity, the remaining broken strand is unable to prime repair DNA synthesis to complete gene conversion. If, instead, DNA replication occurs prior to 3' nonhomologous tail removal, template switching could produce both an intact chromosome of the switched mating type and a broken chromosome. Segregation of these chromosomes to daughter cells could then lead to the "one switched, one dead" phenotype (Table 2.3), whereas repair of the broken chromosome by an inefficient nuclease could yield two viable, switched cells as is seen in wild-type (Figure 2.5). In further support of replication-mediated repair, another study found that mating type switching in G1-arrested cells led to a much more severe reduction in product formation (37% product formation at 5 hrs) in *rad1*Δ mutants than is seen in this study in cycling cells, with product formation in *rad1*Δ mutants only reduced to ~90% of wild-type at 4 hrs (Holmes and Haber 1999). Additional evidence for this model of replication-mediated recombination is discussed below.

We show that mating type switching in mutants lacking Rad1-Rad10 or Slx4 induces a G2/M cell cycle delay involving both the DNA damage and spindle

checkpoints (Table 2.4). Interestingly, the arrest phenotypes correlated with the viability phenotypes observed by pedigree analysis. Those cells that produced two viable, switched daughter cells exhibited shorter cell cycle delays (~2 hours) that were completely dependent upon the spindle checkpoint, whereas cells that produced two dead cell clusters or one switched colony and one dead cell cluster exhibited longer arrests (~3.5 hours) and were only partially dependent on the spindle checkpoint (Table 2.4).

Several studies have indicated potential links between the DNA damage and spindle checkpoints (Garber and Rine 2002; Kim and Burke 2008). It is not surprising that DNA damage that triggers the damage checkpoint might also impede the correct attachment and formation of tension between the chromosomes and the mitotic spindle. It was recently demonstrated that the spindle assembly checkpoint arrests cells in response to MMS-induced DNA damage in a Mec1- and Tel1-dependent manner, independent of a functional kinetochore (Kim and Burke 2008). We show here that in response to a single DSB at the *MAT* locus, the DNA damage response factor Rad9 appears to be required for both the DNA damage and spindle checkpoints, as *rad1*Δ*rad9*Δ mutants exhibit no G2/M arrest and *rad1*Δ*mad2*Δ mutants exhibit shorter arrests than *rad1*Δ single mutants (1 hr vs. ~3.5 hrs; Table 2.5). In contrast to other studies, we do not see residual G2/M arrest in *rad9*Δ mutants in these experiments (Aylon and Kupiec 2003; Kim and Burke 2008).

Previous work has shown that the length of G2/M arrest in response to DNA damage correlates with the amount of single-stranded DNA present (Lee *et al.* 1998). Our results are consistent with this, as *rad1*Δ mutants exhibit shorter arrests relative to *donorless* strains; *rad1*Δ mutants are able to initiate strand invasion, whereas *donorless* mutants accumulate ssDNA because they cannot initiate repair (Lee *et al.* 1998). We also observed distinct adaptation phenotypes in the *rad1*Δ and *donorless*

strains. *donorless* strains adapted for one cell cycle only and died at the next G2/M transition, whereas *rad1*Δ mutants exhibited a classical break adaptation phenotype and died as 8-cell clusters (See appendix, Supplementary Fig. 2.8). Since dying *rad1*Δ mutants exhibit a cell cycle delay followed by adaptation, it is possible that repair in this subset of the population occurs by break-induced replication (BIR) or by crossing over. BIR initiated from the *MAT* locus by strand invasion into *HML***α** would lead to loss of half of Chromosome *III* including the centromere, and crossing over would similarly create an intrachromosomal deletion. Such repair would be expected to be associated with delayed product formation as well as a DNA damage checkpoint- and spindle checkpoint-dependent G2/M arrest, as seen in our pedigree analysis (McEachern and Haber 2006).

The fact that Msh2 localization to the *MAT* locus is prolonged in *rad1*Δ and *donorless* mutants implies the presence of unrepaired recombination intermediates several hours after DSB formation. While this is expected in *donorless* mutants that lack homologous donor sequences, the fact that *rad1*Δ mutants exhibit *donorless*-like Msh2 localization highlights that repair occurs aberrantly in these cells. The prolonged presence of Msh2 in both mutants is also consistent with the fact that these mutants have an activated DNA damage response, and may indicate a role for Msh2 in this checkpoint.

In contrast to proposed models of mating type switching and to gene conversion involving a 3' nonhomologous tail on the invading strand, Rad1-Rad10-dependent 3' nonhomologous tail removal on the second, non-invading strand appears to be independent of Msh2-Msh3. Viability was only slightly reduced in *msh2*Δ mutants undergoing mating type switching, and *msh2*Δ mutants did not exhibit the unique viability pattern characteristic of *rad1*Δ and *slx4*Δ mutants in pedigree analysis. In this way, Rad1-Rad10-dependent 3' nonhomologous tail removal during mating

type switching is analogous to its role in cleavage of 3' DNA-bound Top1 lesions, which is also Msh2-Msh3-independent (Vance and Wilson 2002).

There are at least two separate error-free lesion bypass pathways in *S. cerevisiae,* one pathway involving the homologous recombination machinery and the Mph1 helicase, and the Rad5-Mms2-Ubc13 branch of the Rad6-Rad18 pathway that is thought to regress replication forks and promote bypass of lesions by template switching (Torres-Ramos *et al.* 2002; Schürer *et al.* 2004; Watts 2006; Blastyák *et al.* 2007). We observed that both of these pathways contributed to the viability and cell cycle phenotypes of cells undergoing mating type switching. Mph1 is a helicase that is known to be in the Rad52 epistasis group, but it is thought to function in recombinational restart of stalled replication forks (Schürer *et al.* 2004; Prakash *et al.* 2005). The fact that the *rad1*Δ and *mph1*Δ mutations were mostly epistatic suggests that Mph1-dependent fork restart is hindered by the presence of the nonhomologous 3' end that remains in *rad1*Δ mutants, though it is unclear why this might be. We cannot rule out that the role of the Mph1 helicase during gene conversion is separate from its role in replication fork restart.

Replicative lesion bypass pathway choice depends on whether the lesion (in this case, a 3' nonhomologous tail followed by a significant single-stranded gap) is on the leading strand versus the lagging strand. Presumably, priming of the next Okazaki fragment on the lagging strand could bypass such a lesion and allow replication to proceed without employing specialized fork restart machinery, which may explain why the decreased viability in *mms2*Δ and *mph1*Δ mutants is relatively subtle. In addition, there is *in vitro* evidence using bacterial proteins that re-priming of DNA synthesis can occur on the leading strand (Heller and Marians 2006). The nearest replication origin to the *MAT* locus is located on the centromere-proximal side, approximately 2.5 kb from the Y region at *MAT* (www.oridb.org,

www.yeastgenome.org), so it may be more likely that the 3' Y**a** tail is replicated by lagging rather than leading strand synthesis.

Mating type switching does not require progression through S-phase, since efficient gene conversion is detected in G2-arrested cells, though *MAT* switching in G1-arrested cells is severely reduced due to the absence of CDK1 (Cdc28) activation (Holmes and Haber 1999; Ira *et al.* 2004; Wang *et al.* 2004). However, DNA replication may contribute to mating type switching by priming DNA synthesis across the top strand of the partially-repaired intermediate pictured in Figure 2.5, bypassing the need to use the cleaved 3' end as a primer for repair synthesis and relaxing the dependence on Rad1-Rad10-Slx4. Indeed, mutations in the genes encoding Polymerase α-primase or Rad27 were shown to greatly reduce mating type switching in G1-arrested cells (Holmes and Haber 1999). While it was later shown that these lagging-strand synthesis factors were dispensable for mating type switching in G2-arrested cells (Wang *et al*. 2004), it is possible that cycling cells might utilize lagging-strand synthesis in addition to specialized lesion bypass pathways to promote efficient completion of gene conversion. Moreover, recent work has shown that endonuclease-induced DSBs formed during G1 are recognized by the RPA subunit Rfa1 only after cells have entered S-phase, and that formation of Rad52 foci following IR treatment required release of G1-arrested cells into S-phase (Barlow *et al.* 2008). Further studies will be necessary in order to parse out the interplay between DNA replication and repair of DSBs by homologous recombination.

In summary, we conclude that gene conversion intermediates containing 3' nonhomologous tails are principally processed by Rad1-Rad10-Slx4, even on the non-invading strand, and we propose that repair is aided by concurrent DNA replication and its associated post-replicative lesion bypass pathways.

Acknowledgments

We thank James Haber and Neal Sugawara for strains, plasmids, advice and comments on the manuscript, Lorraine Symington and John Rouse for insights regarding the *rad1*Δ and *slx4*Δ mutant phenotypes, Aaron Plys for construction of *mms2*Δ and *pol3-01* strains, and members of the Alani lab for comments on the manuscript. A.M.L. was supported by a GAANN fellowship from the U. S. Department of Education and a National Institutes of Health Training Grant, T.G. by a Natural Sciences and Engineering Research Council of Canada PGSB Award, and E.A. by National Institutes of Health grant GM53085. Experiments shown in Figures 2.2 and 2.3 were performed by T. Goldfarb.

REFERENCES

Aylon, Y. and M. Kupiec (2003). "The checkpoint protein Rad24 of *Saccharomyces cerevisiae* is involved in processing double-strand break ends and in recombination partner choice." Mol. Cell. Biol. **23**(18): 6585-6596.

Aylon, Y., B. Liefshitz, G. Bitan-Banin and M. Kupiec (2003). "Molecular dissection of mitotic recombination in the yeast *Saccharomyces cerevisiae*." Mol. Cell. Biol. **23**(4): 1403-1417.

Bardwell, A., L. Bardwell, A. Tomkinson and E. Friedberg (1994). "Specific cleavage of model recombination and repair intermediates by the yeast Rad1-Rad10 DNA endonuclease." Science **265**(5181): 2082-5.

Barlow, J. H., M. Lisby and R. Rothstein (2008). "Differential regulation of the cellular response to DNA double-strand breaks in G1." Mol. Cell **30**(1): 73-85.

Blastyák, A., L. Pintér, I. Unk*, et al.* (2007). "Yeast Rad5 protein required for postreplication repair has a DNA helicase activity specific for replication fork regression." Mol. Cell **28**(1): 167-175.

Church, G. M. and W. Gilbert (1984). "Genomic sequencing." Proc. Natl. Acad. Sci. **81**(7): 1991-5.

Colaiácovo, M. P., F. Pâques and J. E. Haber (1999). "Removal of one nonhomologous DNA end during gene conversion by a *RAD1*- and *MSH2*-independent pathway." Genetics **151**: 1409-23.

Evans, E., N. Sugawara, J. E. Haber and E. Alani (2000). "The *Saccharomyces cerevisiae* Msh2 mismatch repair protein localizes to recombination intermediates *in vivo*." Mol. Cell **5**: 189-99.

Fishman-Lobell, J. and J. Haber (1992). "Removal of nonhomologous DNA ends in double-strand break recombination: the role of the yeast ultraviolet repair gene *RAD1*." Science **258**(5081): 480-4.

Flott, S., C. Alabert, G. W. Toh*, et al.* (2007). "Phosphorylation of Slx4 by Mec1 and Tel1 regulates the single-strand annealing mode of DNA repair in budding yeast." Mol. Cell. Biol. **27**(18): 6433-45.

Flott, S. and J. Rouse (2005). "Slx4 becomes phosphorylated after DNA damage in a Mec1/Tel1-dependent manner and is required for repair of DNA alkylation damage." Biochem. J. **391**(2): 325-33.

Garber, P. M. and J. Rine (2002). "Overlapping roles of the spindle assembly and DNA damage checkpoints in the cell-cycle response to altered chromosomes in *Saccharomyces cerevisiae*." Genetics **161**(2): 521-534.

Gietz, R. D. and R. H. Schiestl (1991). "Applications of high efficiency lithium acetate transformation of intact yeast cells using single-stranded nucleic acids as carrier." Yeast **7**: 253-263.

Goldfarb, T. and E. Alani (2004). Chromatin immunoprecipitation to investigate protein-DNA interactions during genetic recombination. Genetic recombination: Reviews and protocols. A. S. Waldman. Totowa, NJ, Humana Press Inc. **262:** 223-37.

Goldfarb, T. and E. Alani (2005). "Distinct roles for the *Saccharomyces cerevisiae* mismatch repair proteins in heteroduplex rejection, mismatch repair and nonhomologous tail removal." Genetics **169**: 563-74.

Guzder, S. N., C. Torres-Ramos, R. E. Johnson*, et al.* (2004). "Requirement of yeast Rad1-Rad10 nuclease for the removal of 3'-blocked termini from DNA strand breaks induced by reactive oxygen species." Genes Dev. **18**(18): 2283-91.

Haber, J. E. (1998). "Mating-type gene switching in *Saccharomyces cerevisiae*." Annu. Rev. Genet. **32**: 561-99.

Harrison, J. C. and J. E. Haber (2006). "Surviving the breakup: The DNA damage checkpoint." Annu. Rev. Genet. **40**(1): 209-235.

Heller, R. C. and K. J. Marians (2006). "Replication fork reactivation downstream of a blocked nascent leading strand." Nature **439**: 557-562.

Holmes, A. and J. E. Haber (1999). "Physical monitoring of HO-induced homologous recombination." Meth. Mol. Biol. **113**: 403-15.

Holmes, A. M. and J. E. Haber (1999). "Double-strand break repair in yeast requires both leading and lagging strand DNA polymerases." Cell **96**: 415-24.

Ira, G., A. Pellicioli, A. Balijja*, et al.* (2004). "DNA end resection, homologous recombination and DNA damage checkpoint activation require *CDK1*." Nature **431**(7011): 1011-1017.

Ira, G., D. Satory and J. E. Haber (2006). "Conservative inheritance of newly synthesized DNA in double-strand break-induced gene conversion." Mol. Cell. Biol. **26**(24): 9424-9.

Ivanov, E. and J. Haber (1995). "*RAD1* and *RAD10*, but not other excision repair genes, are required for double-strand break-induced recombination in *Saccharomyces cerevisiae*." Mol. Cell. Biol. **15**(4): 2245-51.

Kang, L. E. and L. S. Symington (2000). "Aberrant double-strand break repair in *rad51* mutants of *Saccharomyces cerevisiae*." Mol. Cell. Biol. **20**(24): 9162-72.

Kim, E. M. and D. J. Burke (2008). "DNA damage activates the SAC in an ATM/ATR-dependent manner, independently of the kinetochore." PLoS Genet. **4**(2): e1000015.

Kirkpatrick, D. T. and T. D. Petes (1997). "Repair of DNA loops involves DNA-mismatch and nucleotide-excision repair proteins." Nature **387**: 929-31.

Klar, A. J. S. and J. N. Strathern (1984). "Resolution of recombination intermediates generated during yeast mating type switching." Nature **310**: 744-8.

Lee, S. E., J. K. Moore, A. Holmes*, et al.* (1998). "*Saccharomyces* Ku70, Mre11/Rad50, and RPA proteins regulate adaptation to G2/M arrest after DNA damage." Cell **94**: 399-409.

Lee, S. E., A. Pellicioli, M. B. Vaze*, et al.* (2003). "Yeast Rad52 and Rad51 recombination proteins define a second pathway of DNA damage assessment in response to a single double-strand break." Mol. Cell. Biol. **23**(23): 8913-23.

Li, F., J. Dong, X. Pan*, et al.* (2008). "Microarray-based genetic screen defines *SAW1*, a gene required for Rad1/Rad10-dependent processing of recombination intermediates." Mol. Cell **30**(3): 325-35.

McEachern, M. J. and J. E. Haber (2006). "Break-induced replication and recombinational telomere elongation in yeast." Annu. Rev. Biochem. **75**(1): 111-35.

McGill, C., B. Shafer and J. Strathern (1989). "Coconversion of flanking sequences with homothallic switching." Cell **57**: 459-67.

McWhir, J., J. Selfridge, D. J. Harrison*, et al.* (1993). "Mice with DNA repair gene (*ERCC-1*) deficiency have elevated levels of p53, liver nuclear abnormalities and die before weaning." Nat. Genet. **5**(3): 217-24.

Moore, J. and J. Haber (1996). "Cell cycle and genetic requirements of two pathways of nonhomologous end-joining repair of double-strand breaks in *Saccharomyces cerevisiae*." Mol. Cell. Biol. **16**(5): 2164-2173.

Pâques, F. and J. E. Haber (1997). "Two pathways for removal of nonhomologous DNA ends during double-strand break repair in *Saccharomyces cerevisiae*." Mol. Cell. Biol. **17**(11): 6765-71.

Pâques, F. and J. E. Haber (1999). "Multiple pathways of recombination induced by double-strand breaks in *Saccharomyces cerevisiae*." Microbiol. Mol. Biol. Rev. **63**(2): 349-404.

Pellicioli, A., S. E. Lee, C. Lucca*, et al.* (2001). "Regulation of *Saccharomyces* Rad53 checkpoint kinase during adaptation from DNA damage-induced G2/M arrest." Mol. Cell **7**: 293-300.

Pellicioli, A., C. Lucca, G. Liberi*, et al.* (1999). "Activation of Rad53 kinase in response to DNA damage and its effect in modulating phosphorylation of the lagging strand DNA polymerase." EMBO J. **18**: 6561-72.

Prakash, R., L. Krejci, S. Van Komen, *et al.* (2005). "*Saccharomyces cerevisiae MPH1* gene, required for homologous recombination-mediated mutation avoidance, encodes a 3' to 5' DNA helicase." J. Biol. Chem. **280**(9): 7854-7860.

Roberts, T. M., M. S. Kobor, S. A. Bastin-Shanower, *et al.* (2006). "Slx4 regulates DNA damage checkpoint-dependent phosphorylation of the BRCT domain protein Rtt107/Esc4." Mol. Biol. Cell **17**(1): 539-48.

Rose, M. D., F. Winston and P. Hieter (1990). Methods in yeast genetics, Cold Spring Harbor Laboratory Press.

Sandell, L. L. and V. A. Zakian (1993). "Loss of a yeast telomere: Arrest, recovery, and chromosome loss." Cell **75**: 729-39.

Saparbaev, M., L. Prakash and S. Prakash (1996). "Requirement of mismatch repair genes *MSH2* and *MSH3* in the *RAD1-RAD10* pathway of mitotic recombination in *Saccharomyces cerevisiae*." Genetics **142**(3): 727-36.

Schürer, K. A., C. Rudolph, H. D. Ulrich and W. Kramer (2004). "Yeast *MPH1* gene functions in an error-free DNA damage bypass pathway that requires genes from homologous recombination, but not from postreplicative repair." Genetics **166**(4): 1673-1686.

Strathern, J., J. Hicks and I. Herskowitz (1981). "Control of cell type in yeast by the mating type locus." J. Mol. Biol. **147**(3): 357-372.

Sugawara, N., E. L. Ivanov, J. Fishman-Lobell, *et al.* (1995). "DNA structure-dependent requirements for yeast *RAD* genes in gene conversion." Nature **373**: 84-6.

Sugawara, N., F. Pâques, M. Colaiacovo and J. E. Haber (1997). "Role of *Saccharomyces cerevisiae* Msh2 and Msh3 repair proteins in double-strand break-induced recombination." Proc. Natl. Acad. Sci. USA **94**: 9214-9.

Sung, P., P. Reynolds, L. Prakash and S. Prakash (1993). "Purification and characterization of the *Saccharomyces cerevisiae* RAD1/RAD10 endonuclease." J. Biol. Chem. **268**(35): 26391-26399.

Surtees, J. A. and E. Alani (2006). "Mismatch repair factor MSH2-MSH3 binds and alters the conformation of branched DNA structures predicted to form during genetic recombination." J. Mol. Biol. **360**(3): 523-6.

Toczyski, D. P., D. J. Galgoczy and L. H. Hartwell (1997). "*CDC5* and CKII control adaptation to the yeast DNA damage checkpoint." Cell **90**: 1097-1106.

Torres-Ramos, C. A., S. Prakash and L. Prakash (2002). "Requirement of *RAD5* and *MMS2* for postreplication repair of UV-damaged DNA in *Saccharomyces cerevisiae*." Mol. Cell. Biol. **22**(7): 2419-2426.

Vance, J. R. and T. E. Wilson (2002). "Yeast Tdp1 and Rad1-Rad10 function as redundant pathways for repairing Top1 replicative damage." Proc. Natl. Acad. Sci. USA **99**(21): 13669-13674.

Vaze, M. B., A. Pellicioli, S. E. Lee*, et al.* (2002). "Recovery from checkpoint-mediated arrest after repair of a double-strand break requires Srs2 helicase." Mol. Cell **10**(2): 373-85.

Wach, A., A. Brachat, R. Pohlmann and P. Philippsen (1994). "New heterologous modules for classical or PCR-based gene disruptions in *Saccharomyces cerevisiae*." Yeast **10**(13): 1793-808.

Wang, X., G. Ira, J. A. Tercero*, et al.* (2004). "Role of DNA replication proteins in double-strand break-induced recombination in *Saccharomyces cerevisiae*." Mol. Cell. Biol. **24**(16): 6891-6899.

Watts, F. Z. (2006). "Sumoylation of PCNA: Wrestling with recombination at stalled replication forks." DNA Repair **5**(3): 399-403.

Weeda, G., I. Donker, J. de Wit*, et al.* (1997). "Disruption of mouse *ERCC1* results in a novel repair syndrome with growth failure, nuclear abnormalities and senescence." Curr. Biol. **7**(6): 427-39.

White, C. I. and J. E. Haber (1990). "Intermediates of recombination during mating type switching in *Saccharomyces cerevisiae*." EMBO J. **9**(3): 663-673.

Wu, X. and J. Haber (1995). "*MAT***a** donor preference in yeast mating-type switching: activation of a large chromosomal region for recombination." Genes Dev. **9**(15): 1922-1932.

Wu, X. and J. E. Haber (1996). "A 700 bp *cis*-acting region controls mating-type dependent recombination along the entire left arm of yeast chromosome III." Cell **87**: 277-85.

Wu, X., C. Wu and J. E. Haber (1997). "Rules of donor preference in *Saccharomyces* mating-type gene switching revealed by a competition assay involving two types of recombination." Genetics **147**(2): 399-407.

http://www.oridb.org

http://www.yeastgenome.org

http://www-sequence.stanford.edu/group/yeast_deletion_project/deletions3.html

http://www.physics.csbsju.edu/stats/t-test_bulk_form.html

CHAPTER 3

Rad1-Rad10-dependent 3' nonhomologous tail removal: Unpublished results and future directions

Introduction

As described in the previous chapters, the Rad1-Rad10 endonuclease plays an important role in removing 3' nonhomologous tails during many homologous recombination events. It is still unclear whether other nucleases are redundant with Rad1-Rad10 for this function during gene conversion involving 3' tails longer than 30 nt, since the most likely candidates, Mus81-Mms4 and the Polymerase δ proofreading activity, do not appear to play a role. It also remains to be seen which factors besides Mms2 and Mph1 might be involved in replication-mediated gene conversion, as proposed in the model in Chapter 2 (Figure 2.5; Lyndaker *et al.* 2008), and whether such a mechanism involves the S-phase checkpoint machinery. The experiments reported in this chapter attempt to address these issues, and the resulting findings both support and extend those in Chapter 2 regarding the roles of Rad1-Rad10 and associated factors in 3' nonhomologous tail removal. Lingering questions and future avenues to pursue are discussed.

Materials and methods

Strains. For *tdp1*Δ, *sae2*Δ, and *mrc1*Δ experiments, the *KANMX* gene deletion was amplified from the Yeast Deletion Collection strain by PCR and transformed into

parent strain EAY745 (wild-type) or EAY853 (*rad1*Δ) to create EAY2138 (*tdp1*Δ), EAY2140 (*rad1*Δ*tdp1*Δ), EAY2127 (*sae2*Δ), EAY2128 (*rad1*Δ*sae2*Δ), and EAY1781 (*mrc1*Δ). All other yeast strains are described in Chapter 2 (Lyndaker *et al.* 2008).

Media and culture conditions. Yeast were grown under the conditions described in Lyndaker *et al.* (2008).

Cell survival assays. Cell survival following galactose-induced mating-type switching was determined as follows. Log-phase asynchronous cultures grown in YP-lactate media (2% w/v lactate) were induced with galactose (US Biological, 2% w/v final concentration) or mock induced with water. After a 30 minute induction, glucose (US Biological, 2% w/v) was added to suppress *HO* expression. Both induced and uninduced cultures were diluted 10,000-fold and plated in triplicate onto YPD plates before and 2 hours after induction. [*It was later realized that some strains (*rad1*Δ mutants single nonhomology strains, all the double nonhomology strains, and *donorless* mutant) exhibit cell cycle delays, and that waiting to plate cells at two hours post-induction in cell viability experiments was misleading given the differences in cell cycle progression. Thus, unlike these experiments, cell survival experiments reported in Chapter 2 (Lyndaker *et al.* 2008) were plated immediately after the 30-minute galactose induction and more accurately reflect the cell viability.] Survival was determined by taking a ratio of the number of colonies growing on plates containing induced cells compared to those from uninduced cells (Table 3.1).

Mating type switching assay. Mating types were determined both before and after galactose-induced mating type switching as described in Lyndaker *et al.* (2008) by crossing to tester strains FY23/EAY235 (*MAT***a** *ura3-52 leu2*Δ*1 trp1*Δ*63*) and

FY86/EAY236 (*MAT*α *ura3-52 leu2*Δ*1 his3*Δ*200*) and selecting for diploids. The percentage of switched cells was determined for each experiment and is shown in Table 3.1 as the mean ± SEM.

Western blotting. Cell samples (10 mls) were collected during a timecourse of galactose-inducible mating type switching and lysed by glass bead lysis in Hepes-based buffer. Lysates were boiled for 10 minutes in 1x sample buffer containing β-mercaptoethanol and SDS and run on 8% SDS-PAGE gels in 1x Tris glycine electrode buffer with SDS at 30 mA after stacking in 5% SDS-PAGE stacking gel at 15 mA. Gels were transferred to nitrocellulose membranes (BioRad Trans-blot transfer medium) in transfer buffer (25 mM Tris pH 7.5, 192 mM glycine, 20% methanol) for one hour at 42 mA using a BioRad Trans-blot SD semi-dry transfer cell (BioRad Laboratories, Inc.). Membranes were blocked overnight in TBST (1x Tris-buffered saline with 0.1% Tween 80, (Sigma)) plus 4% dry milk or 4% ECL Advance blocking agent (Amersham, GE Healthcare). Blocked membranes were incubated with yC-19 goat polyclonal anti-Rad53 antibody (1:2000 dilution; Santa Cruz Biotechnology, Inc.) in TBST + 2% blocking agent for one hour, washed with TBST, and incubated 1-2 hours with donkey anti-goat IgG-HRP secondary antibody (1:5000 dilution; Santa Cruz Biotechnology, Inc.) in TBST + 1% blocking agent. Detection was carried out using either ECL Plus or ECL Advance (Amersham, GE Healthcare).

Preparation of genomic DNA by spheroplasting. For most PCR-based assays and previous Southern blots, genomic DNA was prepared by glass bead lysis as described in Lyndaker *et al.* 2008. In some preliminary PCR-based experiments, DNA was prepared by spheroplasting to potentially preserve any intact single-stranded DNA. Spheroplasting was carried out essentially as described in the Lichten lab protocol (T.

Goldfarb, personal communication) and Allers and Lichten (2000). 30 mls of mid-log phase cells were harvested at the relevant time point before or after induction of mating type switching and treated with 8 mls of 50% glycerol, 0.5% sodium azide on ice. Cells were pelleted, washed with 10 mls of ice cold spheroplasting buffer pH 7.5 (1 M sorbitol, 50 mM Potassium phosphate pH 7.0, 10 mM EDTA pH 8.0) plus 20% glycerol, resuspended in 1 ml of the same buffer, and frozen. Cells were thawed on ice, pelleted, resuspended in 500 µl of spheroplasting buffer containing zymolase, 1% (v/v) β-mercaptoethanol, and 20% glycerol, and incubated at 37° C for 5 minutes. Samples were pelleted and resuspended in 500 µl stop solution (100 mM NaCl, 50 mM Tris pH 8.0, 50 mM EDTA pH 8.0), followed by the addition of 1 volume of equilibrated phenol. Samples were rocked for 15 minutes, spun, treated with 24:1 chloroform:isoamyl alcohol, and spun down. Nucleic acids were precipitated by addition of 1/10 volume of 5 M NaCl and 1 volume of isopropanol and pellets dried overnight. Pellets were resuspended in 300 µl TE containing 0.05 µg/ml RNase A and incubated 30 minutes at 37° C. DNA was precipitated by adding 30 µl of 3 M NaAcetate and 200 µl isopropanol, and pellets were washed with 70% ethanol. Before use, DNA was resuspended in 50 µl TE.

BND-cellulose enrichment for ssDNA. The protocol for enrichment of ssDNA from genomic DNA preparations using BND-cellulose was obtained from Dr. Joel Huberman (Roswell Park Cancer Institute, SUNY Buffalo, Buffalo, NY) and is adapted from Gamper *et al.* (1985). Benzoylated napthoylated DEAE (BND)-cellulose beads (Sigma) were suspended in 10 mls of 5 M NaCl, pelleted gently at 2000 rpm, and washed 4 times in 10 mls 5 M NaCl. The bead pellet was washed once in 3 volumes of water, then washed twice with 10 mls 1.0 M NET (1.0 M NaCl, 10

mM Tris pH 8.0, 1 mM EDTA pH 8.0), resuspended in 10 mls of the same buffer, and stored at 4° C until use.

Genomic DNA (prepared by glass bead lysis or spheroplasting, resuspended in TE) was brought up to 1.0 M NaCl using 5 M NaCl in twice the volume of the BND-cellulose packed volume. DNA samples were added to BND-cellulose, mixed gently for 30 seconds, and centrifuged gently for 20 seconds. Beads were washed 5 times with one volume of 1.0 M NET and 6 times with 1.0 M NET + 1.6% caffeine. Caffeine wash fractions were pooled and centrifuged at 10,000 rpm in Eppendorf tubes for 10 minutes to pellet the BND-cellulose. An equal volume of isopropanol was added to each tube, and samples were incubated at -20° C for at least 30 minutes. Chilled samples were then spun at 10,000 rpm for 90 minutes at 4° C. Pellets were dried in the fume hood and resuspended in 150 µl TE. DNA was treated with 1/9 volume 4 M NaAcetate and 2.2 volumes of ethanol and incubated at -20° C for at least 30 minutes. Samples were spun 30 minutes at 4° C, rinsed with 70% ethanol, and when dry, resuspended in 20 µl TE.

The resulting genomic DNA enriched for ssDNA was used as a template in PCR reactions with primer sets (AO1048 + AO1049) and (AO1042 + AO1044), and samples were run on 1.5% agarose gels, stained with EtBr (Figure 3.2), and quantified using ImageJ.

PCR detection of strand invasion intermediates. Genomic DNA samples prepared for Southern blot experiments (Lyndaker *et al.* 2008) were used as substrates in a PCR-based strand invasion assay (White and Haber 1990). PCR reactions were performed as described previously in 50 µl reactions each containing 0.1 µl of genomic DNA and primers pA (AO1056) and pB (AO1057) (White and Haber 1990).

All PCR samples were electrophoresed in 1.5% TAE-agarose gels and bands were quantified relative to the *CRY1* control product using Image J (see Figure 3.3).

Chromatin immunoprecipitation and semi-quantitative PCR. Samples from mating type switching time course experiments were chromatin immunoprecipitated as described previously (Goldfarb and Alani 2004). Msh2-HA_4 was immunoprecipitated from yeast cell extracts using the α-HA 12CA5 monoclonal antibody. All strains used in ChIP experiments contained a deletion of the *HMR***a** donor so that the *MAT***a** locus could be specifically amplified by PCR. This deletion still allows mating type switching from *MAT***a** to *MAT*α since intact *HML*α is available. PCR reactions, electrophoresis conditions, and quantification were similar to those described in Evans *et al.* (2000), but with different primers. To detect sequences adjacent to the DSB, a 267 bp fragment containing Y**a** sequence was amplified with primers AO1048 (5'TCACCCCAAGCACGGGCATT) and AO1049 (5'CTGTTGCGGAAAGCTGAAAC). The loading control *CRY1* locus is situated far from the *MAT* locus on Chromosome *III*. Samples were run on 1.5% TAE-agarose gels and bands were quantified relative to the zero time point using Scion Image (Figure 3.4).

Results and Discussion

Rad53 is not appreciably phosphorylated in *rad1*Δ mutants during mating type switching. Yeast lacking the Rad1-Rad10 endonuclease exhibit a G2/M cell cycle delay in response to a single DSB at the mating type locus, as described in Chapter 2 (Lyndaker *et al.* 2008). This checkpoint response is dependent upon both *RAD9* and *MAD2*, factors critical for the DNA damage checkpoint and spindle checkpoint,

respectively, suggesting that the cell cycle is delayed due to unrepaired or aberrantly repaired DNA. To test whether this cell cycle arrest is associated with activation of the Rad53 branch of the DNA damage checkpoint, we analyzed the phosphorylation status of Rad53 by Western blotting. In *donorless* mutant strains, which arrest in G2/M due to an inability to repair the DSB at the mating type locus by gene conversion, several higher mobility Rad53 species were observed (see Figure 3.1), indicative of multiply-phosphorylated Rad53 and consistent with previous studies (Pellicioli *et al.* 2001). In *rad1*Δ mutants, higher mobility Rad53 bands were not detected (Figure 3.1). While these results are not conclusive, they are consistent with *rad1*Δ mutant strains lacking Rad53 phosphorylation despite an ongoing *RAD9*-dependent cell cycle arrest.

There are two plausible explanations for the lack of Rad53 phosphorylation in *rad1*Δ mutants: 1) The DNA damage-responsive checkpoint response in *rad1*Δ mutants induced for mating type switching may proceed via a Rad9-dependent, Rad53-independent pathway. There is evidence that a Rad53-independent DNA damage response exists in *S. cerevisiae*, which might depend on the type or extent of DNA damage, and such responses are instead dependent upon Chk1 (Sun and Fasullo 2007; Segurado and Diffley 2008). 2) The extent of checkpoint activation in *rad1*Δ mutants during mating type switching may be sufficiently lower than in *donorless* cells, and the amount of Rad53 phosphorylation may be low enough that we cannot detect it by Western blots. This is consistent both with the incomplete arrest in *rad1*Δ cells, as observed by FACS analysis, and with the amount of detectable gene conversion product formation in *rad1*Δ mutants, which is nearly wild-type despite activation of the G2/M DNA damage checkpoint (Lyndaker *et al.* 2008). The latter interpretation of the data seems more likely given the mixture of both wild-type and repair-defective phenotypes exhibited by *rad1*Δ mutants undergoing double-strand

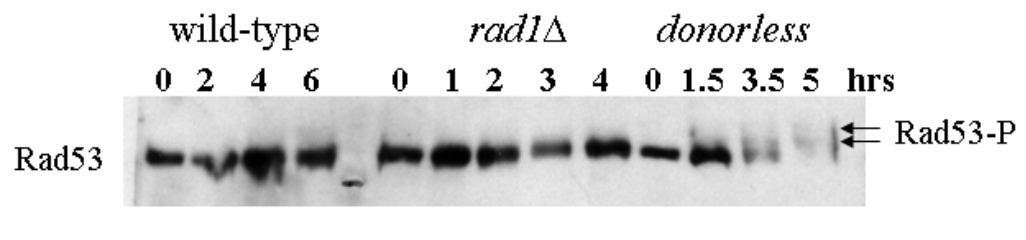

Figure 3.1. Western blot analysis of Rad53 during mating type switching in wild-type, *rad1*Δ, and *donorless* strains. Cultures of wild-type, *rad1*Δ, and *donorless* mutants were induced for mating type switching and cell samples were taken at relevant time points. Cell lysates were run on 8% SDS-PAGE gels and blotted with α-Rad53 antibody. Arrows indicate the higher mobility phosphorylated forms of Rad53 that appear in response to DNA damage.

break repair during mating type switching.

The Ya 3' tail is removed in *rad1*Δ mutants during mating type switching. The proposed role of Rad1-Rad10 during mating type switching is cleavage of the 3' Y**a** nonhomologous tail to allow completion of gene conversion. In order to detect whether the 3' Y**a** sequence remains attached in *rad1*Δ mutants, genomic DNA prepared during mating type switching was enriched for ssDNA using BND-cellulose prior to PCR detection of Y**a**. As shown in Figure 3.2, Y**a** signal was equal to control signal prior to mating type switching (t = 0) and decreased in intensity by 3 hours post-DSB induction. The ratio of Y**a**/control signal was not consistently significantly different in *rad1*Δ mutants relative to wild-type cells, despite a trend towards more Y**a** in *rad1*Δ mutants at 2 and 3 hours post-induction. Southern blots of the Y**a** sequence suggest that there is no significant difference in loss of the Ya sequence between wild-type and *rad1*Δ strains (Appendix, Supplementary Figure 2.7; Lyndaker *et al.* 2008). Thus, it appears that even in the absence of Rad1-Rad10, the 3' nonhomologous Y**a** tail is removed.

In earlier studies, we found that completion of gene conversion was more strictly dependent upon Msh2-Msh3 and Rad1-Rad10 when nonhomologous sequence was present on both sides of the break (two 3' nonhomologous tails) compared to "normal" mating type switching involving only one 3' nonhomologous tail (Chapter 2; Lyndaker *et al.* 2008). Since product formation is severely limited in these cells, we wanted to test whether product formation was inhibited at the early step of strand invasion, when a 3' nonhomologous tail sits on the very 3' end of the invading strand, or whether the cumulative delay in having to remove two 3' tails was sufficient to impair repair (See Chapter 1, Figure 1.2 for diagram of gene conversion involving two 3' nonhomologous tails). Previously, White and Haber (1990) developed a PCR assay

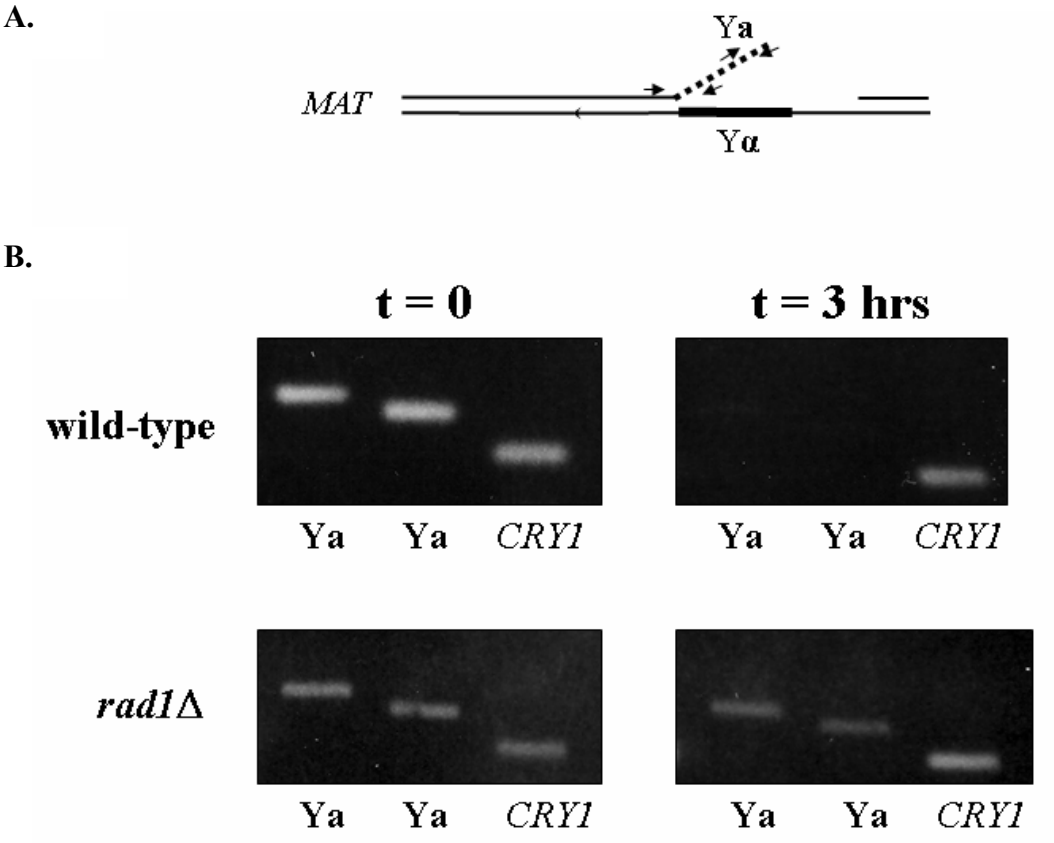

Figure 3.2. PCR detection of the Ya 3' tail in wild-type and *rad1*Δ mutants undergoing mating type switching following BND-cellulose enrichment for ssDNA. A. Primer sets AO1048 + AO1049 (3' Y**a**) and AO1042 + AO1044 (Y**a** base) used for detection of Y**a** by semi-quantitative PCR. B. PCR detection of Y**a** and *CRY* control DNA sequences in BND-cellulose-treated genomic DNA isolated from wild-type and *rad1*Δ mutants prior to (t = 0) or during (t = 3) mating type switching.

to monitor the formation of a strand invasion intermediate containing new DNA synthesis off the invading 3' end (Figure 3.3B). To test whether such an intermediate can form in double nonhomology strains, genomic DNA isolated during mating type switching was PCR-amplified using primers specific for DNA distal to *MAT* (pB) and the Y**α** (pA) sequence (Figure 3.3A; White and Haber 1990).

For "normal" (single nonhomology) mating type switching, the timing of invasion product formation was similar in wild-type, *rad1*Δ, and *msh3*Δ strains (Figure 3.3C), and was similar to that of final product formation as detected previously (Lyndaker *et al.* 2008). A delay was seen in the formation of the strand invasion intermediate in the wild-type double nonhomology strains compared to the single nonhomology strains; this is in agreement with previous studies indicating that recombination is delayed when nonhomologous sequence must be removed from the invading strand (Colaiácovo *et al.* 1999). Very little PCR product was detected in the *rad1*Δ and *msh3*Δ double nonhomology strains (Figure 3.3C), consistent with the physical and genetic analyses of product formation and viability presented earlier (Chapter 2; Lyndaker *et al.* 2008). Thus, mating type switching in wild-type double nonhomology strains appears to be inhibited at the strand invasion step rather than at later time points during repair, and both Rad1 and Msh3 are critical for processing the 3' tail on the invading strand.

Msh2 localization to *MAT* is prolonged in wild-type double nonhomology strains.

While Msh2-Msh3 is dispensable for 3' nonhomologous tail removal during mating type switching when only one side of the DSB is nonhomologous to the donor sequence, Msh2 localizes to the DSB region following DSB formation and leaves with kinetics consistent with product formation (Chapter 2; Lyndaker *et al.* 2008).

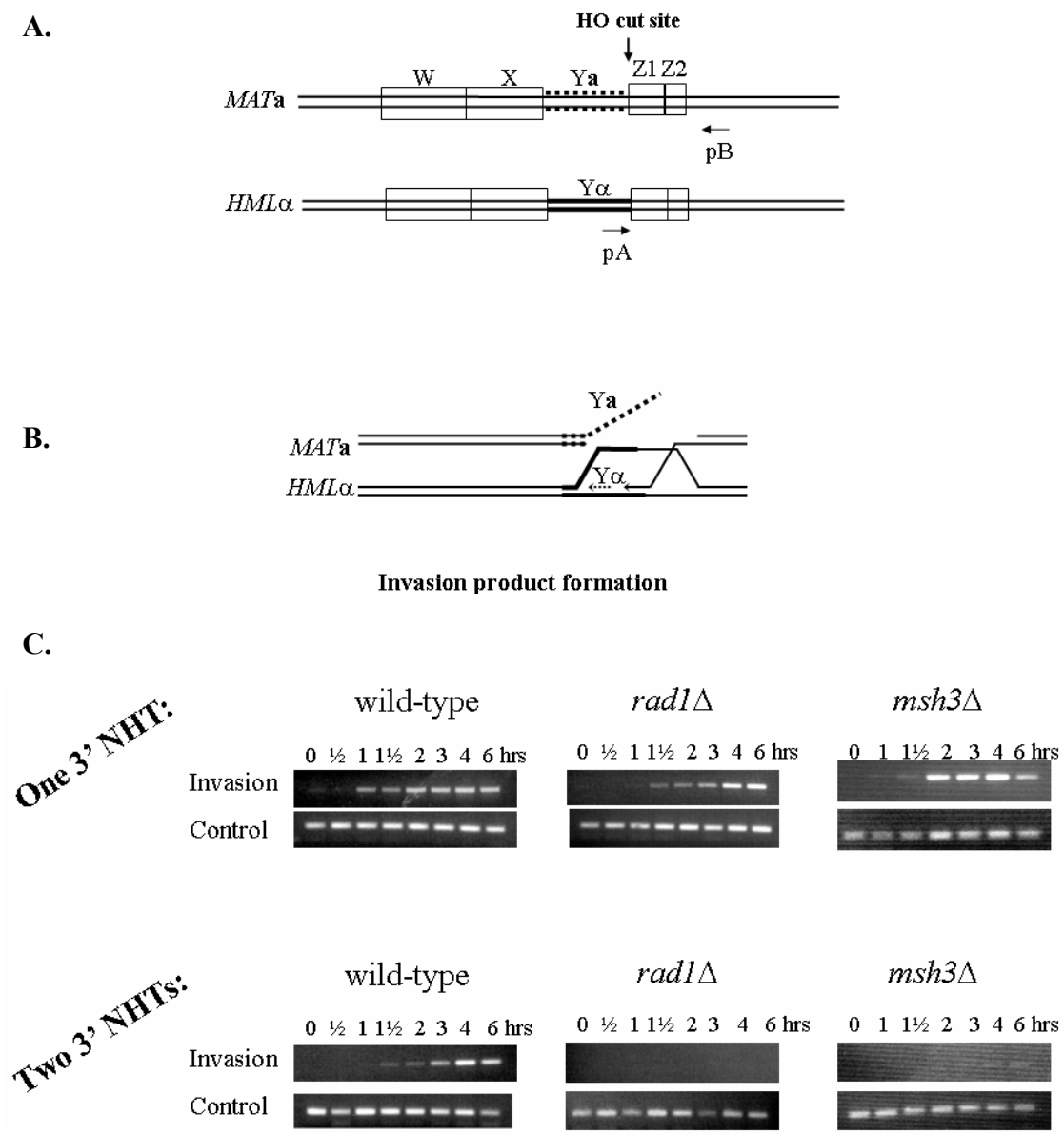

Figure 3.3. PCR detection of synthesis off the invading 3' end in single nonhomology and double nonhomology wild-type, *rad1*Δ, and *msh3*Δ strains induced for mating type switching. A. Location of primers pA and pB for detection of invasion PCR products following invasion of the distal 3' end at *MAT* into the *HML***α** donor sequence. Adapted from White and Haber (1990). B. Predicted intermediate capable of being detected by this PCR assay. Synthesis off the 3' end must reach the site of primer pA in order to be detected. C. Semi-quantitative PCR of genomic DNA extracted at the shown time points following induction of mating type switching from wild-type, *rad1*Δ, and *msh3*Δ strains harboring nonhomologous sequence on one or both sides of the DSB.

Previous studies of DSB repair on plasmids found that Msh2 localizes rapidly to DSBs containing nonhomologous sequence on both sides of the break (Evans *et al.* 2000). Thus, we analyzed localization of Msh2 to the mating type locus when the DSB is flanked by two nonhomologous sequences. Using Msh2-HA_4 and α-HA antibody as described in Chapter 2, Msh2 was found to be similarly recruited to the DSB in double nonhomology strains (Figure 3.4), though slightly later, and exhibited prolonged localization in these strains relative to single nonhomology strains. It remains unclear whether the localization is extended in *rad1*Δ or *msh3*Δ double nonhomology strains relative to wild-type in these strains as in the single nonhomology strains, despite the narrow localization peaks shown in this representative experiment (Figure 3.4; Chapter 2; Lyndaker *et al.* 2008). ChIP to these sequences near the DSB is complicated by the fact that repair does not occur appreciably in *rad1*Δ or *msh3*Δ double nonhomology mutants, and the DNA at the *MAT* locus is degraded at later time points.

***rad1*Δ mutant phenotypes are not due to defective removal of Topoisomerase I during mating type switching.** *rad1*Δ mutants exhibit a mixture of near-wild-type and repair-defective phenotypes during mating type switching in *S. cerevisiae* (Lyndaker *et al.* 2008). Product formation in *rad1*Δ mutants appears wild-type in both PCR-based assays and Southern blots, as do the kinetics and extent of 3' Y**a** nonhomologous tail loss. On the other hand, *rad1*Δ mutants exhibit a *RAD9*-dependent G2/M cell delay during mating type switching similar to that of *donorless* strains that are unable to complete gene conversion. Pedigree experiments following single cells induced for mating type switching previously revealed a unique phenotype in which a single cell induced for a DSB divide to produce one switched cell and one dead cell (Lyndaker *et al.* 2008). While we favored the idea that the dying cells

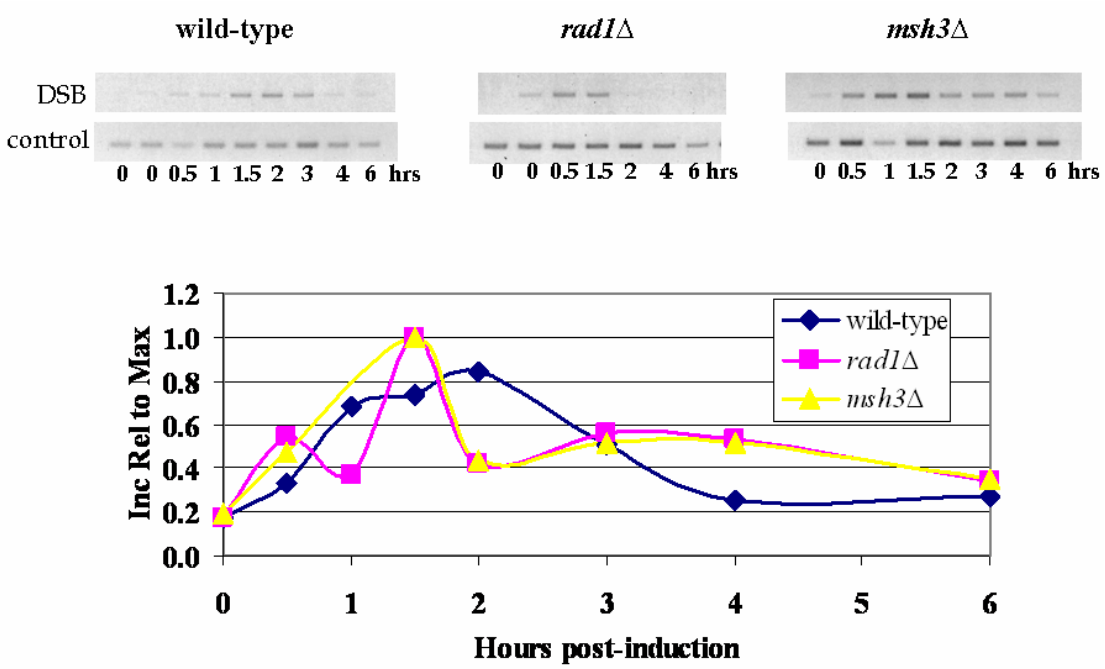

Figure 3.4. Msh2 ChIP to the mating type locus during mating type switching in double nonhomology strains. Representative experiment of Msh2 ChIP localization to *MAT* as detected by semi-quantitative PCR with primers adjacent to the DSB in wild-type, *rad1*Δ, and *msh3*Δ double nonhomology strains.

contained uncleaved 3' Y**a** tails and the surviving cells completed gene conversion by replicating partially repaired gene conversion intermediates, it seemed plausible that cells could be dying from a Rad1-dependent defect on one DNA strand that is independent of the 3' nonhomologous tail.

One potential candidate for this defect concerns the role of Rad1-Rad10 in removing Topoisomerase I that is covalently attached to DNA. TopI relieves topological stress in DNA during replication and repair processes, and it is possible that the process of gene conversion creates enough supercoiling to require TopI function. Following relief of supercoiling, TopI remains covalently attached to a 3' single-stranded DNA end at its site of action and must be removed. There are several mechanisms by which TopI is removed from DNA: 1) TopI can remove itself, 2) Rad1-Rad10 can cleave the 3' flap of DNA that TopI is attached to, or 3) the Tdp1 protein, Tyrosyl-DNA Phosphodiesterase I, can hydrolyze the 3' phosphor-tyrosyl bond attaching TopI to the DNA (Raymond and Burgin 2006). The Tdp1- and Rad1-Rad10-dependent TopI removal mechanisms are redundant with each other, as evidenced by the increased sensitivity of *tdp1*Δ*rad1*Δ double mutants to camptothecin, which requires TopI function to repair DNA damage (Deng *et al.* 2005). I therefore tested whether the *rad1*Δ mating type switching phenotypes changed in mutants lacking *TDP1*.

In cell survival experiments, *tdp1*Δ mutants exhibited decreased viability when induced for mating type switching (47% ± 4 vs. 65% ± 4 in wild-type), whereas *tdp1*Δ*rad1*Δ double mutant viability was comparable to that of *rad1*Δ mutants (32% ± 3 vs. 34% ± 3; Table 3.1). The percentage of surviving cells that switched mating type was similar for all genotypes (Table 3.1). Thus, the defect in *rad1*Δ mutants appears to be unrelated to removal of TopI from DNA. However, it might be interesting to follow up on why cell survival is reduced in *tdp1*Δ single mutants during mating type

switching. Perhaps the cell cycle arrest in *rad1*Δ mutants is sufficient for resolving whatever defect the *tdp1*Δ mutants have in completing efficient repair.

S-phase checkpoint signaling may be important for efficient completion of mating type switching. Given the hypothesis presented in Chapter 2 that both wild-type cells and *rad1*Δ mutants complete mating type switching with the aid of replication, and the fact that *rad1*Δ mutants exhibit a Rad9-dependent cell cycle arrest (Lyndaker *et al.* 2008), it seemed likely that damage signaling might occur at or associated with replication forks. To test this hypothesis, mutants lacking Mrc1, the yeast Claspin homolog and S-phase counterpart of Rad9 in the DNA damage response (Pasero *et al.* 2003), were assayed for cell survival and mating type switching efficiency. As shown in Table 3.1, *mrc1*Δ mutants exhibited a decrease in cell viability in comparison to wild-type strains yet efficient switching in surviving cells, indicating a potential role for Mrc1 in either completion of repair or in efficient cell cycle signaling during mating type switching. Attempts to create *rad1*Δ*mrc1*Δ double mutants were unsuccessful and resulted in gene duplications during homologous integration. Further studies are necessary in order to understand the intriguing potential role of Mrc1 in the DNA damage response during gene conversion.

Loss of Sae2 reduces mating type switching. Since *rad1*Δ mutants form gene conversion products with near-wild-type kinetics, it was of interest to look for other nucleases that might be redundant with Rad1-Rad10 during mating type switching. Mus81-Mms4 and the proofreading activity of Polymerase δ were tested previously and found to have little effect on mating type switching in the *rad1*Δ mutant background (Lyndaker *et al.* 2008). The Sae2 endonuclease, which cleaves DNA with a preference for single-stranded DNA near ssDNA/dsDNA junctions

Table 3.1. Cell survival and mating type switching efficiency of wild-type and mutant strains. The indicated strains were induced for mating type switching from *MAT***a** to *MAT*α and assayed for mating type as described in Materials and Methods.

	% Survival		% Switched		N
wild-type	65	± 4	93	± 1	41
*tdp1*Δ	47	± 4	94	± 2	7
*mrc1*Δ	43	± 6	100	± 0	5
*sae2*Δ	43	± 4	90	± 2	7
*rad1*Δ	34	± 3	91	± 1	25
*rad1*Δ*tdp1*Δ	32	± 3	84	± 4	7
*rad1*Δ*sae2*Δ	22	± 2	76	± 3	13

(Lengsfeld *et al.* 2007), was tested for its potential to act during mating type switching. *sae2*Δ (43% ± 4) and *rad1*Δ*sae2*Δ mutants (22% ± 2) exhibited decreased viability relative to wild- type (65% ± 4) and *rad1*Δ mutants strains (34% ± 3), respectively (Table 3.1). *rad1*Δ*sae2*Δ double mutants also showed a defect in the percentage of surviving cells that switched mating type (76% ± 3 vs. 91% ± 1 in *rad1*Δ mutants). While these results might suggest that Sae2 aids in the removal of 3' tails during mating type switching, recent work has shown that Sae2 plays a critical role in the 5' to 3' resection of DSBs (Mimitou and Symington 2008; Zhu *et al.* 2008). Slowed resection in the absence of Sae2 may cause a delay in mating type switching or in cell cycle progression during switching that is unrelated to 3' nonhomologous tail removal. Detection of the 3' Y**a** tail by Southern blot or PCR-based assay in wild-type vs. *sae2*Δ mutants could aid in discerning between these possibilities and lead to a better understanding the role of Sae2 in mating type switching.

Together, the results presented here extend the findings of previous studies on the role of the Rad1-Rad10-Slx4 complex and Msh2-Msh3 in 3' nonhomologous tail removal, and shed new light on potential roles for TdpI, Sae2, and Mrc1 in the completion of gene conversion during mating type switching. Aside from further work on these factors, future avenues of interest with regard to Rad1-Rad10-dependent 3' nonhomologous tail removal are discussed below.

Future directions

Mutation of the Mec1/Tel1 phosphorylation sites on Slx4 abolishes the ability of Slx4 to function in 3' nonhomologous tail removal during single-strand annealing (Flott *et al.* 2007). Presumably, this checkpoint-regulated function of Slx4 in SSA is the Rad1-Rad10-dependent removal of 3' nonhomologous tails, given that the

phosphorylation-defective mutants of Slx4 are just as deficient as *slx4*Δ*, rad1*Δ*,* or *saw1*Δ null mutants (Flott *et al.* 2007; Li *et al.* 2008). Consistent with this, we previously found that *slx4*Δ deletion mutants are as defective as *rad1*Δ mutants in mating type switching (Lyndaker *et al.* 2008). Since DSB repair by SSA normally involves activation of the DNA damage checkpoint and mating type switching does not, it would interesting to test the phosphorylation-deficient mutants of Slx4 in mating type switching assays. Like *rad1*Δ mutants, *slx4*Δ mutants exhibit cell cycle delays (though shorter) following initiation of mating type switching (Lyndaker *et al.* 2008), indicating that the DNA damage checkpoint response to DSBs is at least partly independent of both *RAD1* and *SLX4*.

In order to further study the checkpoint response in cells undergoing mating type switching, future experiments should be performed in synchronized cells. To do this, strains can be deleted for the *BAR1* gene to sensitize them to α-factor, and cultures can be synchronized in α-factor and released prior to DSB induction. Since a significant fraction of *rad1*Δ mutants do not arrest when induced for mating type switching during asynchronous growth (Chapter 2, Figure 2.4; Lyndaker *et al.* 2008), the molecular analysis in our previous studies reflects repair occurring at various stages of the cell cycle. The extent of gene conversion defects in *rad1*Δ*, msh2*Δ*,* and other mutants could be clarified by repeating the Southern blots and ChIP experiments in cells synchronized in α-factor prior to DSB formation.

It would be interesting to run pulsed-field gels of *rad1*Δ mutants that had undergone mating type switching to see if there is any indication for break-induced replication that initiates by invasion of the *MAT* 3' end into *HML***α** and continues to the end of the chromosome. Such an event would be expected to create a switched Y**α** product, but could potentially delete the centromere and more than half of Chromosome III (See Figure 3.5). A BIR mechanism could explain the involvement

Figure 3.5. Mating type switching from *MAT*a to *MATα*: Poised for break-induced replication? A. Initiation of mating type switching by HO-mediated DSB formation at the *MAT* locus. Following 3' to 5' resection of the DSB, the distal 3' end performs strand invasion into the homologous sequence at *HML***α**. DNA synthesis initiates from the invading 3' end to begin gene conversion. B. Diagram of Chromosome *III* including the mating type locus (*MAT***a**), centromere, and donor locus (*HML***α**).

A.

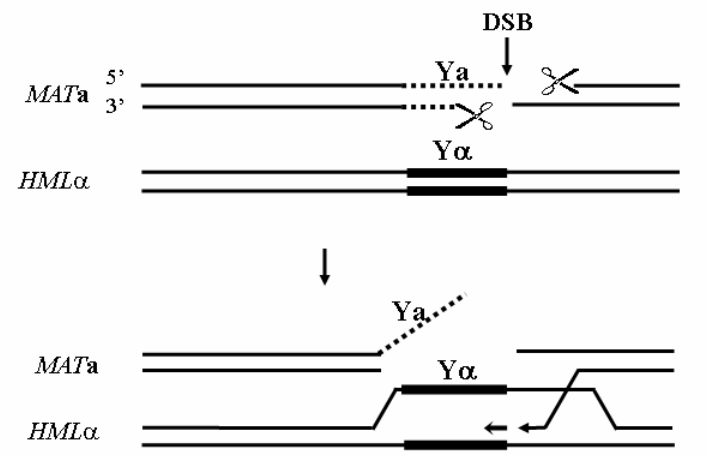
DSB
Ya
MATa 5'
3'
Yα
HMLα
Ya
MATa
Yα
HMLα

B.

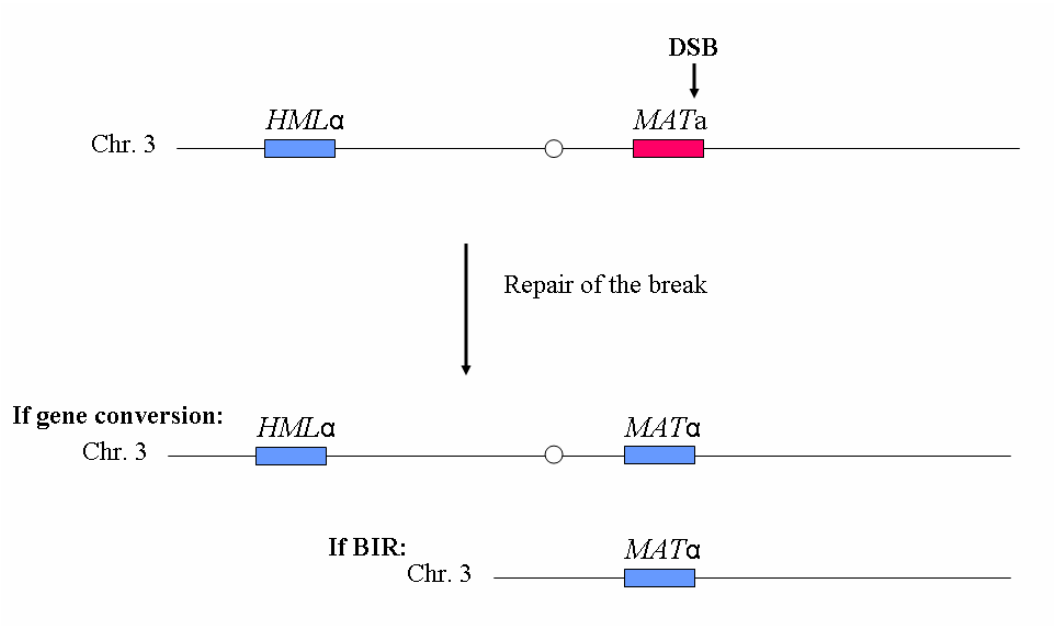
DSB
Chr. 3
HMLα
MATa
Repair of the break
If gene conversion:
Chr. 3
HMLα
MATα
If BIR:
Chr. 3
MATα

of the spindle checkpoint in the G2/M arrest in *rad1*Δ mutants, though cells of the "two switched" pedigree category with presumably wild-type-like gene conversion products also undergo *MAD2*-dependent cell cycle arrest. While the products of BIR may not be stable, they might be visible on a pulsed-field gel, especially if the gel is probed for *MAT*-specific sequences. BIR initiating from *MAT* invasion into *HML***α** might also be followed by single-strand annealing or other repeat-mediated recombination events to create unique products that we detect by Southern blot as gene conversions, and might better explain the G2/M DNA damage checkpoint response observed in *rad1*Δ mutants.

A recent study showed that Rad54 controls access to the 3' OH after Rad51-mediated strand invasion (Li and Heyer 2008). Rad54 dissociates Rad51 from double-stranded DNA at the end of the Rad51-dsDNA filament after strand invasion in order to allow DNA polymerase to access the free 3' hydroxyl and prime DNA synthesis. Rad54 is also thought to act at earlier steps in stimulating Rad51-dependent strand invasion, perhaps to convert unstable paranemic structures formed upon strand invasion into more stable plectonemic joints (Sugawara *et al.* 2003; Li and Heyer 2008). 3' nonhomologous tail removal may be intimately linked with this process, since cleavage of nonhomologous tails frees the 3' end for priming of DNA synthesis. It has been proposed that the role of Msh2-Msh3 in 3' nonhomologous tail removal may be to stabilize paranemic joints, such as those formed upon strand invasion, to prepare them for Rad1-Rad10-dependent cleavage, and also that the requirement for Rad1-Rad10 in 3' end processing may vary for paranemic vs. plectonemic joints (reviewed in Lyndaker and Alani 2009). It will be interesting to see how Rad54-dependent removal of Rad51 and Rad1-Rad10-Slx4- and Msh2-Msh3-dependent 3' nonhomologous tail removal are intertwined.

REFERENCES

Allers, T. and M. Lichten (2000). "A method for preparing genomic DNA that restrains branch migration of Holliday junctions." Nucl. Acids Res. **28**(2): e6.

Colaiácovo, M. P., F. Pâques and J. E. Haber (1999). "Removal of one nonhomologous DNA end during gene conversion by a *RAD1*- and *MSH2*-independent pathway." Genetics **151**: 1409-23.

Deng, C., J. A. Brown, D. You and J. M. Brown (2005). "Multiple endonucleases function to repair covalent Topoisomerase I complexes in *Saccharomyces cerevisiae*." Genetics **170**(2): 591-600.

Evans, E., N. Sugawara, J. E. Haber and E. Alani (2000). "The *Saccharomyces cerevisiae* Msh2 mismatch repair protein localizes to recombination intermediates *in vivo*." Mol. Cell **5**: 189-99.

Flott, S., C. Alabert, G. W. Toh*, et al.* (2007). "Phosphorylation of Slx4 by Mec1 and Tel1 regulates the single-strand annealing mode of DNA repair in budding yeast." Mol. Cell. Biol. **27**(18): 6433-45.

Gamper, H., N. Lehman, J. Piette and J. E. Hearst (1985). "Purification of circular DNA using benzoylated naphthoylated DEAE-cellulose." DNA **4**(2): 157-64.

Goldfarb, T. and E. Alani (2004). Chromatin immunoprecipitation to investigate protein-DNA interactions during genetic recombination. Genetic recombination: Reviews and protocols. A. S. Waldman. Totowa, NJ, Humana Press Inc. **262:** 223-37.

Lengsfeld, B. M., A. J. Rattray, V. Bhaskara*, et al.* (2007). "Sae2 is an endonuclease that processes hairpin DNA cooperatively with the Mre11/Rad50/Xrs2 complex." Mol. Cell **28**(4): 638-51.

Li, F., J. Dong, X. Pan*, et al.* (2008). "Microarray-based genetic screen defines *SAW1*, a gene required for Rad1/Rad10-dependent processing of recombination intermediates." Mol. Cell **30**(3): 325-35.

Li, X. and W.-D. Heyer (2008). "RAD54 controls access to the invading 3'-OH end after RAD51-mediated DNA strand invasion in homologous recombination in *Saccharomyces cerevisiae*." Nucl. Acids Res. **37**(2): 638-46.

Lyndaker, A. M. and E. Alani (2009). "A tale of tails: Insights into the coordination of 3' end processing during homologous recombination." BioEssays **In press**.

Lyndaker, A. M., T. Goldfarb and E. Alani (2008). "Mutants defective in Rad1-Rad10-Slx4 exhibit a unique pattern of viability during mating type switching in *Saccharomyces cerevisiae*." Genetics **179**(4): 1807-21.

Mimitou, E. P. and L. S. Symington (2008). "Sae2, Exo1 and Sgs1 collaborate in DNA double-strand break processing." Nature **455**(7214): 770-4.

Pasero, P., K. Shimada and B. P. Duncker (2003). "Multiple roles of replication forks in S phase checkpoints." Cell Cycle **2**(6): 568-72.

Pellicioli, A., S. E. Lee, C. Lucca*, et al.* (2001). "Regulation of *Saccharomyces* Rad53 checkpoint kinase during adaptation from DNA damage-induced G2/M arrest." Mol. Cell **7**: 293-300.

Raymond, A. C. and A. B. Burgin, Jr. (2006). "Tyrosyl-DNA Phosphodiesterase (Tdp1) (3'-Phosphotyrosyl DNA Phosphodiesterase)." Meth. Enzymol. **409**: 511-24.

Segurado, M. and J. F. X. Diffley (2008). "Separate roles for the DNA damage checkpoint protein kinases in stabilizing DNA replication forks." Genes Dev. **22**(13): 1816-27.

Sugawara, N., X. Wang and J. E. Haber (2003). "*In vivo* roles of Rad52, Rad54, and Rad55 proteins in Rad51-mediated recombination." Mol. Cell **12**: 209-19.

Sun, M. and M. Fasullo (2007). "Activation of the budding yeast securin Pds1 but not Rad53 correlates with double-strand break-associated G2/M cell cycle arrest in a *mec1* hypomorphic mutant." Cell Cycle **6**(15): 1896-902.

White, C. I. and J. E. Haber (1990). "Intermediates of recombination during mating type switching in *Saccharomyces cerevisiae*." EMBO J. **9**(3): 663-73.

Zhu, Z., W. Chung, E. Shim*, et al.* (2008). "Sgs1 helicase and two nucleases Dna2 and Exo1 resect DNA double-strand break ends." Cell **134**(6): 981-94.

CHAPTER 4

Insights into the roles of the Sgs1 helicase and Msh2-Msh6 mismatch recognition complex in heteroduplex rejection during homologous recombination

Abstract

Recombination between slightly divergent sequences in the genome can lead to chromosomal rearrangements such as insertions, deletions, inversions, and translocations. DNA mismatch repair proteins are known to actively inhibit recombination between homeologous sequences while allowing recombination between completely homologous substrates. Mismatch repair-dependent prevention of homeologous recombination is thought to occur via heteroduplex rejection, which is hypothesized to entail mismatch recognition and binding by the Msh2-Msh6 complex within heteroduplex DNA and either recruitment or stimulation of the Sgs1 helicase leading to unwinding of inappropriate recombination intermediates. This chapter describes the biochemical purification of Msh2-Msh6 and a helicase-proficient soluble fragment of Sgs1, $Sgs1_{400\text{-}1268}$, and demonstrates that Msh2-Msh6 and Sgs1 physically interact in coimmunoprecipitation experiments. When added to helicase assays, Msh2-Msh6 appears to inhibit Sgs1-dependent unwinding of short 3' overhang substrates. Studies of the effect of Msh2-Msh6 on Sgs1 helicase activity are ongoing.

Introduction

Although homologous recombination often serves as a DNA repair mechanism, recombination between slightly divergent or so-called homeologous sequences in the genome can lead to chromosomal rearrangements, including deletions, duplications, inversions, and translocations. This is especially true for higher eukaryote genomes that contain many repeated sequences. Chromosomal rearrangement and instability is observed in cancerous cells, so understanding how recombination fidelity is regulated may also aid in our understanding of cancer progression and susceptibility. Aside from maintaining genome stability, inhibition of homeologous recombination also preserves species diversity and isolation by preventing recombination between different species (Radman and Wagner 1993).

DNA mismatch repair. DNA mismatch repair factors play a role in maintaining the fidelity of recombination by inhibiting recombination between somewhat divergent homologous sequences. The DNA mismatch repair (MMR) system primarily functions to repair errors incurred during DNA replication. In *E. coli* MMR, multimers of the MutS protein recognize and bind to mismatched bases. Subsequent binding of the MutL proteins to MutS activates the nuclease activity of MutH at a downstream hemimethylated GATC site, allowing for strand discrimination and excision of the newly-synthesized strand. DNA resynthesis and ligation follow to form the final repaired product (Modrich and Lahue 1996; Harfe and Jinks-Robertson 2000; Schofield and Hsieh 2003).

In the yeast *Saccharomyces cerevisiae,* there are 6 MutS homologs, Msh1-Msh6, as well as 4 MutL homologs, Mlh1-Mlh3 and Pms1. The major components of post-replicative DNA mismatch repair are Msh2, Msh3, Msh6, Mlh1, and Pms1. As

shown in Figure 4.1, mismatch recognition is carried out by either the Msh2-Msh6 (MutSα) or Msh2-Msh3 (MutSβ) heterodimer; Msh2-Msh6 has binding specificity for single base-base mismatches and single nucleotide insertion/deletions, whereas Msh2-Msh3 recognizes insertion/deletion loops of one to 16 nucleotides. Recent work suggests that Msh2-Msh3 also binds specifically to base-base mismatches (Harrington and Kolodner 2007). Mismatch recognition is followed by binding of the Mlh1-Pms1 "matchmaker" heterodimer to the Msh heterodimer, which, through an unknown mechanism, allows recruitment of downstream factors for completion of excision, resynthesis, and ligation (see Figure 4.1).

Downstream factors in mismatch repair include the ExoI exonuclease, the PCNA processivity clamp, replication factor C (RFC), DNA polymerases δ and ε, and the RPA single-strand binding protein, though the mechanism of these downstream steps in eukaryotic MMR remains unclear (reviewed in Harfe and Jinks-Robertson 2000; Harfe and Jinks-Robertson 2000; Schofield and Hsieh 2003). Eukaryotes lack both the post-replicative GATC hemimethylation and the MutH endonuclease that direct nascent strand recognition and the downstream excision steps in the bacterial MMR system. Recent work has shown that Mlh1-Pms1 exhibits nuclease activity *in vitro,* and the conserved metal-binding motif present in Pms1 is also conserved in Mlh3, though it is unclear what the exact function of this activity is *in vivo* (Kadyrov *et al.* 2007; Nishant *et al.* 2008). It is striking that this endonuclease motif is conserved in MutL homologs from organisms that lack the MutH strand-discrimination system, though it is unclear how this Mlh1-Pms1 nicking activity might provide a strand discrimination signal.

MMR in higher eukaryotes is thought to occur in a similar manner to that in *S. cerevisiae,* with high conservation of the Msh2, Msh6, Msh3, Mlh1, and Pms1 (hPms2) proteins throughout evolution. Human Pms2 is the homolog of *S. cerevisiae*

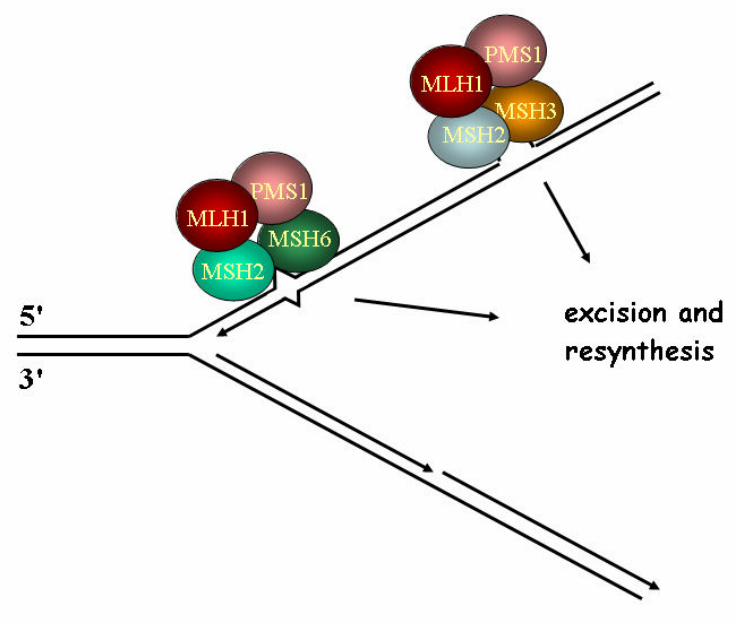

Figure 4.1. Post-replicative DNA mismatch repair in *S. cerevisiae*. Adapted from a figure obtained from Dr. Julie Heck. The MutS homolog heterodimers Msh2-Msh6 and Msh2-Msh3 recognize mismatches resulting from misincorporation errors at replication forks. Msh2-Msh6 primarily recognizes base-base mismatches and single nucleotide insertion/deletions, whereas Msh2-Msh3 recognizes larger insertion/deletion mismatches. Binding of the MutL homolog heterodimer Mlh1-Pms1 to MutS homologs bound at mismatches promotes subsequent steps in mismatch repair including strand excision, repair synthesis, and ligation. Downstream factors in mismatch repair include the ExoI exonuclease, the PCNA processivity clamp, Rfc, DNA polymerases δ and ε, and the RPA single-strand binding protein.

Pms1, and the hMlh1-Pms2 complex (MutLα) is thought to be the major MutL complex in post-replicative MMR. Germline mutations in the human *MSH2, MSH6, MSH3, MLH1, PMS2*, *MLH3* and *EXO1* mismatch repair genes are associated with Lynch syndrome, an autosomal dominant condition characterized primarily by microsatellite instability and early-onset colon and endometrial cancers (Peltomaki 2003; Boland *et al.* 2008). Mutations in *MSH2*, *MLH1, MSH6,* and *PMS2* are found in up to 80% of hereditary non-polyposis colorectal cancer (HNPCC) families, and *MSH2* and *MLH1* mutations confer consistently higher levels of microsatellite instability than the remaining MMR mutations (Peltomaki 2003). Biallelic inheritance of MMR mutations can also lead to Constitutional Mismatch Repair-Deficiency (CMMR-D) syndrome, characterized by childhood cancers, brain tumors, early-onset colon cancers, and neurofibromatosis type 1 phenotypes (Wimmer and Etzler 2008). Mutations and aberrant epigenetic regulation of MMR genes have also been identified in a variety of sporadic cancers (Lynch and de la Chapelle 2003; Peltomaki 2003; Chaksangchaichot *et al.* 2006).

Mismatch repair factors have a variety of roles outside the canonical post-replicative MMR functions at the replication fork. Msh2-Msh6, Msh2-Msh3, and Mlh1-Pms1 also correct mismatches in heteroduplexes during homologous recombination. Msh2-Msh3 is important for Rad1-Rad10-dependent processing of 3' nonhomologous tail intermediates during homologous recombination (see Chapters 1 and 2), while Msh4-Msh5 and Mlh1-Mlh3 are critical players in meiotic crossover recombination. At least in higher eukaryotes, Msh2 interacts with DNA damage checkpoint factors and is involved in promoting apoptosis in response to DNA damaging agents (Seifert and Reichrath 2006). Msh2-Msh6 is also important for somatic hypermutation and class switch recombination during antibody generation

(Slean *et al.* 2008). As discussed below, both Msh2-Msh6 and Mlh1-Pms1 act to prevent recombination between homeologous substrates.

Double-strand break repair via homologous recombination. Like post-replicative mismatch repair, double-strand break (DSB) repair pathways help to maintain the integrity of the genome. Repair of DSBs is primarily carried out by either homologous recombination (HR) or non-homologous end-joining (NHEJ). These repair pathways are crucial, since unrepaired DSBs can lead to chromosome rearrangements, chromosome loss, and cell death. DSB repair via homologous recombination can occur through a variety of mechanisms, including gene conversion, crossing over, break-induced replication (BIR), and single-strand annealing (SSA) (reviewed in Pâques and Haber 1999; Symington 2002). These mechanisms each involve some degree of pairing between two homologous sequences, and can involve nucleolytic and helicase activities, Holliday junction formation, migration, and resolution, DNA synthesis, and ligation. All HR mechanisms are largely dependent on Rad52, which binds to ssDNA and mediates strand annealing. Of the Rad52-dependent HR pathways, gene conversion pathways are highly dependent upon Rad51, a RecA homolog that forms nucleoprotein filaments that perform strand invasion into duplex DNA, and others, like SSA, are Rad51-independent. In addition, many HR mechanisms require Rad59, which anneals complementary DNA strands in a similar manner to Rad52. Requirements for Rad51 and Rad59 are not mutually exclusive (Pâques and Haber 1999; Symington 2002; Spell and Jinks-Robertson 2003).

Homologous recombination repair of DSBs is often considered to be an error-free DNA repair mechanism, and this is true for the majority of gene conversion events. Gene conversion results in a non-reciprocal transfer of DNA sequence from

one region of the genome to another that can result in either noncrossover or crossover products. Noncrossovers are thought to occur via a synthesis-dependent strand annealing (SDSA) mechanism as discussed in Chapter 2, where strand invasion into a homologous donor sequence and DNA synthesis off of the donor template are followed by annealing back to the native locus. This is in contrast to earlier predicted models of noncrossover formation by alternative resolution of double Holliday junctions (reviewed in Pâques and Haber 1999). Crossovers entail the reciprocal exchange of DNA strands, and are hypothesized to form when strand invasion into a donor sequence and second end capture form a double Holliday junction intermediate that is then resolved by nucleolytic cleavage. Crossovers can be associated with varying extents of gene conversion depending both on the extent of Holliday junction migration and the degree of homology between the two recombining regions.

Some HR pathways are less conservative and, while they serve their purpose in repairing lethal DSBs, can lead to deletions and gross chromosomal rearrangements, especially when DSBs are located within repetitive DNA sequences (Argueso *et al.* 2008). Single-strand annealing (SSA) occurs when a DSB is formed between repeated sequences, and results in deletion of the intervening sequence (which can be up to 15 kb) and one copy of the repeat (see Figure 4.2; reviewed in Pâques and Haber 1999). Break-induced replication (BIR) begins with strand invasion similarly to simple gene conversion, but is followed by extensive replication that can span the full arm of a chromosome. Repeated cycles of template switching are likely to play a role, and can lead to complex chromosomal rearrangements. BIR includes both Rad51-dependent and -independent pathways (Pâques and Haber 1999; McEachern and Haber 2006).

Mismatch repair factors in recombination. Given the complexity of HR and the importance of repairing breaks in the genome, it is critical that this recombination be

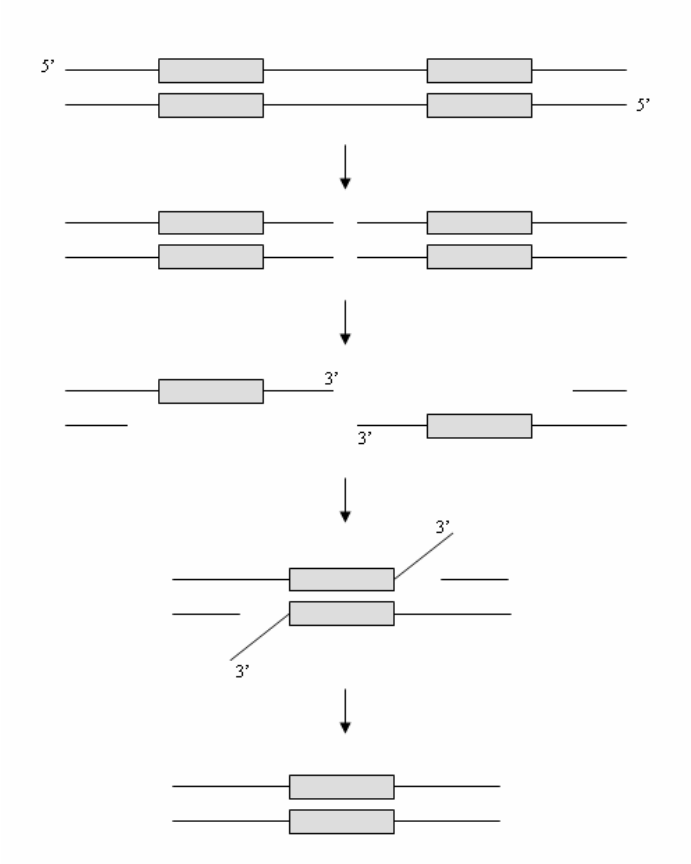

Figure 4.2. Single-strand annealing (SSA) mechanism of DSB repair. Gray boxes indicate a repeated sequence. DSBs can be repaired by SSA when homologous DNA sequences reside on both sides of the break. Following DSB formation, the ends are resected 5' to 3' until homologous sequences are revealed. Annealing of these repeats deletes the intervening sequence and leaves 3' nonhomologous tails on either side of the annealed intermediate. 3' nonhomologous tail removal, repair synthesis, and ligation allow for completion of repair.

regulated. Aside from their roles in post-replicative MMR, mismatch repair proteins have been implicated in the regulation of homologous and homeologous recombination events, and it is clear that the effect of MMR on HR is directly related to the level of sequence divergence (Chambers *et al.* 1996; Datta *et al.* 1996; Hunter *et al.* 1996; Porter *et al.* 1996). In bacterial systems, mutation of *mutS* or *mutL* leads to a 1,000-fold increase in recombination between the *E. coli* and *S. typhimurium* genomes, which are approximately 20% divergent (Rayssiguier *et al.* 1989). In addition, recombination between 9% divergent phage and plasmid DNA in *E. coli* occurs 15-fold more often in *mutS* mutants than in wild-type cells (Shen and Huang 1989), and duplications are formed by homeologous recombination 10-fold more frequently in *mutS* and *mutL* mutant *E. coli* strains than in wild-type (Petit *et al.* 1991).

Similar MMR-dependent effects have been observed in yeast, where *msh2*Δ and *msh3*Δ mutations increase recombination between 25% divergent substrates by 17- and 10-fold, respectively, and *msh2*Δ*msh3*Δ double mutants exhibit a 43-fold increase (Selva *et al.* 1995). Work in the Jinks-Robertson lab has shown that mutation of yeast *MSH2* causes the greatest defect in anti-recombination activity of all the MMR proteins tested (Datta *et al.* 1996; Nicholson *et al.* 2000). Msh2 also plays an important role in mammalian recombination, as *msh2* mutant mouse ES cells show a 10-fold increase compared to wild-type cells in DSB-induced recombination between substrates with 1.5% sequence divergence (Elliott and Jasin 2001). *msh2*$^{-/-}$ homozygous mutant mouse ES cells also have approximately equivalent frequencies of homologous and homeologous (0.6% divergent) recombination (de Wind *et al.* 1995). *msh3*Δ mutants have some defect in anti-recombination, but to a lesser extent than *msh2*Δ mutants (Selva *et al.* 1995; Datta *et al.* 1996; Nicholson *et al.* 2000). Mutation of the MutL homologs has less of an effect on anti-recombination than the MutS homologs in a variety of assays (Selva *et al.* 1995; Chambers *et al.* 1996; Datta

et al. 1996; Hunter *et al.* 1996; Chen and Jinks-Robertson 1999; Nicholson *et al.* 2000; Sugawara *et al.* 2004).

Though Msh2 may play an integral role in regulation of HR, studies of its anti-recombination role are complicated by the fact that Msh2 also acts in recombination along with Msh3, Rad1, and Rad10 to remove non-homologous 3' single-stranded tails that can form as HR intermediates, as described in Chapters 1 and 2 (Pâques and Haber 1997; Sugawara *et al.* 1997; Studamire *et al.* 1999; Goldfarb 2005; Goldfarb and Alani 2005; Lyndaker *et al.* 2008). Many studies of Msh2 in anti-recombination were initiated prior to the discovery of Msh6. The anti-recombination effect of mutation of *MSH6* was first shown by Nicholson *et al.* (2000), and has since been confirmed (Sugawara *et al.* 2004; Goldfarb and Alani 2005). Unlike Msh2 and Msh3, the specific effect of Msh6 on anti-recombination is easier to study because it is not involved in 3' non-homologous tail removal (Pâques and Haber 1999; Harfe and Jinks-Robertson 2000).

DNA sequence requirements for homologous recombination. There is a direct correlation of both the percentage and length of DNA sequence homology with the frequency of HR events (Singer *et al.* 1982; Liskay *et al.* 1987; Ahn *et al.* 1988; Deng and Capecchi 1992; Mezard *et al.* 1992; Sugawara and Haber 1992; Radman and Wagner 1993; Zawadzki *et al.* 1995; Datta *et al.* 1996; Datta *et al.* 1997; Vulic *et al.* 1997; Chen and Jinks-Robertson 1999; Fujitani and Kobayashi 1999). This seems intuitive, since the longer a stretch of homology, the more likely it is that stable strand invasion or annealing intermediates can be formed. The idea of a requirement during recombination for a minimum length of homology was first proposed by Shen and Huang (1986), and this region was referred to as the MEPS, or minimal efficient processing segment. In their work, the MEPS for initiation of RecBC- and RecF-

dependent recombination in *E. coli* was found to be 23-27 bp and 44-90 bp, respectively (Shen and Huang 1986). Consistent with this, the frequency of recombination between plasmids and phage in *E. coli* switched from exponential to linear dependence on the length of homology at 74 bp (Watt *et al.* 1985). Thus, the minimal efficient length of homology in *E. coli* is less than 100 bp. In mammalian cells, the MEPS is estimated at approximately 200 bp (Rubnitz and Subramani 1984; Liskay *et al.* 1987; Waldman and Liskay 1988).

Work in the yeast system assessing recombination between both interchromosomal repeats and intrachromosomal direct and inverted repeats has estimated the MEPS for these events to be 248, 271, and 280 bp, respectively (Jinks-Robertson *et al.* 1993). For the process of single-strand annealing, which does not involve strand invasion into duplex DNA as other HR events do, the MEPS is estimated to be between 63 and 89 bp (Sugawara and Haber 1992). While this value is the minimum length of homology for *efficient* recombination, HR can occur between sequences with as little as 13 bp of homology (Ahn *et al.* 1988). Similarly, work by Datta and colleagues suggests that 20 bp of homology is sufficient for initiation of heteroduplex formation (Datta *et al.* 1997).

Requirements for anti-recombination. Presumably the MEPS allows for stable pairing during strand invasion and/or annealing, and it is likely that active anti-recombination activities occur after formation of a stable heteroduplex; If stable pairing cannot be accomplished (i.e., the two sequences are too divergent), recombination will not be initiated, as depicted in Figure 4.3. Mismatches present within a stable heteroduplex present yet another barrier to completion of HR events (Figure 4.3). Studies in bacteria have supported the idea that mismatches in a heteroduplex intermediate lead to decreased recombination frequencies (Zhart and

Maloy 1997). Further support has come from fine-resolution analysis of intrachromosomal conversion tract lengths in mammals, where rearrangements caused by homeologous recombination are regulated by the amount of sequence divergence at the site of recombination initiation (Yang and Waldman 1997).

One mismatch within 53 bp of homology (1.9% divergence) decreases recombination 4-fold in *E. coli* (Watt *et al.* 1985). Similarly, Shen and Huang found that a single mismatch in 31 bp (3.2% divergence) is sufficient to inhibit recombination between phage and plasmid DNA in *E. coli,* and recombination frequency is reduced 240-fold when substrates differ in homology by 9% (Shen and Huang 1989). In a different assay, these authors saw a 40-fold reduction in recombination with 10% divergent substrates (Shen and Huang 1986). In yeast, one mismatch present in 350 bp of an inverted repeat (effectively 0.29% divergence) is sufficient for anti-recombination to take effect (Datta *et al.* 1997; Chen and Jinks-Robertson 1999). There is also a 6-fold reduction in single-strand annealing when repeats are 3% divergent compared to identical sequences (7 mismatches within 205 bp; Sugawara *et al.* 2004). The effect of a small number of mismatches on mitotic recombination is also slightly higher than on meiotic recombination events (Chen and Jinks-Robertson 1999), indicating that mitotic recombination may be a more effective system for studying the mechanistic details of heteroduplex rejection.

Work in mammalian cells has found that the rate of intrachromosomal recombination depends on the amount uninterrupted homology rather than the number of mismatches (Waldman and Liskay 1988). This distinction between the length of perfect identity and the absolute number of mismatches within a given region may allow us to better understand the molecular mechanism of heteroduplex rejection. A region of homology as long as the MEPS should allow initiation, and it is likely that the recombination frequency may increase as stretches of homology increase in length

above the size of the MEPS, since more initiation of HR can occur when there are more MEPS. However, it is not clear how the length of sequence identity affects HR efficiency after stable initiation has occurred. Anti-recombination can be triggered by a single mismatch in 350 bp (Datta *et al.* 1997), but it is not known whether the location of the mismatch within the 350 bp has a significant effect. It has been estimated that approximately 610 bp of homology is required in order to bypass the MMR-dependent anti-recombination effect (Datta *et al.* 1997), which suggests that homology plays a further role in regulation of HR aside from the MEPS.

In *E. coli,* different locations of single mismatches within a 31 bp substrate (3.2% divergence) were shown to decrease recombination frequencies anywhere from 2- to 12-fold (Shen and Huang 1989). In yeast, studies using different locations of one mismatch within a HR substrate (Datta *et al.* 1997; Chen and Jinks-Robertson 1999) have not been systematic, and have effectively only tested two locations: one mismatch at position 137/140 and one at position 193/194 out of ~350 bp. Both substrates yielded similar recombination frequencies and MMR-dependence (Datta *et al.* 1997). The effect of one mismatch and its location in single-strand annealing has not been systematically studied. Given the immense number of repeat sequences and regions of homology in the human genome, more studies are needed to determine the sequence requirements for anti-recombination and to further our understanding of how cells maintain the fidelity of homologous recombination events. Future experiments to address these questions are discussed at the end of this chapter.

The mechanism of anti-recombination by MMR factors has been suggested to occur in various ways, shown in Figure 4.3, including limitation of branch migration or Holliday junction resolution to limit heteroduplex extension, or rejection of intermediates by nucleolytic destruction or unwinding of the heteroduplex DNA (Sugawara *et al.* 2004; Surtees *et al.* 2004; Goldfarb and Alani 2005; Waldman 2008).

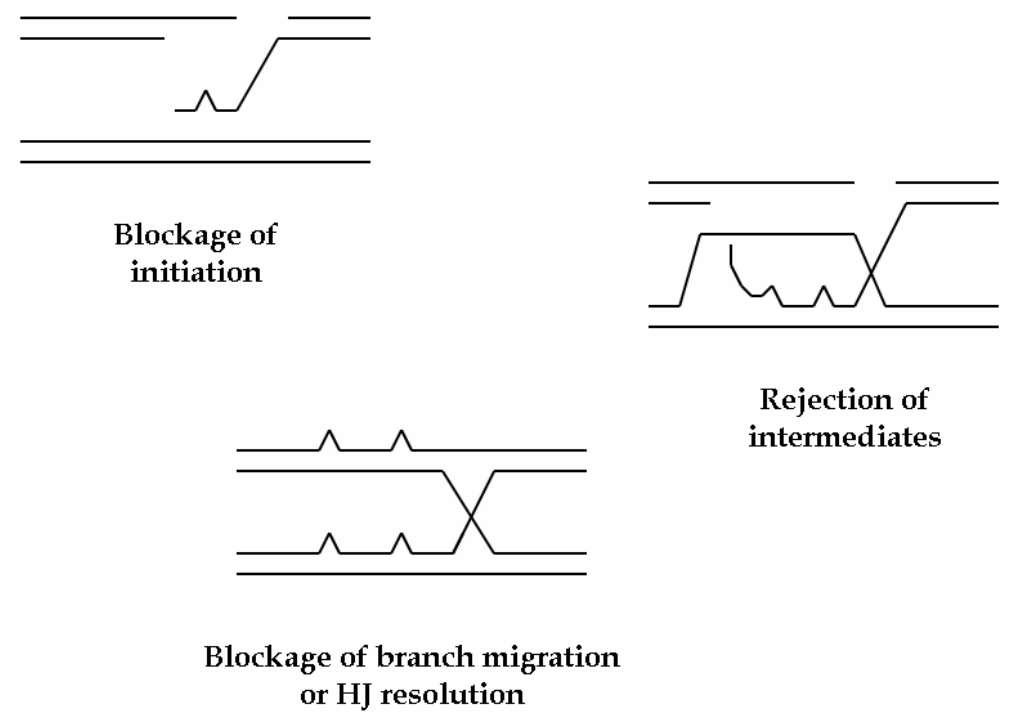

Figure 4.3. Potential mechanisms of mismatch-dependent anti-recombination. Sequence divergence can limit initiation of recombination when there is insufficient homology to create a stable strand invasion (during gene conversion) or annealed (during SSA) intermediate. Anti-recombination by mismatch repair factors is proposed to occur via nucleolytic or helicase-driven heteroduplex rejection and/or by limiting Holliday junction migration or resolution.

Support for an effect of MMR factors on Holliday junctions includes the fact that MutS can block RecA-mediated strand exchange *in vitro* (Worth *et al.* 1994). Mitotic and meiotic gene conversion tract lengths are 50-65% longer in MMR mutants compared to wild-type, suggesting that at least part of the MMR anti-recombination activity entails blockage of Holliday junction migration or resolution (Chen and Jinks-Robertson 1998; Chen and Jinks-Robertson 1999). *S. cerevisiae* Msh2 binds to Holliday junctions *in vitro* (Alani *et al.* 1997), and the Msh2-Msh6 complex has an affinity for Holliday junctions that is comparable to its affinity for mismatched bases (Marsischky *et al.* 1999). However, recent evidence has provided strong support for a helicase-dependent heteroduplex rejection model (see below) (Sugawara *et al.* 2004; Goldfarb and Alani 2005). Heteroduplex rejection and blockage of branch migration are not mutually exclusive, as blockage of migration could serve as a signal for helicase recruitment, though processes such as single-strand annealing could solely utilize an unwinding mechanism of anti-recombination since no Holliday junctions are formed.

Roles for Sgs1 in anti-recombination. Within the past 12 years it has become evident that the Sgs1 helicase is crucial for the maintenance of genome stability (Lu *et al.* 1996; Watt *et al.* 1996; Myung *et al.* 2001; Cobb *et al.* 2002). Sgs1 is a 3' to 5' helicase of the RecQ family that was identified both as a suppressor of the slow growth phenotype of *S. cerevisiae* Topoisomerase III (*TOP3*) mutants (Gangloff *et al.* 1994; Lu *et al.* 1996), and as a protein that interacts with Topoisomerase II (Watt *et al.* 1995). Sgs1 is the only RecQ homolog in *S. cerevisiae,* and homologs in other species include *E. coli* RecQ, *S. pombe* Rqh1, and the human homologs Blm, Wrn, RecQL4, RecQL5, RecQL1 (Bennett and Keck 2004). Blm, Wrn, and RecQL4 are mutated in Bloom's Syndrome, Werner's Syndrome, and Rothmund-Thomson Syndrome,

respectively, which are characterized by genomic instability and cancer susceptibility (reviewed in Chakraverty and Hickson 1999; Bennett and Keck 2004). Although there are 5 RecQ homologs in humans, Blm appears to be the closest functional homolog of Sgs1 (Watt *et al.* 1996).

The 164 kDa Sgs1 protein consists of 1447 amino acids and contains 7 conserved helicase motifs, a C-terminal conserved region (Ct domain), and an HRD (Helicase and RNase D) C-terminal domain, as well as a serine-rich, highly acidic region located more towards the N-terminal region (see Fig. 4.4). The seven conserved motifs are found in variety of RNA and DNA helicases, and are designated I, Ia, II, III, IV, V, and VI. Sgs1 also contains an additional motif located N-terminal to motif I that is designated as motif 0. Motifs I and II house the Walker A and B motifs, and these are important, along with motif 0, in ATP binding and hydrolysis (reviewed in Bennett and Keck 2004). The HRD domain is found in all RecQ homologs as well as in RNase D homologs, and is thought to play a role in nucleic acid binding (Morozov *et al.* 1997). Interestingly, this domain is not required for helicase or ATPase activity, but does seem to be required for suppression of some mutant phenotypes (Bennett and Keck 2004). The Ct domain contains both a Zn^{++} binding region and a winged-helix domain, which may play a role in DNA binding and protein-protein interactions (Figure 4.3; Bennett and Keck 2004).

Sgs1 has been implicated in the intra-S phase checkpoint, the replication checkpoint, DNA replication, and telomere maintenance, as well as in various meiotic and mitotic recombination processes (Cobb *et al.* 2002; Bachrati and Hickson 2003). *sgs1* mutants show elevated mitotic HR (Watt *et al.* 1996) and an increase in gross chromosomal rearrangements comparable to that in a *msh2*Δ mutant (Myung *et al.* 2001). In addition, yeast *sgs1*Δ mutants exhibit premature aging and shorter life span (Sinclair *et al.* 1997), not unlike homozygous mutations in *WRN* that lead to Werner's

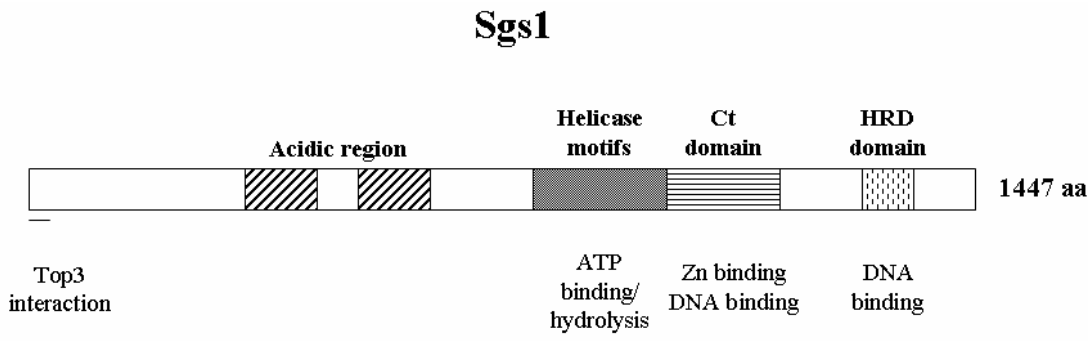

Figure 4.4. Domain structure of the Sgs1 protein. The N-terminus of Sgs1 contains the Top3 interaction domain and a serine-rich acidic domain. The central portion of the protein contains the conserved helicase motifs, the first few of which are critical for ATP binding and hydrolysis. The Ct domain contains both a Zn^{++} binding region and a winged-helix domain, which may play a role in DNA binding and protein-protein interactions. The C-terminal HRD domain is conserved in RecQ helicases and RNase D homologs, but is not required for helicase or ATPase activity. The structure and function of Sgs1 are reviewed in Bennett and Keck (2004). The $Sgs1_{400\text{-}1268}$ recombinant protein purified in this study lacks the first 399 amino acids and the last 179 amino acids, thus retaining all of these domains except for the Top3-interacting region.

syndrome in humans (Bachrati and Hickson 2003). Homozygous *sgs1*Δ diploids are highly sensitive to ionizing radiation, which is suggestive of defective recombinational repair (Gangloff *et al.* 2000). *sgs1* mutants are also sensitive to the alkylating agent methyl methane sulfonate (MMS) and to hydroxyurea (HU), which causes replication fork collapse (Yamagata *et al.* 1998; Mullen *et al.* 2000; Bennett and Wang 2001). When an *sgs1*Δ mutation is combined with that of another helicase, Srs2, *sgs1*Δ*srs2*Δ double mutants have low viability that is dependent upon functional recombination pathways (Gangloff *et al.* 2000).

The full-length Sgs1 protein has not been purified because it is insoluble when overexpressed (Bennett *et al.* 1998). Initial experiments thus employed an *in vitro* rabbit reticulocyte coupled transcription/translation system to obtain the full-length protein (Lu *et al.* 1996). More recent experiments have shown that fragments of the Sgs1 protein can be overexpressed successfully and purified from yeast (Bennett *et al.* 1998). Bennett *et al.* purified amino acids 400-1268 from yeast and found that the resulting protein exhibited DNA-dependent ATPase activity and ATP-dependent 3' to 5' helicase activity on dsDNA and DNA-RNA heteroduplexes (Bennett *et al.* 1998). The recombinant Sgs1 protein binds *in vitro* to ds/ssDNA junctions with 3' overhangs and forms DNaseI- and hydroxyl radical-protected regions on both strands (Bennett *et al.* 1999).

Heteroduplex rejection via an unwinding mechanism. Genetic studies in several labs have implicated Sgs1 in anti-recombination during HR (Myung *et al.* 2001; Spell and Jinks-Robertson 2004; Sugawara *et al.* 2004; Goldfarb and Alani 2005), and the helicase activity of Sgs1 is required for this anti-recombination role (Spell and Jinks-Robertson 2004; Goldfarb and Alani 2005). Consistent with these findings, a study by Sugawara *et al.* using a 3-repeat SSA competition assay showed that heteroduplex

rejection is likely to occur through an unwinding mechanism rather than by nucleolytic degradation (Sugawara *et al.* 2004). In their system, a DSB could be repaired by SSA with a choice of two different repeats on one side of the break. While wild-type cells completed SSA using both repeats at equal frequencies when all three repeats were completely homologous, insertion of mismatches into one repeat led to an increase in SSA events using the completely identical repeat and disfavoring the divergent repeat. If heteroduplex rejection were to occur via nucleolytic degradation of inappropriate intermediates, one would expect that abortion of recombination between the mismatched repeats would destroy the intermediate, precluding any further chances at SSA. Instead, it appears that recombination initiated between the mismatched repeats followed by rejection does not inhibit a further homology search and later SSA at an identical repeat sequence.

The bias in repeat choice in the above assay in the presence of one divergent and one identical repeat was also dependent upon the Sgs1 helicase and Msh6 (Sugawara *et al.* 2004). Further genetic studies using a standard two-repeat SSA assay found that mismatch binding (*msh2-K564E, msh6-F337A*) and ATP binding and hydrolysis mutants (*msh2-S656P, msh2-R730W, msh6-G987D*) of Msh2-Msh6 were defective in heteroduplex rejection during SSA between repeats with 3% sequence divergence, suggesting that both of these functions are required for rejection (Goldfarb and Alani 2005). Deletion of domain I of Msh2 (*msh2*Δ*1*), which is important for DNA binding during Msh2-Msh3-dependent repair, had no effect on rejection (Goldfarb and Alani 2005; Lee *et al.* 2007). Consistent with these genetic studies, a physical interaction between the Sgs1 helicase and Msh6 has been detected in a large-scale TAP-tagging screen (Gavin *et al.* 2002). Based on this mounting evidence, Goldfarb and Alani (2005) proposed that heteroduplex rejection during single-strand annealing in *S. cerevisiae* entails mismatch recognition and binding by Msh2-Msh6

and either recruitment of the Sgs1 helicase to improper recombination intermediates or stimulation of its unwinding activity to facilitate their dissolution, as depicted in Figure 4.5.

Studies in the human system support this unwinding model of heteroduplex rejection. Three of the five known human Sgs1 homologs have been shown to interact with the mismatch repair machinery: Blm and hMsh6 physically interact both *in vivo* and *in vitro* (Pedrazzi *et al.* 2003), RecQ1 interacts with ExoI, Mlh1, and Msh2-Msh6 in coIP and ELISA assays (Doherty *et al.* 2005), and Wrn physically interacts with Msh2-Msh6, Msh2-Msh3, and Mlh1-Pms2 through distinct protein domains (Saydam *et al.* 2007). The hMsh2-Msh6 complex is reported to stimulate the helicase activity of Blm on Holliday junctions (Yang *et al.* 2004) and also stimulates the helicase activity of RecQ1 (RecQL1) on flapped DNA substrates containing both double-stranded and single-stranded arms (Doherty *et al.* 2005). Perhaps most convincingly, hMsh2-Msh6 stimulates the helicase activity of Wrn on DNA substrates containing 3' single-stranded flaps, and this stimulation is enhanced in the presence of a single G/T mismatch (Saydam *et al.* 2007). Comparable studies with the yeast proteins have not been reported. The goal of the work explained below is to test the unwinding model of heteroduplex rejection proposed in Figure 4.5 *in vitro* using purified *S. cerevisiae* Sgs1 and Msh2-Msh6 proteins by assessing physical interactions, DNA binding, and helicase activity.

Materials and Methods

Purification of $Sgs1_{400\text{-}1268}$. The expression plasmid and strain for the 6-His-tagged, HA-tagged soluble fragment of Sgs1 containing amino acids 400-1268 of 1447 was created in the Wang lab at Harvard University (Bennett *et al.* 1998) and

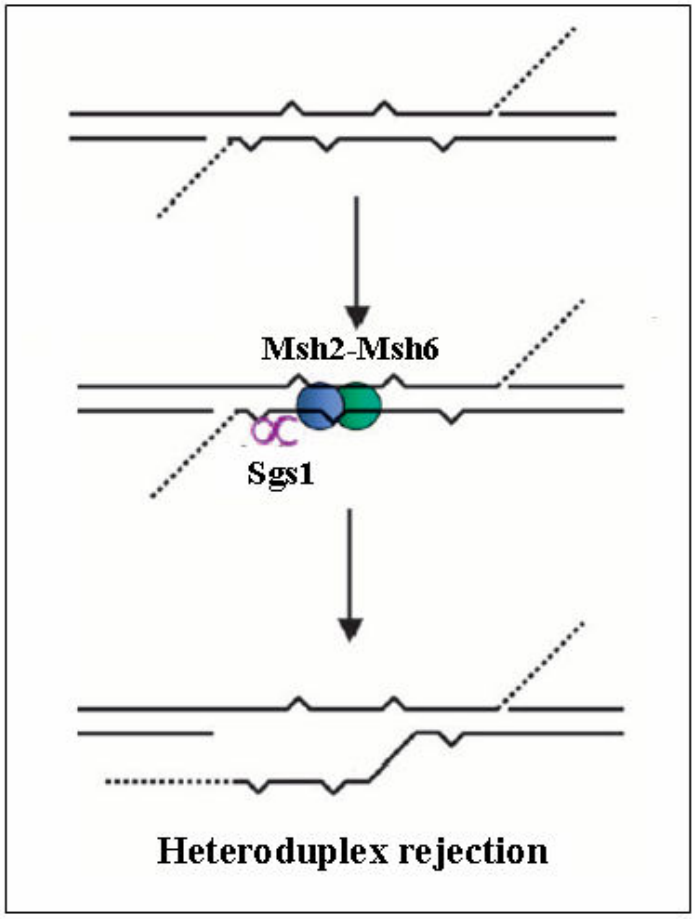

Figure 4.5. Model for heteroduplex rejection during single-strand annealing. This figure is adapted from Goldfarb and Alani (2005). The top figure represents a single-strand annealing intermediate that contains five mismatches. It is proposed that Msh2-Msh6 recognizes and binds to DNA mismatches revealed in the heteroduplex upon annealing of homologous sequences. Msh2-Msh6 may recruit and/or stimulate the Sgs1 helicase to facilitate unwinding of mismatched recombination intermediates.

obtained from the Lahue lab (University of Nebraska Medical Center). The expression plasmid (pRB222; pEAE265) was later put into the Alani lab expression strain, EAY33. The resulting EAY2339 Sgs1 expression strain was grown to saturation at 30° C in synthetic complete medium lacking uracil. Six liters of yeast-peptone medium containing 2% lactate, 3% (v/v) glycerol were inoculated with approximately 20 ml saturated culture per liter of growth medium to an OD_{600nm} of 0.1 and grown in a 30° C shaker. At OD_{600nm} of 0.3 - 0.4, protein expression was induced by the addition of galactose to a 2% (w/v) final concentration. Following a six-hour induction, cells were pelleted by centrifugation at 4,000 rpm for 30 minutes at 4° C in a Beckman J6B rotor. Pellets were washed and combined using 10 mls Lysis buffer (20 mM Tris pH 7.5, 200 mM KCl, 2% (v/v) glycerol) and pelleted in a 250 ml plastic centrifuge bottle at 13,000 rpm for 30 minutes in a GSA rotor in a 4° C Sorvall centrifuge. The cell pellet was resuspended in 10 mls Lysis buffer and dropped drip-by-drip into liquid nitrogen to form popcorn-like beads. Beads of frozen cells were stored at -80° C in a freezer box lined with plastic wrap until lysis.

All biochemical solutions were made and stored in acid-washed glassware, and all purification buffers contained 1 mM PMSF and 10 mM β-mercaptoethanol (Sigma-Aldrich). Cell beads were ground with dry ice in a coffee grinder for one minute with constant agitation. Lysate/dry ice powder was stored in 50 ml conical tubes with loosened caps at -20° C for 1-2 days until no dry ice remained. Lysed cell powder was thawed on ice, resuspended and combined in 10 ml Lysis buffer + 1 mM PMSF and spun in 40 ml glass centrifuge tubes for 30 minutes at 19,000 rpm at 4° C in a SS-34 rotor in the Sorvall centrifuge to clear the lysate. 1 M imidazole was added to bring the lysate to 20 mM imidazole for subsequent column chromatography steps. Ni-NTA beads (Qiagen) resuspended in 1 ml of 20 mM Tris pH 7.5, 200 mM NaCl, 20 mM imidazole were added to the cleared lysate in a 50 ml conical tube and incubated at 4°

C on an orbital rocker for 1 hour. The lysate/bead suspension was added to a disposable 0.8 x 4 cm Poly-Prep column (BioRad) previously washed with 5 mls of 20 mM Tris pH 7.5, 200 mM NaCl, 20 mM imidazole. The Ni-NTA column was then washed with 10 mls of 20 mM Tris pH 7.5, 200 mM NaCl, 40 mM imidazole, and the Sgs1 protein was eluted off the column using 5 mls of 20 mM Tris pH 7.5, 200 mM NaCl, 80 mM imidazole and collected in 0.5 ml fractions in 1.5 ml Eppendorf tubes. 8 µl samples of each fraction were boiled 10 minutes in SDS loading dye and loaded on an 8% SDS-PAGE gel alongside appropriate amounts of the pre- and post-induction whole-cell lysates, cleared lysate, column flowthrough, and washes.

Fractions containing high amounts of Sgs1 and relatively few contaminants were pooled, concentrated using Centricon 30 kDa-, 50 kDa-, or 100 kDa-cutoff spin concentrators (Amicon, Inc.) and dialyzed using Spectra/Por 12,-14,000 Da-cutoff 25 mm dialysis tubing (Spectrum Laboratories/VWR Scientific) overnight in 1 L of 20 mM Tris pH 8.0, 50 mM NaCl, 25% (v/v) glycerol, 1 mM β-mercaptoethanol. Protein aliquots were snap-frozen in liquid nitrogen and stored at -80° C until use. Protein concentrations were determined by incubating protein samples for 5 minutes in BioRad Protein Assay reagent (BioRad) and water, taking absorbance readings at 595 nm, and comparing to a BSA (BioRad Protein Assay Standard II) standard curve created using Excel. Use of a second column, PBE94 Polybuffer Exchanger (Amersham Biosciences), and elution on a 0.2 – 1.0 M NaCl gradient did not significantly improve $Sgs1_{400\text{-}1268}$ protein purity as judged by SDS-PAGE and Coomassie staining, and thus was not done for later preparations. Representative gels from purification of $Sgs1_{400\text{-}1268}$ are shown in Figure 4.6. Pre-stained broad range protein ladder (New England Biolabs, Inc.) was used to assess protein size. $Sgs1_{400\text{-}1268}$ protein purified from a single Nickel column in this manner exhibits ATP-

dependent 3' to 5'-specific DNA helicase activity with as little as 1 nM helicase (see below).

A helicase-dead (Sgs1-hd; Sgs1-K706A; Lu *et al.* 1996) version of the $Sgs1_{400-1268}$ expression construct was made by creation of a single lysine to alanine change at position 706 in the Sgs1 protein in the wild-type expression vector to yield pEAE276, which was then expressed in the EAY33 protease-deficient strain to allow purification of the mutant protein as described above (mutagenesis and protein purification by Eric Alani). The helicase-dead protein exhibited no helicase activity with up to 20 nM helicase per reaction as shown in Figure 4.8, consistent with the lack of helicase activity exhibited by the Sgs1-hd full-length protein synthesized *in vitro* using a rabbit reticulocyte transcription/translation system (Lu *et al.* 1996).

Purification of Msh2-Msh6. *MSH2* and *MSH6* were co-overexpressed from *GAL10* promoters on 2 μm plasmids pEAE9 and pEAE218 in the protease-deficient yeast strain EAY960 (EAY33 derivative; same genotype as Sgs1 expression strain). Four liters of ura- trp- synthetic dropout medium + 2% lactate and 3% (v/v) glycerol were inoculated with 20 ml of saturated overnight cultures grown in 2% (w/v) glucose. At $OD_{600nm} = 0.7 – 0.8$, protein expression was induced with galactose (2% (w/v) final concentration) for 7 hours. Cells were harvested by centrifugation in 1 L plastic bottles at 4,000 rpm in a J6-B rotor for 30 minutes at 4° C. Pellets were washed in 25 mM Tris pH 7.5, 1 mM EDTA, 0.3 M NaCl, frozen as beads in liquid nitrogen, and stored at -80° C.

Beads were lysed with dry ice in a coffee grinder and stored in 50 ml conical tubes in the -20° C freezer for 2 days. Lysates were thawed on ice and cleared by centrifugation at 19,000 rpm for 40 minutes in an SS-34 rotor in the Sorvall centrifuge at 4° C. Subsequent chromatography steps were similar to those in Alani (1996). The

supernatant was loaded on an equilibrated PBE94 anion exchange column (resin from Amersham Biosciences) and washed with 5 volumes of 25 mM Tris pH 7.5, 1 mM EDTA, 0.3 M NaCl. Protein was eluted from the column on a 0.3 – 1.0 M NaCl gradient and collected in 3 ml fractions. Fractions containing the majority of Msh2-Msh6 and lacking the main contaminant (which runs just below Msh2 on an 8% SDS-PAGE gel) were pooled. NaCl concentration of the pooled sample was determined by measuring the conductivity (Wilson laboratory conductivity meter) and comparing to known NaCl concentrations on a standard curve. The pooled sample was gently diluted down to 0.2 M NaCl in 25 mM Tris pH 7.5, 1 mM EDTA.

Pooled protein was loaded onto an equilibrated single-stranded DNA-cellulose column (single-stranded deoxyribonucleic acid-cellulose from calf thymus DNA; Sigma), washed with 0.2 M NaCl, eluted with 0.5 M NaCl, and collected in 0.75 ml fractions at 20 ml/hr. Fractions containing the most protein were pooled and diluted to 0.3 M NaCl prior to loading on a second PBE94 column. After washing with 0.3 M NaCl, protein was eluted using 0.5 M NaCl and collected in 0.75 ml fractions. Fractions containing concentrated protein were pooled and concentrated using a Centricon 50 kDa- or 100 kDa-cutoff spin concentrator (Amicon, Inc.) before snap-freezing aliquots in liquid nitrogen and storing at -80° C. The Msh2 and Msh6 proteins have been purified in our lab previously (Alani 1996). A representative gel showing the purity of Msh2-Msh6 following each chromatography step is shown in Figure 4.10.

DNA substrates. DNA oligonucleotides used in this study are listed in Table 4.1. HPLC-purified synthetic DNA oligo substrates (Integrated DNA Technologies, Inc.) were 5' end-labeled with ^{32}P using T4 Polynucleotide kinase (New England Biolabs) and γ^{32}P-ATP (Perkin Elmer). 250 pmol of oligo resuspended in 10 mM Tris pH 7.6,

50 mM NaCl, 1 mM EDTA was labeled in a 50 µl reaction at 37° C for at least 30 minutes followed by 20 minutes at 60° C to kill the kinase. Excess nucleotide and storage dye was removed from oligo-labeling reactions using Micro Bio-Spin P-30 Tris chromatography columns (BioRad). To make double-stranded and partially double-stranded substrates for helicase and gel shift experiments, labeled oligos were annealed to the relevant unlabeled oligos or φX174 virion DNA (New England Biolabs) in 1x oligo buffer (10 mM Tris pH 7.6, 50 mM NaCl, 1 mM EDTA) by heating for 5 minutes at 95° C in an oil heat block and letting cool slowly to room temperature. Substrates used in this study are listed in Table 4.2. Substrates were diluted appropriately in 1x oligo buffer prior to use.

Gel shifts. Electrophoretic gel mobility shift assays were performed using up to 200 nM purified Msh2-Msh6 and/or $Sgs1_{400\text{-}1268}$ proteins incubated 5 minutes at room temperature in 1x binding buffer (200 mM Tris pH 7.5, 40 µg/ml BSA, 1 mM DTT, 50 mM NaCl), 100 nM radiolabeled DNA substrate, and 8% sucrose. Samples were run on 4% native acrylamide/0.5x TBE gels at 130 volts for 45 minutes and dried on 3mm Whatman paper using a BioRad Model 583 gel dryer at 80º C for 1 hour. Following overnight exposure to a phosphor storage screen (Molecular Dynamics), gels were visualized using a Storm 280 phosphorimager (Molecular Dynamics/GE Healthcare) and bands were quantified using ImageQuant (GE Healthcare).

Helicase assays. Helicase assays were performed in 20 µl reactions in 20 mM Tris pH 7.5, 2 mM ATP, 2 mM $MgCl_2$, 2 mM DTT, 100ug/ml BSA (New England Biolabs, Inc.), 50-150 mM NaCl, 1 nM DNA substrate, and 10 nM unlabeled single-stranded DNA competitor identical to the labeled strand (unless otherwise noted) at 30º C for 30 minutes and stopped by the addition of 5 µl stop buffer (100 mM Tris,

Table 4.1. DNA Oligos used in this study.

Name	Sequence (5' to 3')	# bases	Source
S1	ACCGAATTCTGACTTGCTAGGACATCTTTGCCCACGTTGA	40	From Surtees and Alani 2006
S2	TCAACGTGGGCAAAGATGTCCTAGCAAGTCAGAATTCGGT	40	From Surtees and Alani 2006
S4	ATGTCCTAGCAAGTCAGAATTCGGTCGATAGATCTCTGAT	40	From Jennifer Surtees, Alani lab
S11	ATGTCCTAGCAAGTCAGAATTCGGT	25	From Jennifer Surtees, Alani lab
S12	TCAACGTGGGCAAAGATGTCCTAGC	25	From Jennifer Surtees, Alani lab
AO2177	ATGTCCTAGCAAGTTAGAATTCGGTCGATAGATCTCTGAT	40	This study; S4 with a C to T change
AO2181	ATGTCCTAGCAAGTTAGAATTCGGT	25	This study; S11 with a C to T change
AO2353	ATGTCCTAGCAAGGTCAGAATTCGGT	26	This study; S11 with a central +1 G insertion
AO2167	GCATCACGCTACCGAATTCTGACTTGCTAGGACATCTTTGCCCACGTTGACCCCGCACCG	60	From Aaron Plys, Alani lab
AO2168	CGGTGCGGGGTCAACGTGGGCAAAGATGTCCTAGCAAGTCAGAATTCGGTAGCGTGATGC	60	From Aaron Plys, Alani lab
AO2188	GACATCTTTGCCCACGTTGACCCCGCACCG	30	From Aaron Plys, Alani lab
AO2385	GACTTGCTAGGACATCTTTGCCCACGTTGACCCCGCACCG	40	This study
AO2273	GTGGGCAAAGATGTCCTAGCAAGTCAGAATTCGGTAGCGTGATGC	45	This study
AO2274	GTGGGCAAAGATGTCCTAGCAGGTCAGAATTCGGTAGCGTGATGC	45	This study; AO2273 with a central A to G change
AO2349	GTGGGCAAAGATGTCCTAGCAAGGTCAGAATTCGGTAGCGTGATGC	46	This study; AO2273 with a central +G insertion
AO2387	CAAAGTAAGAGCTTCTCGAGCTGCGC	26	Oligo 9 in Whitby *et al.* 1994 EMBO J.
AO2388	CAAAGTAAGAGCTTTCTCGAGCTGCGC	27	This study; AO2387 with a central +T
AO2389	CAAAGTAAGAGCTTCTCGAGCTGCGCAAGGATAGGTCGAATTTTCTCATTTT	52	Oligo 4 in Whitby *et al.* 1994 EMBO J.
AO2390	CAAAGTAAGAGCTTCTCGAGCTGCGCCAAGGATAGGTCGAATTTTCTCATTTT	53	This study; AO2389 with a central +C insertion

Table 4.2. DNA substrates used for helicase and gel shift assays.

Name	Structure	Nucleotides	Mismatches
S1/S2	duplex	40/40	none
S1/S3	forked	40/40	none
S1/S4	two 3' overhangs	40/40	none
S1/AO2177	two 3' overhangs	40/40	central G/T
S1/S11	3' overhang	40/25	none
S1/AO2181	3' overhang	40/25	central G/T
S1/AO2353	3' overhang	40/26	central +1 G
S1/S12	5' overhang	40/25	none
AO2167/AO2168	duplex	60/60	none
AO2168/AO2188	3' overhang	60/30	none
AO2168/AO2385	3' overhang	60/40	none
AO2167/AO2273	3' overhang	60/45	none
AO2167/AO2274	3' overhang	60/45	central G/T
AO2167/AO2349	3' overhang	60/46	central +1 G
AO2387/φX174	oligo + circle	26/5386	none
AO2388/φX174	oligo + circle	27/5386	central +1 T
AO2389/φX174	oligo + circle	52/5386	none
AO2390/φX174	oligo + circle	53/5386	central +1 C

200 mM EDTA, 0.5% (w/v) Proteinase K (New England Biolabs), 2.5% (w/v) SDS) and incubation at 37º C for 15 to 30 minutes (derived from Bennett *et al.* 1998; Bennett *et al.* 1999). Samples were run on 6%, 8%, or 10% native polyacrylamide/1x TBE gels in DNA loading dye (Bromophenol blue, Xylene cyanol, glycerol) and run for 45 minutes to 3 hours depending on substrate size. Gels were dried on 3 mm Whatman paper using a BioRad Model 583 gel dryer at 80º C for 1 – 2 hours, exposed to a phosphor storage screen for several days, and scanned and quantified as described above.

Coimmunoprecipitation of purified proteins. Equimolar amounts of purified Msh2-Msh6 and $Sgs1_{400\text{-}1268}$ proteins were incubated with 20 U of DNase I in 20 mM Tris pH 7.5, 100 mM NaCl, 3 mM $MgCl_2$ for 30 minutes at room temperature. DNase I activity was confirmed by digestion of 1 µg of control DNA and agarose gel analysis. 1 µl of 12CA5 mouse monoclonal anti-HA antibody (Roche) or 0.5 µl of anti-Msh2 polyclonal antibody were added per reaction and incubated 1 hour at 4º C. Protein A agarose beads were suspended 1:1 (v/v) in 50 mM Tris pH 7.5, 100 mM NaCl, 1 mM EDTA and 20 µl of the suspension were incubated with each sample for 1 hour. Beads were washed three times with 200 µl of 50 mM Tris pH 7.5, 100 mM NaCl, 1 mM EDTA, 0.1% NP-40 and twice with 200 µl of 50 mM Tris pH 7.5, 50 mM NaCl, 1 mM EDTA, 0.1% NP-40. Beads were boiled in SDS-PAGE loading dye for ten minutes, and samples were run on 8% SDS-PAGE gels followed by staining with Coomassie blue.

Gel filtration. Gel filtration was carried out at the Cornell Core facility for Protein Purification and Characterization with the help of Dr. Cynthia Kinsland. The apparatus used was an AKTA FPLC with a 24 ml Superdex 200 10/300 GL gel

filtration column (GE Healthcare). Experiments were performed in 20 mM Tris pH 7.5, 150 mM NaCl (200 mM NaCl for runs containing Msh2-Msh6) and run at a flow rate of 0.5 ml/min. Pressure and conductivity readings remained constant at approximately 1.1 MPa and 15 mS/cm, respectively. Standard proteins Ferritin (440 kDa), Catalase (250 kDa), and Aldolase (158 kDa) obtained from GE Healthcare were resuspended in 20 mM Tris pH 7.5, 150 mM NaCl. All samples were injected at 50 µg or 100 µg in a 0.5 ml injection volume using a 2 ml injection loop. Peak elution volumes for standard proteins were plotted over the log of the protein molecular weight (kDa) to form a standard curve and linear trend lines were calculated in Excel.

Aliquots of $Sgs1_{400\text{-}1268}$ protein were thawed on ice, pooled, and concentrated using a Centricon 30 kDa-cutoff spin concentrator (60 µg input for minimum of 29 µg needed for sample) to a final volume of approximately 300 µl. 200 µl (71 µg) of Msh2-Msh6 were added to the concentrated Sgs1 protein and incubated on ice overnight prior to gel filtration. Following injection into the FPLC, 250 µl fractions were collected in 96-well plates in serpentine rows along the entire 24 ml elution volume of the column. In order to analyze the contents of the fractions, samples were precipitated with ¼ volume 100% (w/v) TCA at 4° C, washed twice with cold acetone, boiled in SDS loading dye, and run on 8% SDS-PAGE followed by Coomassie blue staining.

Results

Purification of $Sgs1_{400\text{-}1268}$. HA-tagged, 6xHis-tagged Sgs1 protein bearing amino acids 400 to 1268 of the full-length 1447 was overexpressed in yeast and purified over a Nickel resin as described in Materials and Methods and shown in Figure 4.6. $Sgs1_{400\text{-}1268}$ eluted primarily in the first few fractions with 80 mM imidazole. In

further chromatography steps, Sgs1 eluted off of a PBE94 column at approximately 0.6 M NaCl, and fractions 12-14 out of 19 were pooled for dialysis (Figure 4.6). A helicase-dead version of the soluble Sgs1 fragment, Sgs1-hd$_{400\text{-}1268}$, was purified similarly by E. Alani. The yield from 6 L of induced culture ranged from 39 to 164 μg of Sgs1$_{400\text{-}1268}$ protein in three separate preparations. The purified recombinant proteins, with predicted molecular weights of 102 kDa (calculated using www.biopeptide.com/PepCalc), run at approximately 125 kDa on 8% SDS-PAGE (see Figure 4.6), consistent with previous studies (Bennett *et al.* 1998).

Purified Sgs1$_{400\text{-}1268}$ protein exhibits 3' to 5' helicase activity. Femtomole quantities of purified Sgs1$_{400\text{-}1268}$ protein were added to helicase reactions containing 2 mM ATP, 2 mM $MgCl_2$, and 1 nM double-stranded duplex (S1/S2), 3' overhang (S1/S11), or 5' overhang (S1/S12) annealed 40mer oligo DNA substrates in the presence of 10 nM unlabeled ssDNA competitor identical to the labeled strand. Purified Sgs1$_{400\text{-}1268}$ exhibits helicase activity specifically on substrates containing 3' single-stranded DNA as shown in Figure 4.7, consistent with its published 3' to 5' helicase activity. No significant helicase activity was observed on double-stranded duplex or 5' overhang substrates (Figure 4.7). Similarly purified Sgs1$_{400\text{-}1268}$-K706A (Sgs1-hd) helicase-dead protein exhibited no significant helicase activity on the 3' overhang substrate (S1/S11) with up to 20 nM protein, compared to detectable helicase activity at as little as 1 nM Sgs1-$_{400\text{-}1268}$ wild-type protein (Figure 4.8). Helicase activity on forked DNA substrates was comparable to that on 3' overhang Detection of helicase activity was particularly sensitive to the presence of unlabeled ssDNA competitor; in its absence, the unwound DNA strands can readily re-anneal, masking any helicase activity.

Figure 4.6. Purification of $Sgs1_{400-1268}$ following overexpression in yeast. Representative 8% SDS-PAGE gels following purification of $Sgs1_{400-1268}$ from 6 L of yeast strain EAY2339 induced for overexpression for 6 hours. A. Cleared lysate was incubated with Ni-NTA resin and $Sgs1_{400-1268}$ eluted with 80 mM imidazole. B. Pooled fractions from the Ni-NTA column were run over a PBE94 anion exchange resin and eluted on a 0.2 – 1.0 M NaCl gradient. C. Summary of Sgs1 purification showing pooled fractions from Ni-NTA and PBE94 columns, sample concentrated by Centricon spin column, and sample dialyzed overnight into storage buffer as described in Materials and Methods. Proteins were visualized on the gel by staining with Coomassie blue. Molecular weight standards are from pre-stained broad range protein marker (New England Biolabs, Inc.).

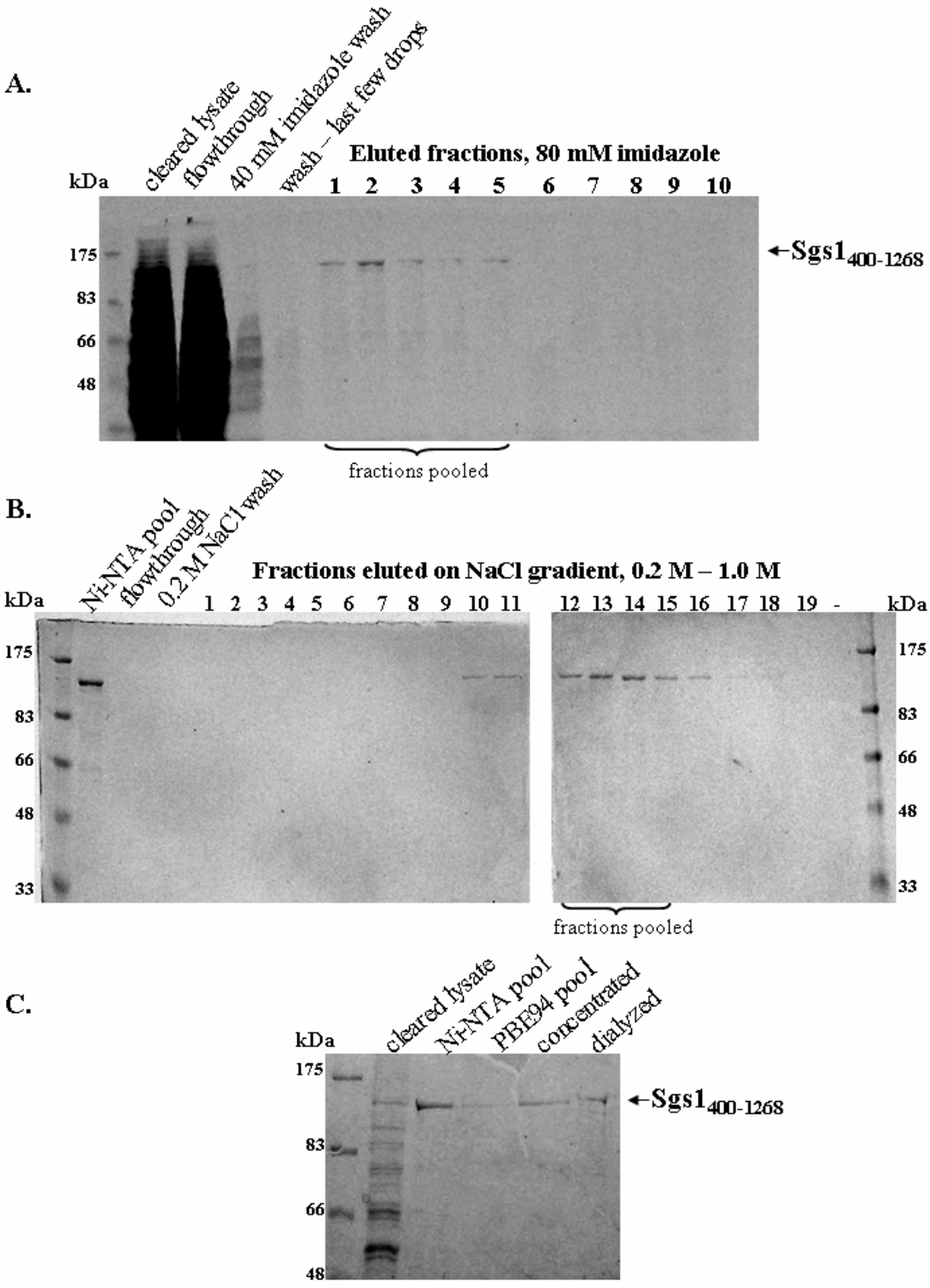
A.
cleared lysate
flowthrough
40 mM imidazole wash
wash – last few drops
Eluted fractions, 80 mM imidazole
kDa
1 2 3 4 5 6 7 8 9 10
175
83
66
48
←Sgs1400-1268
fractions pooled
B.
Ni-NTA pool
flowthrough
0.2 M NaCl wash
Fractions eluted on NaCl gradient, 0.2 M – 1.0 M
kDa
1 2 3 4 5 6 7 8 9 10 11
12 13 14 15 16 17 18 19 -
kDa
175
83
66
48
33
fractions pooled
C.
cleared lysate
Ni-NTA pool
PBE94 pool
concentrated
dialyzed
kDa
175
83
66
48
←Sgs1400-1268

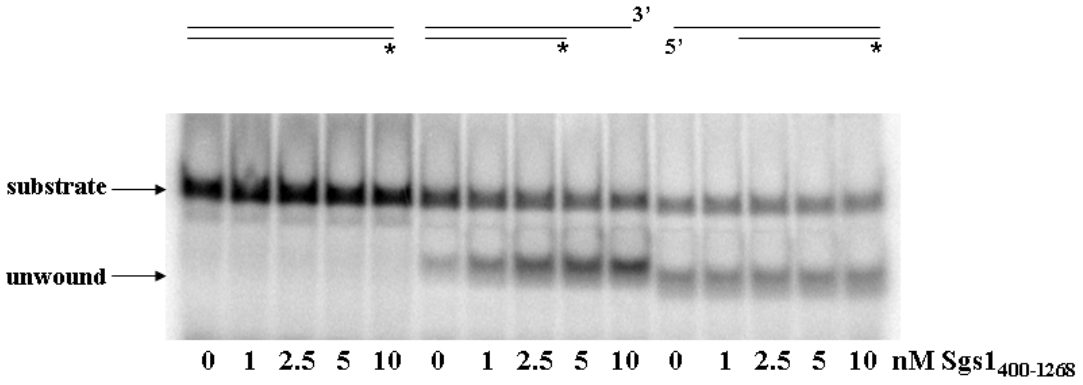

Figure 4.7. Substrate specificity of $Sgs1_{400-1268}$ helicase. 1 nM radiolabeled double-stranded duplex (S1/S2), 3' overhang (S1/S11), and 5' overhang substrates (S1/S12) were incubated with 0 to 10 nM purified $Sgs1_{400-1268}$ in 2 mM ATP, 2 mM $MgCl_2$ in the presence of 10 nM unlabeled competitor ssDNA for 30 min at 30° C. Samples were run on a 10% native polyacrylamide/1x TBE gel, dried, and exposed to a phosphor storage screen.

On 1 nM S1/S11 3' overhang substrate, which contains 25 bp of homoduplex DNA plus a 15 nucleotide 3' overhang, Sgs1 helicase activity peaks at 5 nM protein (See Figures 4.7 and 4.8). While helicase activity is detectable on 3' overhang substrates of various lengths, only those with short (25 bp) duplexes are efficiently unwound under these conditions, as shown graphically in Figure 4.9. 3' overhang substrates containing duplex regions of 30 bp (AO2168/AO2188) and 45 bp (AO2167/2273) exhibited very little unwinding in the presence of up to 10 nM Sgs1 helicase (Figure 4.9), in contrast to published studies of Sgs1 efficiently unwinding substrates with duplexes as long as 140 bp (Bennett *et al.* 1998). These difficulties in detecting helicase activity using substrates with longer than 25 bp duplexes hold true for annealed oligo substrates as well as oligos annealed to φX174 virion DNA, with detectable but inefficient (~3% of total substrate) observable helicase activity (data not shown).

$Sgs1_{400\text{-}1268}$ helicase activity is dependent upon NaCl concentration. Previous studies using the $Sgs1_{400\text{-}1268}$ soluble fragment did not report the effect of NaCl concentration helicase activity. By titrating in NaCl in standard helicase reactions containing unlabeled competitor ssDNA, Sgs1 helicase activity on 3' overhang substrates (S1/S11; 25 bp duplex) was found to be optimal between 75 and 200 mM NaCl (Figure 4.10). For this reason, most helicase experiments were performed at 100 mM NaCl unless otherwise specified. Increasing the $MgCl_2$ concentration was found to have an inhibitory effect on Sgs1 helicase activity (data not shown). Other salts have not been tested in this study.

Purification of Msh2-Msh6. The Msh2-Msh6 complex was overexpressed and purified from yeast as described in Materials and Methods and shown in Figure 4.11.

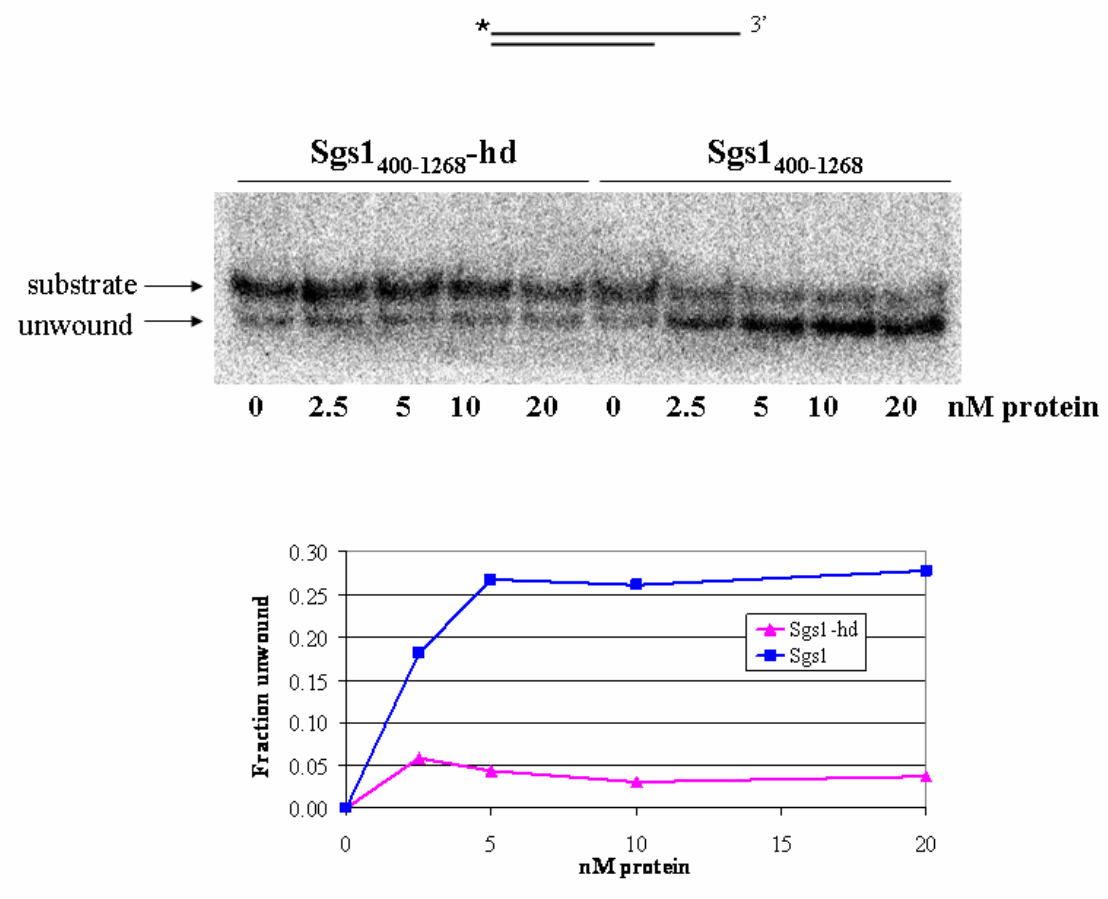

Figure 4.8. $Sgs1_{400\text{-}1268}$ vs. $Sgs1\text{-}hd_{400\text{-}1268}$ helicase activity on 3' overhang substrates. Helicase reactions containing 0 to 20 nM of $Sgs1_{400\text{-}1268}$ or $Sgs1\text{-}hd_{400\text{-}1268}$, 1 nM 3' overhang substrate (S1/S11), and 10 nM cold competitor DNA were run on a 10% native polyacrylamide/1x TBE gel, dried, and exposed to a phosphor storage screen. $Sgs1_{400\text{-}1268}$ exhibits efficient helicase activity on 3' overhang DNA substrates that peaks at 5 nM protein. Similarly purified $Sgs1\text{-}hd_{400\text{-}1268}$ helicase-dead protein exhibits no significant helicase activity with up to 20 nM protein per reaction.

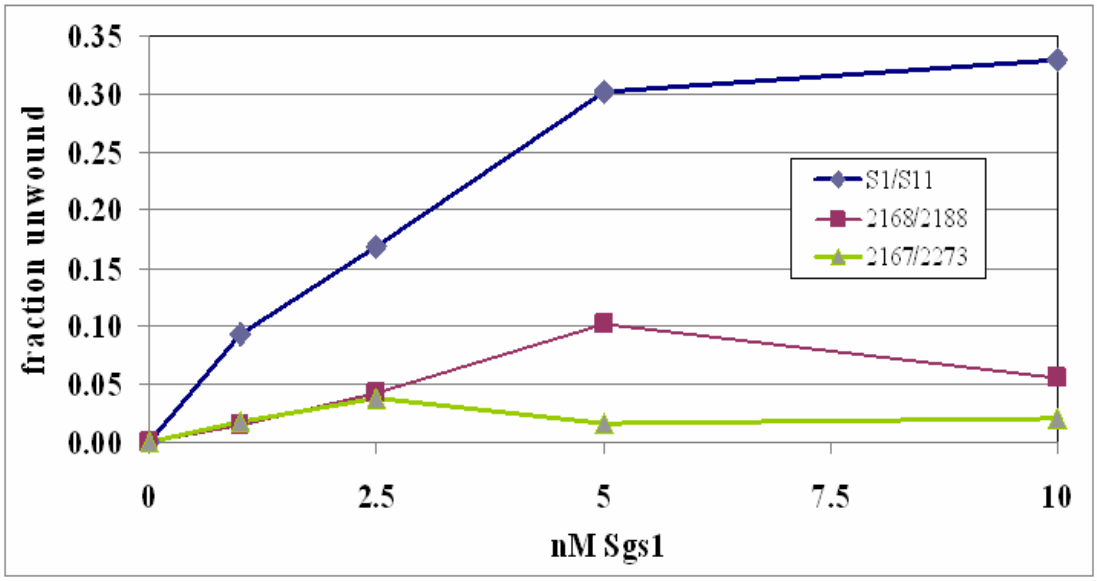

Figure 4.9. $Sgs1_{400\text{-}1268}$ helicase activity on 3' overhang substrates of various lengths. S1/S11 has a 25 bp duplex plus 15 nt overhang, 2168/2188 has a 30 bp duplex plus 30 nt overhang, and 2167/2273 has a 45 bp duplex plus 15 nt overhang. All three substrates are detectably unwound by Sgs1, but only S1/S11 shows unwinding of a significant fraction of the input DNA.

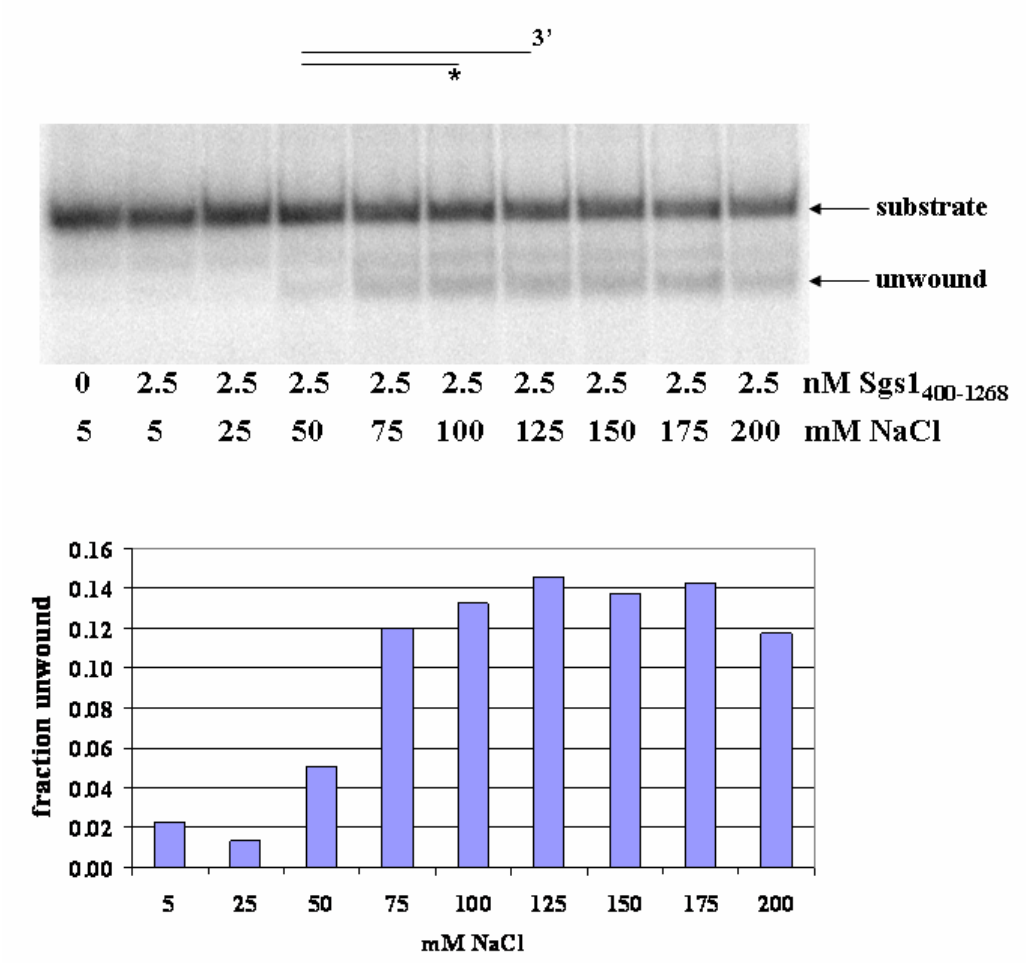

Figure 4.10. Salt dependence of Sgs1$_{400\text{-}1268}$ helicase activity on short 3' overhang substrates. Helicase assays containing 0 to 2.5 nM Sgs1$_{400\text{-}1268}$, 1 nM S1/S11 substrate, unlabeled competitor DNA, and increasing concentrations of NaCl.

Msh2-Msh6 eluted off of the first PBE94 column at approximately 0.5 M NaCl, and fractions were chosen based on SDS-PAGE of individual fractions. Pooled fractions were loaded on subsequent ssDNA and PBE94 columns, and fractions off of these columns containing the most protein were pooled and concentrated. As shown in Figure 4.11, the majority of contaminating bands visible by SDS-PAGE after the first column were removed in subsequent chromatography steps. Total protein yield ranged from 63 μg from 2 L of culture to 670 μg from 4 L of culture in 3 separate protein preparations.

Purified Msh2-Msh6 protein binds to DNA with a preference for mismatches. Purified Msh2-Msh6 protein was analyzed by electrophoretic gel mobility shift assay using annealed oligo substrates S1/S4 and S1/AO2177 that are identical except for one central mismatch in S1/AO2177. Increasing amounts of Msh2-Msh6 protein exhibited increased DNA binding as determined by an increase in shifted DNA, as shown in Figure 4.12. The preference for binding to mismatched DNA is consistent with previous observations (Alani 1996; Alani *et al.* 1997; Habraken *et al.* 1998).

Sgs1 and Msh2-Msh6 purified proteins physically interact. In order to test whether there is a direct physical interaction between the Msh2-Msh6 heterodimer and the Sgs1 helicase, purified Msh2-Msh6 and HA-tagged $Sgs1_{400\text{-}1268}$ were used for Msh2-Msh6 eluted off of the first PBE94 column at approximately 0.5 M NaCl, and

To further show that Msh2-Msh6 and Sgs1 form a stable complex, gel filtration was performed using a Superdex 200 10/300 GL 24 ml gel filtration column run at 0.5 ml/min by FPLC. Injection of Msh2-Msh6 resulted in two distinct elution peaks, shown in Figure 4.14. The late-eluting peak at 11.4 mls is consistent with the 249 kDa molecular weight of the Msh2-Msh6 heterodimer (predicted molecular

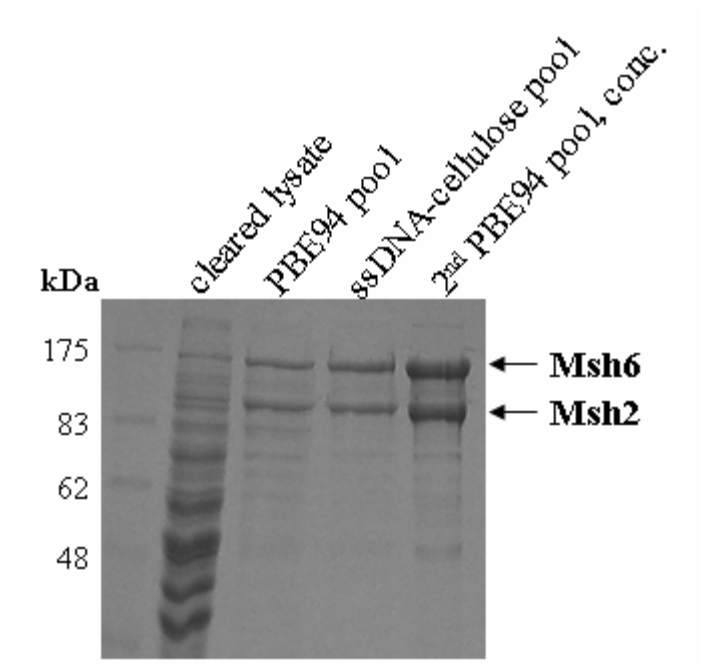

Figure 4.11. Purification of Msh2-Msh6. Msh2 and Msh6 were co-overexpressed in yeast and purified over a PBE94 anion exchange column on a 0.3 to 1.0 M NaCl gradient followed by a ssDNA-cellulose column and concentration on a third PBE94 column as described in Materials and Methods.

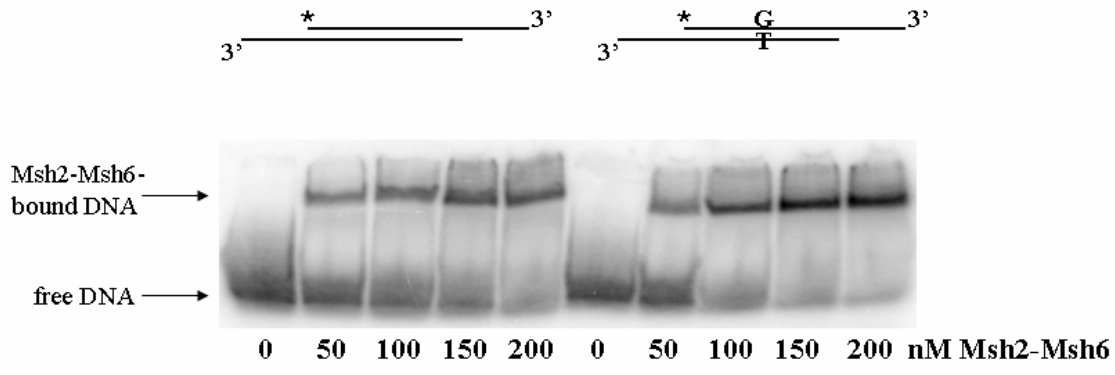

Figure 4.12. Gel mobility shift assay of Msh2-Msh6 binding to matched and mismatched DNA oligo substrates. Increasing amounts of purified Msh2-Msh6 protein were incubated with radiolabeled DNA substrates for 5 minutes at room temperature and run on a 4% native polyacrylamide/0.5x TBE gel for 45 minutes at 130 volts.

weight of this peak assuming one globular protein is 332 kDa, based the elution volumes of known protein standards). An earlier eluting peak at 8.4 mls may be a higher-order complex or simply an aggregate of protein, with a predicted molecular weight 4 times that of the earlier peak, and elutes relatively close to the predicted void volume of this column.

Consistent with the coIP experiments, preliminary gel filtration experiments using Msh2-Msh6 plus $Sgs1_{400-1268}$ show two distinct peaks similar to those observed with Msh2-Msh6 alone, but both peaks are shifted to earlier elution volumes (11.2 and 7.9 mls compared to 11.4 and 8.4 mls with Msh2-Msh6 alone; Figure 4.14). The earlier eluting peak at 7.9 mls has a predicted molecular weight 4 times that of the later peak at 11.2 mls (1518 kDa vs. 371 kDa). This result may be evidence against the elution volume of the first peak in the Msh2-Msh6 runs being equal to the void volume. In very preliminary experiments, the proteins appear to co-elute at least in earlier fractions containing potentially higher-order complexes of Msh2-Msh6 and $Sgs1_{400-1268}$ when gel filtration fractions are TCA-precipitated and analyzed by SDS-PAGE (data not shown). Further gel filtration studies are required to confirm this result.

For future experiments, Blue dextran 2000 should be used as a standard to determine whether the early-eluting peak in the Msh2-Msh6 and Msh2-Msh6-$Sgs1_{400-1268}$ samples is the void volume, as the elution volume of Blue dextran 200 is equal to the void volume. The void volume of this column is predicted to be approximately 8 mls, or 30% of the 24 ml bed volume (GE Healthcare). Changing the salt concentration of the sample may also allow analysis of more Msh2-Msh6 heterodimers in solution, since it appears that an aggregate is formed under these buffer conditions (20 mM Tris pH 7.5, 200 mM NaCl). Cleaner protein preparations

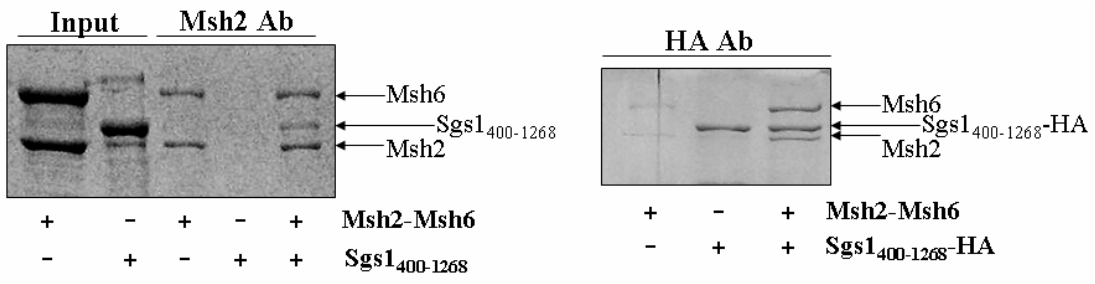

Figure 4.13. Coimmunoprecipitation of purified $Sgs1_{400-1268}$ and Msh2-Msh6. 24 pmol each of purified Msh2-Msh6 and $Sgs1_{400-1268}$ were incubated with either α-HA antibody or α-Msh2 antibody and Protein A-Sepharose beads following treatment with DNaseI and analyzed by 8% SDS-PAGE and Coomassie blue stain.

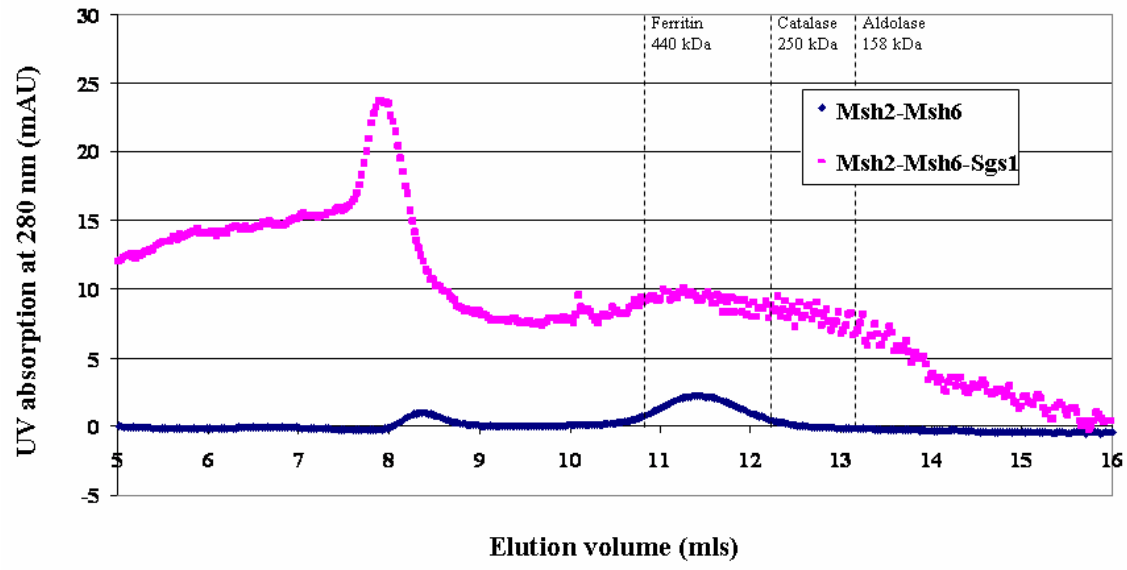

Figure 4.14. Preliminary gel filtration of Msh2-Msh6 with and without $Sgs1_{400-1268}$. Samples consisting of 71 µg of Msh2-Msh6 or 100 µg of Msh2-Msh6 plus $Sgs1_{400-1268}$ were injected into a Superdex 200 10/300 GL gel filtration column via FPLC at 0.5ml/min. Two distinct peaks are detected in both samples: 8.4 mls and 11.4 mls for Msh2-Msh6 and 7.9 and 11.2 for Msh2-Msh6 plus $Sgs1_{400-1268}$. Elution volumes of standard proteins of known molecular weights are indicated with dotted lines.

might also help. Aggregation appeared to be enhanced by the addition of Sgs1 (Figure 4.14).

Msh2-Msh6 and Sgs1 do not simultaneously bind to 25 bp duplex, 15 nt 3' overhang substrates. Since Msh2-Msh6 and Sgs1 physically interact, it was of interest to test whether the two proteins together can also bind DNA. Both Msh2-Msh6 and Sgs1 are known to bind to DNA on their own (Alani 1996; Bennett *et al.* 1999). Electrophoretic gel mobility shift assays were performed using 100 nM each of purified Msh2-Msh6 and $Sgs1_{400\text{-}1268}$ proteins in the absence of ATP. Using DNA substrates S1/AO2818 and S1/AO2353, which have 25 bp duplex regions containing either a G/T mismatch or a +1 G insertion in addition to 15 nt 3' single-stranded tails, $Sgs1_{400\text{-}1268}$ and Msh2-Msh6 both bound to DNA singly, but did not form a super-shifted complex suggestive of a DNA-Msh2-Msh6- $Sgs1_{400\text{-}1268}$ complex (Figure 4.15). A subtle, higher-migrating band visible in the Msh2-Msh6 + $Sgs1_{400\text{-}1268}$ lane was also present in the $Sgs1_{400\text{-}1268}$ alone lane. In the presence of $Sgs1_{400\text{-}1268}$, less Msh2-Msh6 bound to the DNA substrate, but the presence of Msh2-Msh6 did not affect the amount of $Sgs1_{400\text{-}1268}$ bound (Figure 4.15). Larger DNA substrates, addition of non-specific competitor DNA, or different binding conditions may allow for future analysis of ternary complex formation on DNA. ATP may be required for stable association of Msh2-Msh6 with Sgs1, as is true for Msh2-Msh6 ternary complex formation with Mlh1-Pms1 on mismatched DNA (Habraken *et al.* 1998). Order-of-addition experiments may also be crucial for this analysis, since Msh2-Msh6 binds a variety of DNA structures quite well and might prevent Sgs1 loading onto DNA. $Sgs1_{400\text{-}1268}$ footprints on DNA primarily on 3' ssDNA adjacent to the junction with dsDNA (Bennett *et al.* 1999), and it may need to bind the DNA substrate first before Msh2-

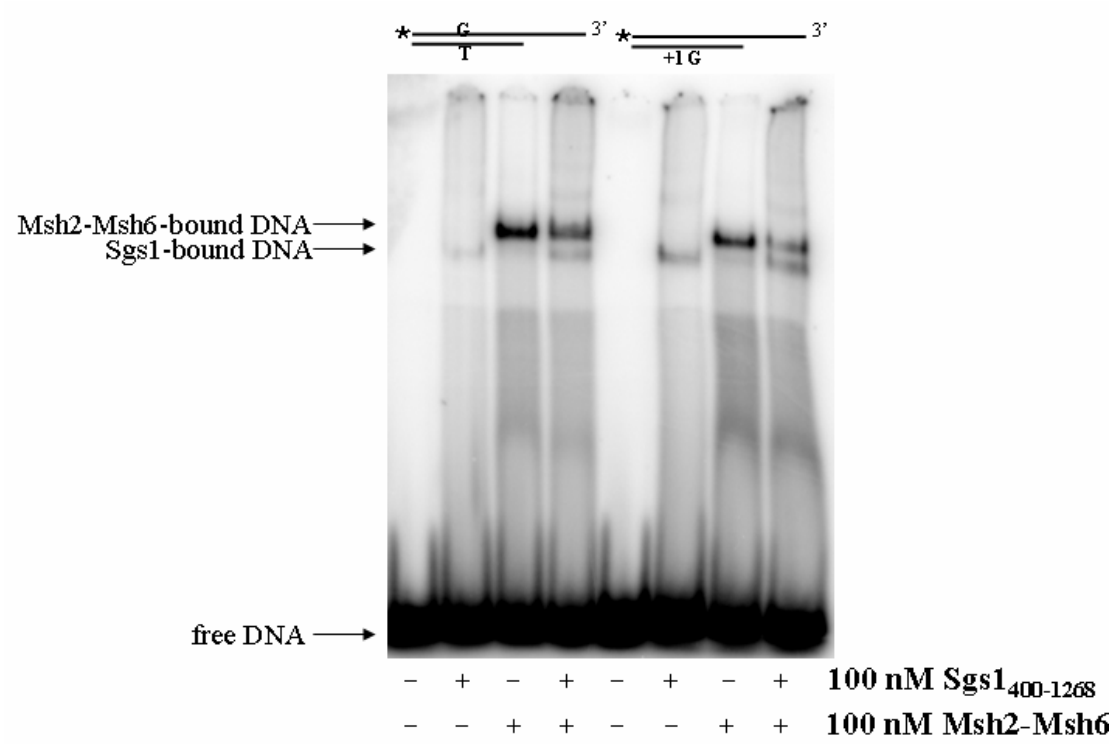

Figure 4.15. Gel mobility shift assay of Msh2-Msh6 and Sgs1$_{400-1268}$ on 3' overhang mismatched substrates. Both Sgs1 and Msh2-Msh6 are able to bind to the 3' overhang substrates (S1/AO2181 and S1/AO2353) alone. The amount of Msh2-Msh6 bound to DNA is reduced in the presence of Sgs1, and no supershift was observed in the presence of both proteins, suggesting that Msh2-Msh6 and Sgs1$_{400-1268}$ cannot both bind to this DNA substrate under these conditions. Order-of-addition experiments, longer DNA substrates, or ATP may be necessary for ternary complex formation.

Msh6 is added. It would also be interesting to see whether pre-bound Msh2-Msh6-Sgs1 protein complexes can bind to DNA.

Msh2-Msh6 inhibits Sgs1 helicase activity on short DNA substrates. To assess whether Msh2-Msh6 can stimulate the helicase activity of Sgs1 *in vitro,* increasing amounts of purified Msh2-Msh6 protein were added to helicase reactions on various DNA substrates with or without mismatches. As exemplified in Figure 4.16, increasing Msh2-Msh6 led to a decrease in unwinding of a homoduplex 3' overhang substrate by Sgs1 at 60 mM NaCl. Similar results have been obtained at salt concentrations ranging from 50 mM to 150 mM NaCl, with and without mismatches in the DNA substrate (S1/S11, S1/AO2181, S1/2353), with and without 10-fold molar excess of unlabeled competitor DNA, and with $Sgs1_{400\text{-}1268}$ concentrations ranging from 1 nM to 10 nM. In some experiments, subtle inhibition was detectable at 2:1 ratios of Sgs1:Msh2-Msh6, while others showed little effect up to 2-fold excess of Msh2-Msh6 over Sgs1, and drastic inhibition was observed at 10-12-fold excess of Msh2-Msh6 over Sgs1, which is in stark contrast to studies with the human proteins. These effects were observed with several different preparations of purified Msh2-Msh6 and Sgs1 proteins. It is unclear whether this inhibitory effect holds true for longer substrates as well. These substrates may be too short to allow efficient loading of Sgs1 and DNA binding (mismatch or otherwise) by Msh2-Msh6. Alternatively, the aggregation of Sgs1 and Msh2-Msh6 suggested by the gel filtration results (Figure 4.14) could be responsible for the inhibition of Sgs1 activity in the presence of increasing Msh2-Msh6 (Figure 4.16).

Subtle stimulation of unwinding was detected in some experiments with approximately equimolar quantities of Sgs1 and Msh2-Msh6, followed by inhibition of unwinding at higher amounts of Msh2-Msh6. One example of such an experiment

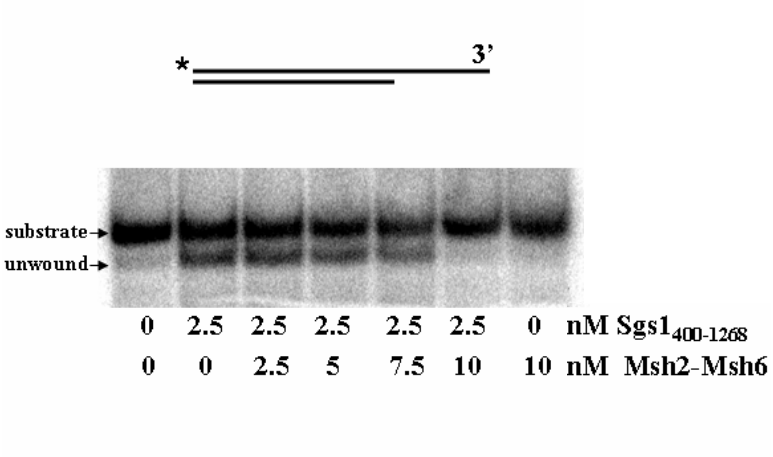

Figure 4.16. Increasing amounts of Msh2-Msh6 inhibit unwinding on short substrates. Helicase assays were performed in 60 mM NaCl at 30° C for 30 minutes as described in Materials and Methods and run on a 10% native acrylamide gel. Increasing amounts of Msh2-Msh6 protein inhibited Sgs1 helicase activity on this homoduplex DNA substrate (S1/S11).

is shown in Figure 4.17, and was carried out in 137 mM NaCl with no unlabeled competitor DNA and 1 nM $Sgs1_{400\text{-}1268}$ by first pre-binding the proteins to the DNA substrate in the absence of ATP and $MgCl_2$ for 5 minutes at room temperature, then incubating for 20 minutes at 30º C following the addition of ATP and $MgCl_2$. A subtle increase in unwinding at 0.25 and 0.5 nM Msh2-Msh6 was observed, followed by decreased unwinding at higher concentrations (Figure 4.17). Unwinding also appeared to increase between 1 nM and 4 nM Msh2-Msh6. Similar results have been obtained under various conditions without clear conclusion. Order-of-addition experiments pre-binding the DNA with either Sgs1 or Msh2-Msh6 have also been inconclusive, but could be a promising avenue for future experiments.

Studies with human Msh2-Msh6 and RecQ homologs detected stimulation of unwinding using less than 1 nM up to 8 nM Msh2-Msh6 with 1 nM Wrn (8-fold excess; 1 nM substrate), 2.5 nM up to 40 nM Msh2-Msh6 with 6 nM Blm (6.7-fold excess; 10 nM substrate), and 3 nM to 25 nM Msh2-Msh6 with 1 nM RecQ1 (25-fold excess; 0.5 nM substrate) (Yang *et al.* 2004; Doherty *et al.* 2005; Saydam *et al.* 2007). It seems most likely that substrates containing duplex regions of longer than 25 bp would be more useful for these studies; however, as described above and below, little helicase activity has been detected with these substrates using Sgs1 alone. Preliminary experiments with longer substrates and increasing Msh2-Msh6 have shown no effect.

Discussion and future directions

The experimental results reported here reveal a direct physical interaction between Sgs1 and Msh2-Msh6 for which amino acids 400 to 1268 of Sgs1 are sufficient. These findings are consistent with previous reports of interactions between the human Msh2-Msh6 complex and three human homologs of Sgs1, Blm, Wrn, and

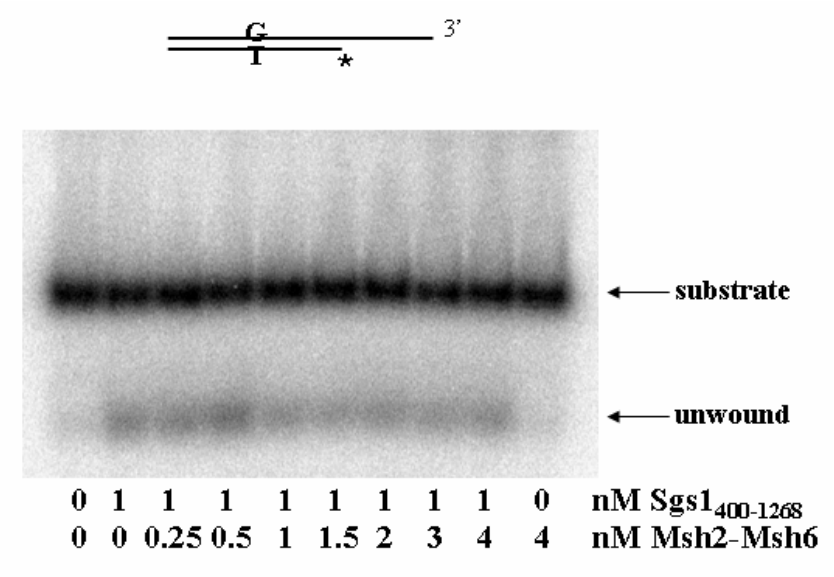

Figure 4.17. Subtle stimulation of $Sgs1_{400-1268}$-dependent unwinding by Msh2-Msh6. In this experiment, both proteins were pre-incubated with the DNA substrate (S1/AO2181) in the absence of ATP and $MgCl_2$, then incubated for 20 minutes at 30º C following addition of ATP and $MgCl_2$. These reactions contain137 mM NaCl and no unlabeled ssDNA competitor.

RecQ1 (Yang *et al.* 2004; Doherty *et al.* 2005; Saydam *et al.* 2007). In particular, the interaction between hMsh2-Msh6 and Wrn was localized to the central conserved DExH helicase domain of Wrn that is also well conserved in Sgs1 (Saydam *et al.* 2007). Considering that an interaction between *S. cerevisiae* Msh6 and Sgs1 was also reported in a large-scale TAP-tagging screen (Gavin *et al.* 2002), the interaction between Msh2-Msh6 and Sgs1 may be mediated via Msh6. This would give specificity to the interaction, since interaction with Msh2 could facilitate both Msh2-Msh3 and Msh2-Msh6 functions. Given the conservation of the Msh2-Msh6-RecQ helicase interaction from *S. cerevisiae* to humans, there is likely to be significant functional relevance for the action of these proteins during DNA repair and recombination.

To date, studies with three distinct human RecQ homologs have shown stimulation of helicase activity in the presence of hMsh2-Msh6 (Yang *et al.* 2004; Doherty *et al.* 2005; Saydam *et al.* 2007). Only the Saydam *et al.* work employs a DNA substrate containing a mismatch, and Msh2-Msh6-dependent stimulation of helicase activity is enhanced in the presence of a mismatch (Saydam *et al.* 2007). The other two studies are also relevant, since Msh2-Msh6 would presumably be recruited to DNA substrates containing mismatches to begin with, and it might not be necessary for mismatches to be present in the particular sequence that the helicase is unwinding. One caveat to these studies is that no trapping oligo or "competitor" DNA is used in the helicase reactions, and as the DNA substrates are unwound, free single-stranded DNA is added to the reaction mixture. This free single-stranded DNA can anneal back to its homologous strand, masking detection of helicase activity, or in the presence of Msh2-Msh6, Msh2-Msh6 might bind and sequester the ssDNA and prevent its re-annealing. In standard helicase reactions, a 10-fold molar excess of unlabeled competitor DNA identical to the labeled strand is often added in order to detect the

labeled, unwound DNA (Bennett *et al.* 1999). In the absence of such competitor, Msh2-Msh6 may appear to stimulate unwinding by simply binding to unwound single-stranded DNA and allowing more of the unwound product to be detected.

The reaction conditions tested here are quite similar to those in Saydam *et al.* (2007), which are performed at 37° C with the human proteins and at 50 mM NaCl. Aside from the temperature difference, the two exceptions are that hMsh2-Msh6 was pre-incubated with the DNA before adding Wrn, and also that the DNA substrates contain a 30 bp duplex region, a 20 bp double-stranded flap, and a 19 nucleotide 3' single-stranded flap (Saydam *et al.* 2007). With this substrate, three distinct unwound products are possible depending on which strand is unwound first. In the work reported in this chapter, very little unwinding was detected using 3' overhang substrates with 30 bp duplexes. Further studies should try using forked substrates containing both double-stranded and single-stranded arms as described above.

In addition to the annealed oligo substrates described in Table 4.2 and used in the helicase assays shown here, DNA substrates were also constructed by annealing oligos of different lengths to single-stranded circular φX174 virion DNA. As described above, very little substrate unwinding was detected using these substrates (~3% maximum), and additionally, the annealing reactions contained an excess of the unpaired labeled oligo despite a 3-fold excess of φX174 virion DNA relative to the oligo. Gel purifying the annealed oligo + φX174 substrate prior to use in helicase assays could address both of these issues.

The initial study that characterized the helicase activity of purified $Sgs1_{400\text{-}1268}$ used the annealed oligo + φX174 substrates and claims to have used a 1 μM DNA substrate concentration for helicase assays in which 5 nM Sgs1 helicase is sufficient to unwind the majority of the substrate in 30 minutes at 30° C (Bennett *et al.* 1998). Since Sgs1 unwinds annealed oligo substrates under similar conditions at a DNA

substrate concentration of 1 nM, it seemed more appropriate in these studies to use nanomolar concentrations of DNA substrate. However, since very little unwinding of these substrates was detected at concentrations ranging from 0.1 nM to 10 nM (data not shown), it is possible that the substrate concentration is a problem. Since the DNA sequence of these substrates and the supplier of the φX174 virion DNA are the same as in previously published studies (Tsaneva *et al.* 1993; Bennett *et al.* 1998), the reason for lack of robust helicase activity on these substrates in our hands is unclear.

Substrate issues aside, it is possible that *S. cerevisiae* Sgs1 is not stimulated by Msh2-Msh6 as its human homologs are, though the physical interaction remains conserved. Or, despite the physical interaction between Msh2-Msh6 and $Sgs1_{400\text{-}1268}$, stimulation of helicase activity may require residues on Sgs1 that are absent in this recombinant soluble fragment. The N-terminal 400 amino acids of Sgs1 that are lacking in $Sgs1_{400\text{-}1268}$ are known to harbor the Top3 interaction site (Fricke *et al.* 2001), but the C-terminal 179 amino acids and remaining portion of the N-terminus that are missing $Sgs1_{400\text{-}1268}$ are of unknown function. These regions of the protein may be required for stimulation of helicase activity by Msh2-Msh6.

Does Sgs1 re-localize to mismatched heteroduplexes following DSB resection in a Msh2-Msh6-dependent manner? Recent work has shown a critical role for Sgs1 in the 5' to 3' resection of DSBs (Gravel *et al.* 2008; Mimitou and Symington 2008; Zhu *et al.* 2008). This role positions Sgs1 at DSBs in the very earliest stages of DSB repair. Since heteroduplex rejection occurs at later stages in recombination following strand invasion and/or strand annealing, the role Sgs1 in heteroduplex rejection is likely to be a separate function of the protein requiring re-localization to recombination intermediates. During resection, Sgs1 would help to unwind the 5' strand in a 3' to 5' direction to allow cleavage by an associated nuclease, which is

proposed to be one of the two prominent long-range resection mechanisms (Gravel *et al.* 2008; Mimitou and Symington 2008; Zhu *et al.* 2008). After this process, Sgs1 would be located at a distance from the single-stranded 3' end, near the 5' end of the opposite strand where resection has ceased. During heteroduplex rejection, the entry point for Sgs1 on recombination intermediates is expected to be one of the 3' single-stranded ends, since *in vitro* unwinding by $Sgs1_{400\text{-}1268}$ requires substrates with 3' single-stranded DNA (This chapter; Bennett *et al.* 1998; Bennett *et al.* 1999). During single-strand annealing, this free 3' end is a nonhomologous tail that is revealed upon Rad52-dependent annealing of the homologous sequences (see Figure 4.2). Hence, heteroduplex rejection is expected to require re-loading of Sgs1 after resection to place it at 3' ends for 3' to 5' unwinding of annealed recombination intermediates.

In order to assess recruitment of Sgs1 to heteroduplexes, future experiments could assay localization of the Sgs1 helicase to mismatched recombination intermediates during the process of SSA by chromatin immunoprecipitation (ChIP). Such experiments could be carried out in wild-type strains harboring either identical (A-A) or 3% divergent (F-A) repeated sequences as well as in derivative *msh6*Δ mutants to test whether recruitment of Sgs1 to intermediates depends on Msh2-Msh6.

Chromatin IPs could be carried out in strains containing the HA-tagged Sgs1 as described previously for $Msh2\text{-}HA_4$ (Goldfarb and Alani 2004), except that the HO cut site would be situated between two direct repeats of *URA3* sequence in Haber A-A/F-A SSA strains (Sugawara *et al.* 2004; Goldfarb and Alani 2005). The homeologous repeats (F-A) have 7 mismatches between them, and rejection is known to occur efficiently in this scenario (Sugawara *et al.* 2004; Goldfarb and Alani 2005). Additionally, the presence of several mismatches may enhance the ChIP signal by having more mismatches for Msh2-Msh6 to bind to. Briefly, cells would be induced with galactose to initiate DSB formation and collected at various time points,

crosslinked with formaldehyde, and lysed. Protein-bound DNA would be sonicated into fragments, then immunoprecipitated with 12CA5 α-HA antibody (Roche). After reversal of crosslinks, DNA would be extracted and used for quantitative or semi-quantitative PCR (Goldfarb and Alani 2004). In order to make sure that Sgs1 is being cleared from the lysate, pre-IP and post-IP samples could be run on 8% SDS-PAGE and analyzed by Western blot using the α-HA antibody.

The strains created for ChIP of Sgs1-HA_3 are EAY1141/1143 (A-A/F-A single-strand annealing strains) transformed with digested pEAI206 to integrate *SGS1-HA_3::KANMX*. The wild-type (EAY1340-EAY1342) and *msh6*Δ (EAY1179, EAY1180) derivatives of EAY1141 were made by Tamara Goldfarb, whereas I created the wild-type (EAY2398, EAY2399) derivatives of EAY1143. Primers to be used for ChIP to the A/A or F/A heteroduplex region have been used previously to look at ChIP localization of the Rad1 protein to SSA intermediates (Li *et al.* 2008). Primer sets pJC1 + pJC2 (AO2379 + AO2380) and pJC3 + pJC4 (AO2381 + AO2382) amplify DNA at the junction of the 3' nonhomologous tails within the annealed heteroduplex, which would be predicted to be the entry point for Sgs1 at a mismatched single-strand annealing intermediate. Primers pJC5 + pJC6 (AO2383 + AO2384) amplify a sequence at the annealed intermediate that is farther from the 3' tails. All signals should be set relative to the PCR signal obtained using control primers located elsewhere in the genome.

Both the extent and timing of Sgs1 localization in wild-type cells of both the A-A and F-A background can be compared to those in *msh6*Δ mutants to see whether Sgs1 recruitment is Msh6-dependent, and similar analyses can be performed in *top3*Δ and *rmi1*Δ strains. Analysis of Sgs1 localization in the absence of Top3 and/or Rmi1 may be more useful than genetic knockout studies of rejection in these mutants since *top3*Δ and *rmi1*Δ strains are slow-growing, sick, and prone to suppressor mutations.

Top3 and Rmi1 are known to form a complex with Sgs1 (Chang *et al.* 2005), and these experiments would help to determine whether these factors are also involved in Sgs1-dependent heteroduplex rejection.

It is yet to be confirmed whether Sgs1-HA_3 can easily be immunoprecipitated, so initial ChIP trials should to be analyzed by Western blot. Studies in several labs have found the Sgs1 protein difficult to detect (Mullen *et al.* 2000). For detection by Western blot, one option is to perform consecutive IPs prior to blotting (as in Mullen *et al.* 2000). Once IP of Sgs1-HA_3 in these strains has been confirmed by Western blot using the α-HA antibody, ChIP experiments could be carried out as described above, with the additional use of the protein-protein crosslinking agent EGS to enhance Sgs1 signal as done in Zhu *et al.* (2008). If immunoprecipitation of Sgs1 is difficult, use of the helicase-dead Sgs1-K706A allele may also enhance the signal.

Additionally, these experiments could be expanded to also look at recruitment of Msh2 and compare the timing of localization to that of Sgs1. Presumably Msh2 and Msh6 bind to the mismatches as a heterodimer during heteroduplex rejection as they do during post-replicative MMR. Since Msh2 is also involved in 3' non-homologous tail removal (Pâques and Haber 1997; Sugawara *et al.* 1997; Studamire *et al.* 1999; Goldfarb 2005), and perhaps in the DNA damage response during SSA (Duckett *et al.* 1999; Franchitto *et al.* 2003; Wang and Qin 2003), Msh2 localization specifically for rejection may be difficult to discern. Comparison of Msh2 localization in identical vs. mismatched repeats and the use of the Msh2Δ1 mutant protein defective in 3' nonhomologous tail removal but proficient in MMR and rejection could be useful in this regard (Lee *et al.* 2007). Msh2-HA_4 localization by ChIP has been done previously in our laboratory (Goldfarb and Alani 2004; Evans *et al.* 2000).

DNA sequence requirements for heteroduplex rejection. How many mismatches are required for Msh2-Msh6- and Sgs1-dependent heteroduplex rejection? It is reported that as little as one mismatch is sufficient to reduce the rate of recombination between two otherwise identical sequences (Datta *et al.* 1997). Is this sufficient in the SSA system? Does it matter what type of mismatch? Are the most-recognized mismatches during rejection the same as those that are best repaired by post-replicative DNA mismatch repair? If several mismatches are required, or if more mismatches increase the robustness of heteroduplex rejection, what is the effect of mismatch spacing? Presumably, a minimum amount of homology (the MEPS) lacking mismatches would need to be present in order for recombination to initiate in the first place.

Are 3' nonhomologous tails required for Sgs1-mediated heteroduplex rejection? Given what is known about the recombination intermediates that Sgs1 unwinds, it would be interesting to test whether the presence of 3' nonhomologous tails is required for Sgs1-mediated heteroduplex rejection. Sgs1 is a 3' to 5' helicase whose *in vitro* helicase activity is most active on substrates containing 3' single-stranded ends. During SSA, as depicted in Figure 4.2, extensive 5' to 3' resection reveals long 3' single-stranded regions of DNA that anneal at homologous sequences. The DNA adjacent to the original DSB site is, in many cases, not homologous to the sequence that is situated on the opposite strand following this annealing. Thus, the 3' ends are nonhomologous tails. As discussed in Chapters 1 and 2, 3' nonhomologous tail removal is a process involved in many homologous recombination events, and as shown in Figure 4.2, removal of these 3' nonhomologous tails is required for completion of DSB repair by SSA. The canonical model of heteroduplex rejection during SSA, depicted in Figure 4.5, follows the same scheme as the repair event

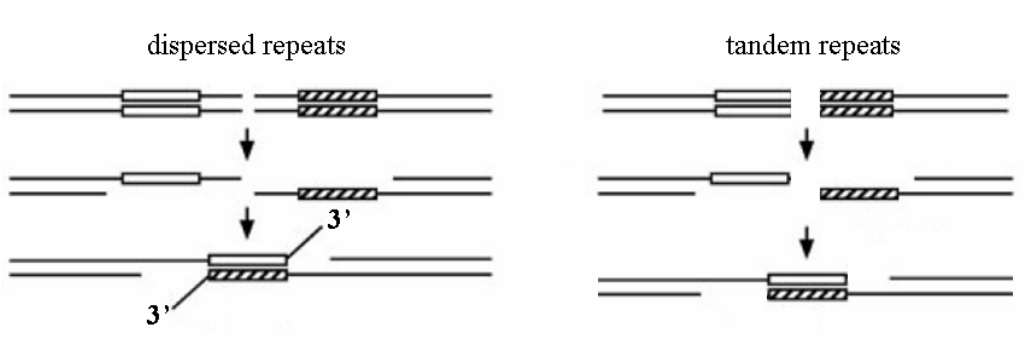

Figure 4.18. Single-strand annealing between dispersed or tandem repeated sequences. During SSA between dispersed repeats, the intervening sequences are not homologous to those flanking the other repeat sequence, thus leaving two 3' nonhomologous tails in the intermediate. Prior to removal of these 3' tails by Rad1-Rad10, they may serve as entry points for the Sgs1 helicase for unwinding during heteroduplex rejection. When a DSB is located in or between tandem repeats, SSA can occur without involving 3' nonhomologous tails. It is unclear whether such intermediates could be efficiently acted upon by Sgs1 to elicit heteroduplex rejection.

depicted in Figure 4.2 up until the 3' nonhomologous tail removal step. In heteroduplex rejection during SSA, it is proposed that Sgs1 would load onto mismatched recombination intermediates via the 3' single-stranded tails. Such entry would allow for 3' to 5' unwinding of inappropriate intermediates, and resumption of a homology search to find a better recombination substrate.

While the proposed model for rejection seems to hold true in many situations, single-strand annealing does not necessarily involve 3' nonhomologous tails. As shown in Figure 4.18, a DSB formed within a repeated sequence or at the edge of a tandemly repeated sequence can be repaired by single-strand annealing without the formation of 3' nonhomologous tails. In such a situation, would Sgs1-dependent heteroduplex rejection be able to occur? One might predict that rejection would be of lower efficiency if Sgs1 could not load as easily onto the DNA substrate via 3' single-stranded tails. It is also possible that recruitment of Sgs1 to mismatched intermediates by Msh2-Msh6 might position Sgs1 on the DNA in such a way that 3' tails would not be required. The proposed necessity for single-stranded 3' tails is based on *in vitro* observations, so it remains possible that the *in vitro* and *in vivo* DNA loading requirements for the helicase may differ.

Does heteroduplex rejection operate similarly during gene conversion and SSA?
It remains to be tested directly whether Msh2-Msh6- and Sgs1-dependent heteroduplex rejection operates via similar mechanisms during single-strand annealing, gene conversion, crossing over, and break-induced replication. As described in the introduction to this chapter, Msh2-Msh6 and Sgs1 are both known to limit the frequency recombination between slightly divergent sequences. However, it is unclear how often both factors act in the same pathway of anti-recombination during non-SSA recombination events. Gene conversion by synthesis-dependent strand

annealing to form noncrossover products can involve one or two 3' nonhomologous tails, as described in Chapters 1, 2, and 3 (See Chapter 1, Figure 1.2). Rejection during gene conversion will depend on where the mismatches are located with respect to the initiating DSB. If mismatches are present between the invading strand sequence and the donor sequence, one might expect rejection to be most effective when there are two 3' nonhomologous tails, since this requires that the invading strand contain a 3' nonhomologous tail, and thus an entry point for Sgs1. If, however, the invading strand contains perfect homology to the donor sequence and it is the newly-replicated (gene converted) sequence copied from the donor that displays mismatches when annealed back to the original locus, one might expect that rejection would be unaffected by the presence or absence of a 3' nonhomologous tail on the invading strand, and would only depend on the presence of a single 3' nonhomologous tail on the non-invading strand.

What is the role of the DNA damage checkpoint in heteroduplex rejection? DSB resection usually produces sufficient single-stranded DNA to induce the DNA damage checkpoint response, stalling the cell cycle to allow for proper DSB repair. It is unclear whether this damage response is activated as a direct result of exposing single-stranded DNA during 5' to 3' resection of the break, or by binding of RPA to the single-stranded DNA. As a critical resection factor (Gravel *et al.* 2008; Mimitou and Symington 2008; Zhu *et al.* 2008), Sgs1 thus plays a key role in allowing checkpoint activation. Following activation of the DNA damage response, DNA repair factors are phosphorylated, activated, and recruited to the break site. It is possible that Sgs1 is recruited by the DNA damage checkpoint machinery to participate in later steps of repair as well as heteroduplex rejection. If the annealed region of a homologous recombination substrate contains mismatched DNA, which might be sensed due to the

resulting perturbations in the DNA backbone or disruptions in the binding of proteins to the annealed DNA, checkpoint factors might aid in recruitment of Msh2-Msh6 as well as Sgs1. Alternatively, mismatch recognition by the Msh2-Msh6 complex could lead to checkpoint-dependent signaling that recruits Sgs1 for heteroduplex rejection. Future experiments in the lab are planned using *rad9*Δ mutants containing single-strand annealing cassettes to test whether checkpoint activation is necessary for heteroduplex rejection. Preliminary results from graduate student Carrie George suggest that the absence of Rad9 leads to increased death specifically in strains bearing divergent repeats (Carrie George, personal communication). It remains to be seen whether this mismatch-dependent death is due to enhanced heteroduplex rejection activity or to an inability to complete rejection or repair at mismatched heteroduplexes in the absence of Rad9. It would be interesting to look at Sgs1 localization to mismatched SSA intermediates by ChIP in *rad9*Δ mutant strains to test whether checkpoint activation is required for Sgs1 recruitment specifically to mismatched intermediates.

As mentioned above, it is unclear whether checkpoint activation is required for heteroduplex rejection during single-strand annealing. While the DNA damage checkpoint is typically activated during SSA, SSA can be completed in the absence of checkpoint activation in *S. cerevisiae*. When SSA occurs between slightly divergent repeats, the activated DNA damage checkpoint response may directly promote heteroduplex rejection at the level of mismatch recognition. Msh6 is known to be a direct phosphorylation target of the Mec1/Tel1 checkpoint kinases (Smolka *et al.* 2007), though it is unclear what the function of this phosphorylation might be. Interestingly, this phosphorylation of Msh6 is independent of Rad53. The predicted SQ phosphorylation sites on Msh6, S102 and S130, lie N-terminal to domain I of the Msh6 protein and C-terminal to the PIP-box that interacts with PCNA (Clark *et al.*

2007; Smolka *et al.* 2007). Future experiments should investigate the necessity of these phosphorylated residues during heteroduplex rejection, which requires Msh2-Msh6 mismatch recognition, but entails quite different downstream events than mismatch repair that are not well understood.

The protein sequence of Sgs1 harbors quite a few S/TQ motifs that could be potential targets of Mec1/Tel1 phosphorylation. It is reported that Sgs1 is phosphorylated *in vivo* (Fricke *et al.* 2001), and also physically interacts with the Rad53 DNA damage checkpoint factor (Bjergbaek *et al.* 2005). Indeed, Sgs1 functions independently of Top3 and Rad51 in stimulating the Rad53 checkpoint kinase in response to HU-dependent replication fork stalling, though this checkpoint function does not require the helicase activity of Sgs1 (Bjergbaek *et al.* 2005). Given the variety of roles that Sgs1 has in maintaining genome integrity, including replication restart/fork integrity, inhibiting crossover formation, 5' to 3' DSB resection, and heteroduplex rejection, it would not be surprising if Sgs1 had roles in checkpoint signaling or activation outside of S-phase.

What is the role of Mlh1 in heteroduplex rejection? In addition to Msh2-Msh6, the Mlh1 mismatch repair factor has also been shown to exhibit anti-recombination properties. The absence of Mlh1 increases the frequency of recombination between divergent sequences in a variety of assays (Chen and Jinks-Robertson 1999; Nicholson *et al.* 2000; Sugawara *et al.* 2004). *mlh1*Δ mutants exhibit a less severe anti-recombination defect in the two 205 bp-repeat SSA assay than *msh6*Δ or *sgs1*Δ mutants, with a divergent/identical repeat recombination ratio of 0.30 to 0.48 in *mlh1*Δ mutants compared to 0.16 in wild-type and 0.64 in *msh6*Δ (Sugawara *et al.* 2004). *mlh1*Δ and *pms1*Δ mutants are also less defective than *msh2*Δ mutants in anti-

recombination between divergent inverted repeats (Chen and Jinks-Robertson 1999; Nicholson *et al.* 2000).

Studies of the human Blm helicase have shown a direct physical interaction with hMlh1 both *in vivo* and *in vitro,* and *S. cerevisiae* Sgs1 interactions with yeast Mlh1 have been detected by yeast two-hybrid and affinity capture-Westerns (Langland *et al.* 2001; Pedrazzi *et al.* 2001; Argueso *et al.* 2002; Argueso *et al.* 2003). Since Mlh1 alone and the Mlh1-Pms1 complex have been purified in our lab (Aaron Plys, personal communication), it would be exciting and feasible to study the effect of Mlh1 on Sgs1 helicase activity *in vitro*. Like the interaction of Msh2-Msh6 with Sgs1, it is possible that this interplay between Mlh1 and Sgs1 could be relevant to post-replicative DNA mismatch repair as well as heteroduplex rejection. Since Mlh1-Pms1 has endonuclease activity (Kadyrov *et al.* 2007), and on its own binds to DNA *in vitro* in electrophoretic gel mobility shift experiments (Aaron Plys, personal communication). Sgs1 might unwind DNA that has been nicked by Mlh1-Pms1. It would be interesting to see whether mutation of the endonuclease motif in Pms1 has an effect on its anti-recombination activity; if not, Mlh1-Pms1 (or Mlh1-Mlh3) might act as a simple matchmaker to enhance the recruitment of Sgs1 helicase to Msh2-Msh6-bound mismatches within recombination intermediates to promote heteroduplex rejection. Mlh3 and Sgs1 have been reported to coimmunoprecipitate during meiosis (Wang and Kung 2002), which might implicate Mlh1-Mlh3 and Sgs1 in meiotic rejection in addition to their roles in regulating meiotic crossing over.

To test the effect of Mlh1 and Mlh1-Pms1 on Sgs1 helicase activity, purified proteins in the range of approximately 20 to 200 fmol could be added to Sgs1 helicase reactions as described in Materials and Methods. 3'-tailed or forked DNA substrates with and without mismatches could be compared to see whether any observed effect depends on the presence of a mismatch. Eventually, both Msh2-Msh6 and Mlh1-

Pms1 complexes could be added to helicase reactions, though this could potential sequester some of the ATP needed by Sgs1. In addition, gel shift assays with Mlh1-Pms1 (or Mlh1 alone) and Sgs1 could be performed to see whether super-shifted complexes containing both proteins form on DNA. Such experiments cannot distinguish between both proteins binding separately to a given piece of DNA or the two proteins binding to each other while one of them is bound to DNA, but the use of various DNA substrates could parse apart these questions. Binding of one protein might preclude binding of the other; this can be tested with order-of-addition experiments by pre-incubating one protein/complex with the DNA for 5 minutes at room temperature prior to the addition of the second protein/complex.

Interestingly, Mlh1 also harbors a Mec1/Tel1 phosphorylation site at S441 whose modification is Rad53-independent (Smolka *et al.* 2007). Use of phosphorylation-defective *mlh1* mutants in *in vivo* anti-recombination assays might further enhance our understanding of the role of checkpoint kinase-dependent Mlh1 phosphorylation. It remains to be seen how this phosphorylation affects the endonuclease activity of Mlh1-Pms1 or its interaction with Msh2-Msh6, and whether abolishing this residue or mimicking constitutive phosphorylation has any effect on post-replicative MMR or homologous recombination.

Characterization of the cell cycle response during heteroduplex rejection. It would be interesting to see if synchronizing the single-strand annealing (A-A/F-A or A-A-A/A-F-A) strains prior to DSB induction would affect 1) SSA timing or efficiency or 2) heteroduplex rejection. While SSA is a slow process that may be unaffected by cell cycle context, heteroduplex rejection efficiency could be greatly affected if it is checkpoint-regulated. If the strains were made *bar1*Δ to sensitize them to α-factor, cells could be synchronized in G1 phase and released prior to DSB

induction. In addition to cell survival and Southern blot analyses that could follow, the ability to synchronize these strains would aid in comparison of the cell cycle arrest in cells harboring identical vs. divergent repeats by FACS analysis of DNA content, pedigree analysis, or Western blots of time course samples to detect phosphorylated checkpoint and DNA repair factors. Are the arrests longer in cells with divergent repeats? Do the arrests have the same genetic requirements? The increased death in *rad9*Δ mutants in F-A strains but not in A-A strains in experiments by Carrie George suggest that the arrests in cells undergoing SSA between divergent repeats have functional consequences that we have yet to understand. Further analysis of the DNA damage response in cells undergoing heteroduplex rejection could employ mass spectrometry technology to assess the differences in phosphorylation of key checkpoint and repair factors in cells undergoing single-strand annealing between identical vs. divergent repeats.

Acknowledgments

Special thanks to the Lahue and Wang labs for the Sgs1 expression plasmid and Dr. Cynthia Kinsland at the Cornell Core facility for Protein Purification and Characterization for help with gel filtration experiments. The first purification of $Sgs1_{400\text{-}1268}$ was performed by Justin Sibert during his lab rotation. The Sgs1-K706A helicase-dead protein was cloned and purified by Dr. Eric Alani. Preliminary coimmunoprecipitation experiments were carried out using Msh2-Msh6 and Msh2Δ1-Msh6 proteins purified by Jennifer Surtees. Protein purification expertise from Aaron Plys, Dr. Jennifer Surtees, and Dr. Eric Alani is much appreciated.

REFERENCES

Ahn, B.-Y., K. J. Dornfeld, T. J. Fagrelius and D. M. Livingston (1988). "Effect of limited homology on gene conversion in a *Saccharomyces cerevisiae* plasmid recombination system." Mol. Cell. Biol. **8**(6): 2442-8.

Al-Minawi, A. Z., N. Saleh-Gohari and T. Helleday (2008). "The ERCC1/XPF endonuclease is required for efficient single-strand annealing and gene conversion in mammalian cells." Nucl. Acids Res. **36**(1): 1-9.

Alani, E. (1996). "The *Saccharomyces cerevisiae* Msh2 and Msh6 proteins form a complex that specifically binds to duplex oligonucleotides containing mismatched DNA base pairs." Mol. Cell. Biol. **16**(10): 5604-15.

Alani, E., S. Lee, M. F. Kane*, et al.* (1997). "*Saccharomyces cerevisiae* MSH2, a mispaired base recognition protein, also recognizes Holliday Junctions in DNA." J. Mol. Biol. **265**: 289-301.

Allers, T. and M. Lichten (2000). "A method for preparing genomic DNA that restrains branch migration of Holliday junctions." Nucl. Acids Res. **28**(2): e6.

Argueso, J. L., A. W. Kijas, S. Sarin*, et al.* (2003). "Systematic mutagenesis of the *Saccharomyces cerevisiae MLH1* gene reveals distinct roles for Mlh1p in meiotic crossing over and in vegetative and meiotic mismatch repair." Mol. Cell. Biol. **23**(3): 873-86.

Argueso, J. L., D. Smith, J. Yi*, et al.* (2002). "Analysis of conditional mutations in the *Saccharomyces cerevisiae* MLH1 gene in mismatch repair and in meiotic crossing over." Genetics **160**: 909-21.

Argueso, J. L., J. Westmoreland, P. A. Mieczkowski*, et al.* (2008). "Double-strand breaks associated with repetitive DNA can reshape the genome." Proc. Natl. Acad. Sci. USA **105**(33): 11845-50.

Aylon, Y. and M. Kupiec (2003). "The checkpoint protein Rad24 of *Saccharomyces cerevisiae* is involved in processing double-strand break ends and in recombination partner choice." Mol. Cell. Biol. **23**(18): 6585-96.

Aylon, Y., B. Liefshitz, G. Bitan-Banin and M. Kupiec (2003). "Molecular dissection of mitotic recombination in the yeast *Saccharomyces cerevisiae*." Mol. Cell. Biol. **23**(4): 1403-17.

Bachrati, C. Z. and I. D. Hickson (2003). "RecQ helicases: Suppressors of tumorigenesis and premature aging." Biochem. J. **374**: 577-606.

Bardwell, A., L. Bardwell, A. Tomkinson and E. Friedberg (1994). "Specific cleavage of model recombination and repair intermediates by the yeast Rad1-Rad10 DNA endonuclease." Science **265**(5181): 2082-5.

Barlow, J. H., M. Lisby and R. Rothstein (2008). "Differential regulation of the cellular response to DNA double-strand breaks in G1." Mol. Cell **30**(1): 73-85.

Bennett, R. J. and J. L. Keck (2004). "Structure and function of RecQ DNA helicases." Crit. Rev. Biochem. Mol. Biol. **39**: 79-97.

Bennett, R. J., J. L. Keck and J. C. Wang (1999). "Binding specificity determines polarity of DNA unwinding by the Sgs1 protein of *S. cerevisiae*." J. Mol. Biol. **289**: 235-48.

Bennett, R. J., J. A. Sharp and J. C. Wang (1998). "Purification and characterization of the Sgs1 DNA helicase activity of *Saccharomyces cerevisiae*." J. Biol. Chem. **273**(16): 9644-50.

Bennett, R. J. and J. C. Wang (2001). "Association of yeast DNA Topoisomerase III and Sgs1 DNA helicase: Studies of fusion proteins." Proc. Natl. Acad. Sci. USA **98**(20): 11108-13.

Bertrand, P., D. X. Tishkoff, N. Filosi*, et al.* (1998). "Physical interaction between components of DNA mismatch repair and nucleotide excision repair." Proc. Natl. Acad. Sci. USA **95**: 14278-83.

Bjergbaek, L., J. A. Cobb, M. Tsai-Plugfelder and S. M. Gasser (2005). "Mechanistically distinct roles for Sgs1p in checkpoint activation and replication fork maintenance." EMBO J. **24**: 405-17.

Blastyák, A., L. Pintér, I. Unk*, et al.* (2007). "Yeast Rad5 protein required for postreplication repair has a DNA helicase activity specific for replication fork regression." Mol. Cell **28**(1): 167-75.

Boland, C. R., M. Koi, D. K. Chang and J. M. Carethers (2008). "The biochemical basis of microsatellite instability and abnormal immunohistochemistry and clinical behavior in Lynch Syndrome: from bench to bedside " Familial Cancer **7**(1): 41-52.

Chakraverty, R. K. and I. D. Hickson (1999). "Defending genome integrity during DNA replication: A proposed role for RecQ family helicases." BioEssays **21**(4): 286-94.

Chaksangchaichot, P., P. Punyarit and S. Petmitr (2006). "Novel *hMSH2, hMSH6,* and *hMLH1* gene mutations and microsatellite instability in sporadic colorectal cancer." J.Canc. Res. Clin. Oncol. **133**(1): 65-70.

Chambers, S. R., N. Hunter, E. J. Louis and R. H. Borts (1996). "The mismatch repair system reduces meiotic homeologous recombination and stimulates recombination-dependent chromosome loss." Mol. Cell. Biol. **16**(11): 6110-20.

Chang, M., M. Bellaoui, C. Zhang*, et al.* (2005). "*RMI1/NCE4*, A suppressor of genome instability, encodes a member of the RecQ helicase/Topo III complex." EMBO J. **24**: 2024-33.

Chen, W. and S. Jinks-Robertson (1998). "Mismatch repair proteins regulate heteroduplex formation during mitotic recombination in yeast." Mol. Cell. Biol. **18**(11): 6525-37.

Chen, W. and S. Jinks-Robertson (1999). "The role of mismatch repair machinery in regulating mitotic and meiotic recombination between diverged sequences in yeast." Genetics **151**: 1299-313.

Church, G. M. and W. Gilbert (1984). "Genomic sequencing." Proc. Natl. Acad. Sci. **81**(7): 1991-5.

Ciccia, A., N. McDonald and S. C. West (2008). "Structural and functional relationships of the XPF/MUS81 family of proteins." Annu. Rev. Biochem. **77**(1): 259-87.

Clark, A. B., L. Deterding, K. B. Tomer and T. A. Kunkel (2007). "Multiple functions for the N-terminal region of Msh6." Nucl. Acids Res. **35**(12): 4114-23.

Cobb, J. A., L. Bjergbaek and S. M. Gasser (2002). "RecQ helicases: At the heart of genetic stability." FEBS Letters **529**: 43-8.

Colaiácovo, M. P., F. Pâques and J. E. Haber (1999). "Removal of one nonhomologous DNA end during gene conversion by a *RAD1*- and *MSH2*-independent pathway." Genetics **151**: 1409-23.

Datta, A., A. Adjiri, L. New*, et al.* (1996). "Mitotic crossovers between diverged sequences are regulated by mismatch repair proteins in *Saccharomyces cerevisiae*." Mol. Cell. Biol. **16**(3): 1085-93.

Datta, A., M. Hendrix, M. Lipsitch and S. Jinks-Robertson (1997). "Dual roles for DNA sequence identity and the mismatch repair system in the regulation of mitotic crossing-over in yeast." Genetics **94**: 9757-62.

de Wind, N., M. Dekker, A. Berns*, et al.* (1995). "Inactivation of the mouse *Msh2* gene results in mismatch repair deficiency, methylation tolerance, hyperrecombination, and predisposition to cancer." Cell **82**: 321-30.

Deininger, P. L. and M. A. Batzer (1999). "*Alu* repeats and human disease." Mol. Genet. Metab. **67**(3): 183-93.

Deng, C., J. A. Brown, D. You and J. M. Brown (2005). "Multiple endonucleases function to repair covalent Topoisomerase I complexes in *Saccharomyces cerevisiae*." Genetics **170**(2): 591-600.

Deng, C. and M. R. Capecchi (1992). "Reexamination of gene targeting frequency as a function of the extent of homology between the targeting vector and the target locus." Mol. Cell. Biol. **12**(8): 3365-71.

Doherty, K. M., S. Sharma, L. A. Uzdilla*, et al.* (2005). "RECQ1 helicase interacts with human mismatch repair factors that regulate genetic recombination." J. Biol. Chem. **280**(30): 28085-94.

Duckett, D. R., S. M. Bronstein, Y. Taya and P. Modrich (1999). "hMutSα- and hMutLα-dependent phosphorylation of p53 in response to DNA methylator damage." Proc. Natl. Acad. Sci. USA **96**(22): 12384-8.

Elliott, B. and M. Jasin (2001). "Repair of double-strand breaks by homologous recombination in mismatch repair-defective mammalian cells." Mol. Cell. Biol. **21**(8): 2671-82.

Elliott, B., C. Richardson and M. Jasin (2005). "Chromosomal translocation mechanisms at intronic *Alu* elements in mammalian cells." Mol. Cell **17**(6): 885-94.

Evans, E., N. Sugawara, J. E. Haber and E. Alani (2000). "The *Saccharomyces cerevisiae* Msh2 mismatch repair protein localizes to recombination intermediates *in vivo*." Mol. Cell **5**: 189-99.

Fishman-Lobell, J. and J. Haber (1992). "Removal of nonhomologous DNA ends in double-strand break recombination: the role of the yeast ultraviolet repair gene *RAD1*." Science **258**(5081): 480-4.

Flott, S., C. Alabert, G. W. Toh*, et al.* (2007). "Phosphorylation of Slx4 by Mec1 and Tel1 regulates the single-strand annealing mode of DNA repair in budding yeast." Mol. Cell. Biol. **27**(18): 6433-45.

Flott, S. and J. Rouse (2005). "Slx4 becomes phosphorylated after DNA damage in a Mec1/Tel1-dependent manner and is required for repair of DNA alkylation damage." Biochem. J. **391**(2): 325-33.

Franchitto, A., P. Pichierri, R. Piergentili*, et al.* (2003). "The mammalian mismatch repair protein MSH2 is required for correct MRE11 and RAD51 relocalization and for efficient cell cycle arrest induced by ionizing radiation in G2 phase." Oncogene **22**: 2110-20.

Fricke, W. M. and S. J. Brill (2003). "Slx1-Slx4 is a second structure-specific endonuclease functionally redundant with Sgs1-Top3." Genes Dev. **17**: 1768-78.

Fricke, W. M., V. Kaliraman and S. J. Brill (2001). "Mapping the DNA Topoisomerase III binding domain of the Sgs1 DNA helicase." J. Biol. Chem. **276**(12): 8848-55.

Fujitani, Y. and I. Kobayashi (1999). "Effect of DNA sequence divergence on homologous recombination as analyzed by a random-walk model." Genetics **153**: 1973-88.

Gamper, H., N. Lehman, J. Piette and J. E. Hearst (1985). "Purification of circular DNA using benzoylated naphthoylated DEAE-cellulose." DNA **4**(2): 157-64.

Gangloff, S., J. P. McDonald, C. Bendixen*, et al.* (1994). "The yeast type I topoisomerase Top3 interacts with Sgs1, a DNA helicase homolog: a potential eukaryotic reverse gyrase." Mol. Cell. Biol. **14**(12): 8391-8.

Gangloff, S., C. Soustelle and F. Fabre (2000). "Homologous recombination is responsible for cell death in the absence of the Sgs1 and Srs2 helicases." Nat. Genetics **25**: 192-4.

Gao, G., C. McMahon, J. Chen and Y. S. Rong (2008). "A powerful method combining homologous recombination and site-specific recombination for targeted mutagenesis in Drosophila." Proc. Natl. Acad. Sci. USA **105**(37): 13999-14004.

Garber, P. M. and J. Rine (2002). "Overlapping roles of the spindle assembly and DNA damage checkpoints in the cell-cycle response to altered chromosomes in *Saccharomyces cerevisiae*." Genetics **161**(2): 521-34.

Gavin, A.-C., P. Aloy, P. Grandi*, et al.* (2006). "Proteome survey reveals modularity of the yeast cell machinery." Nature **440**(7084): 631-6.

Gavin, A.-C., M. Bosche, R. Krause*, et al.* (2002). "Functional organization of the yeast proteome by systematic analysis of protein complexes." Nature **415**: 141-7.

Gietz, R. D. and R. H. Schiestl (1991). "Applications of high efficiency lithium acetate transformation of intact yeast cells using single-stranded nucleic acids as carrier." Yeast **7**: 253-63.

Goldfarb, T. (2005). Distinct Roles for the *Saccharomyces cerevisiae* Mismatch Repair Proteins in Heteroduplex Rejection, Mismatch Repair, and Non-homologous Tail Removal. Molecular Biology and Genetics. Ithaca, NY, Cornell University**:** 175.

Goldfarb, T. and E. Alani (2004). Chromatin immunoprecipitation to investigate protein-DNA interactions during genetic recombination. Genetic recombination: Reviews and protocols. A. S. Waldman. Totowa, NJ, Humana Press Inc. **262:** 223-37.

Goldfarb, T. and E. Alani (2005). "Distinct roles for the *Saccharomyces cerevisiae* mismatch repair proteins in heteroduplex rejection, mismatch repair and nonhomologous tail removal." Genetics **169**: 563-74.

Gravel, S., J. R. Chapman, C. Magill and S. P. Jackson (2008). "DNA helicases Sgs1 and BLM promote DNA double-strand break resection." Genes Dev. **22**(20): 2767-72.

Guzder, S. N., C. H. Sommers, L. Prakash and S. Prakash (2006). "Complex formation with damage recognition protein Rad14 is essential for *Saccharomyces cerevisiae* Rad1-Rad10 nuclease to perform its function in nucleotide excision repair *in vivo*." Mol. Cell. Biol. **26**(3): 1135-41.

Guzder, S. N., P. Sung, L. Prakash and S. Prakash (1996). "Nucleotide excision repair in yeast is mediated by sequential assembly of repair factors and not by a pre-assembled repairosome." J. Biol. Chem. **271**(15): 8903-10.

Guzder, S. N., C. Torres-Ramos, R. E. Johnson*, et al.* (2004). "Requirement of yeast Rad1-Rad10 nuclease for the removal of 3'-blocked termini from DNA strand breaks induced by reactive oxygen species." Genes Dev. **18**(18): 2283-91.

Haber, J. E. (1998). "Mating-type gene switching in *Saccharomyces cerevisiae*." Annu. Rev. Genet. **32**: 561-99.

Habraken, Y., P. Sung, L. Prakash and S. Prakash (1996). "Binding of insertion/deletion DNA mismatches by the heterodimer of yeast mismatch repair proteins MSH2 and MSH3." Curr. Biol. **6**(9): 1185-7.

Habraken, Y., P. Sung, L. Prakash and S. Prakash (1998). "ATP-dependent assembly of a ternary complex consisting of a DNA mismatch and the yeast MSH2-MSH6 and MLH1-PMS1 protein complexes." J. Biol. Chem. **273**(16): 9837-41.

Harfe, B. D. and S. Jinks-Robertson (2000). "DNA mismatch repair and genetic instability." Annu. Rev. Genet. **34**: 359-99.

Harfe, B. D. and S. Jinks-Robertson (2000). "Mismatch repair proteins and mitotic genome stability." Mut. Res. **451**: 151-67.

Harrington, J. M. and R. D. Kolodner (2007). "*Saccharomyces cerevisiae* Msh2-Msh3 acts in repair of base-base mispairs." Mol. Cell. Biol. **27**(18): 6546-54.

Harrison, J. C. and J. E. Haber (2006). "Surviving the breakup: The DNA damage checkpoint." Annu. Rev. Genet. **40**(1): 209-35.

Hedges, D. J. and P. L. Deininger (2007). "Inviting instability: Transposable elements, double-strand breaks, and the maintenance of genome integrity." Mut. Res. **616**(1-2): 46-59.

Heller, R. C. and K. J. Marians (2006). "Replication fork reactivation downstream of a blocked nascent leading strand." Nature **439**: 557-62.

Holmes, A. and J. E. Haber (1999). "Physical monitoring of HO-induced homologous recombination." Meth. Mol. Biol. **113**: 403-15.

Holmes, A. M. and J. E. Haber (1999). "Double-strand break repair in yeast requires both leading and lagging strand DNA polymerases." Cell **96**: 415-24.

Hunter, N., S. R. Chambers, E. J. Louis and R. H. Borts (1996). "The mismatch repair system contributes to meiotic sterility in an interspecific yeast hybrid." EMBO J. **15**(7): 1726-33.

Ira, G., A. Pellicioli, A. Balijja*, et al.* (2004). "DNA end resection, homologous recombination and DNA damage checkpoint activation require *CDK1*." Nature **431**(7011): 1011-7.

Ira, G., D. Satory and J. E. Haber (2006). "Conservative inheritance of newly synthesized DNA in double-strand break-induced gene conversion." Mol. Cell. Biol. **26**(24): 9424-9.

Ito, T., T. Chiba, R. Ozawa*, et al.* (2001). "A comprehensive two-hybrid analysis to explore the yeast protein interactome." Proc. Natl. Acad. Sci. USA **98**(8): 4569-74.

Ivanov, E. and J. Haber (1995). "*RAD1* and *RAD10*, but not other excision repair genes, are required for double-strand break-induced recombination in *Saccharomyces cerevisiae*." Mol. Cell. Biol. **15**(4): 2245-51.

Jaspers, N. G. J., A. Raams, M. C. Silengo*, et al.* (2007). "First reported patient with human *ERCC1* deficiency has cerebro-oculo-facio-skeletal syndrome with a mild defect in nucleotide excision repair and severe developmental failure." Am. J. Hum. Genet. **80**(3): 457-66.

Jensen, L. E., P. A. Jauert and D. T. Kirkpatrick (2005). "The large loop repair and mismatch repair pathways of *Saccharomyces cerevisiae* act on distinct substrates during meiosis." Genetics **170**(3): 1033-43.

Jinks-Robertson, S., M. Michelitch and S. Ramcharan (1993). "Substrate length requirements for efficient mitotic recombination in *Saccharomyces cerevisiae*." Mol. Cell. Biol. **13**(7): 3937-50.

Kadyrov, F. A., S. F. Holmes, M. E. Arana*, et al.* (2007). "*Saccharomyces cerevisiae* MutLα is a mismatch repair endonuclease." J. Biol. Chem. **282**(51): 37181-90.

Kang, L. E. and L. S. Symington (2000). "Aberrant double-strand break repair in *rad51* mutants of *Saccharomyces cerevisiae*." Mol. Cell. Biol. **20**(24): 9162-72.

Kearney, H. M., D. T. Kirkpatrick, J. L. Gerton and T. D. Petes (2001). "Meiotic recombination involving heterozygous large insertions in *Saccharomyces cerevisiae*: Formation and repair of large, unpaired DNA loops." Genetics **158**(4): 1457-76.

Kim, E. M. and D. J. Burke (2008). "DNA damage activates the SAC in an ATM/ATR-dependent manner, independently of the kinetochore." PLoS Genet. **4**(2): e1000015.

Kirkpatrick, D. T. and T. D. Petes (1997). "Repair of DNA loops involves DNA-mismatch and nucleotide-excision repair proteins." Nature **387**: 929-31.

Klar, A. J. S. and J. N. Strathern (1984). "Resolution of recombination intermediates generated during yeast mating type switching." Nature **310**: 744-8.

Kolomietz, E., S. M. Meyn, A. Pandita and J. A. Squire (2002). "The role of *Alu* repeat clusters as mediators of recurrent chromosomal aberrations in tumors." Gen. Chrom. Canc. **35**: 97-112.

Krogan, N. J., G. Cagney, H. Yu*, et al.* (2006). "Global landscape of protein complexes in the yeast *Saccharomyces cerevisiae*." Nature **440**(7084): 637-43.

Lander, E., L. Linton, B. Birren*, et al.* (2001). "Initial sequencing and analysis of the human genome." Nature **409**(6822): 860-921.

Langland, G., J. Kordich, J. Creaney*, et al.* (2001). "The Bloom's syndrome protein (BLM) interacts with MLH1 but is not required for DNA mismatch repair." J. Biol. Chem. **276**(32): 30031-5.

Langston, L. D. and L. S. Symington (2005). "Opposing roles for DNA structure-specific proteins Rad1, Msh2, Msh3, Sgs1 in yeast gene targeting." EMBO J. **24**: 2214-23.

Lee, S. D., J. A. Surtees and E. Alani (2007). "*Saccharomyces cerevisiae* Msh2-Msh3 and Msh2-Msh6 complexes display distinct requirements for DNA binding domain I in mismatch recognition." J. Mol. Biol. **366**(1): 53-66.

Lee, S. E., J. K. Moore, A. Holmes, *et al.* (1998). "*Saccharomyces* Ku70, Mre11/Rad50, and RPA proteins regulate adaptation to G2/M arrest after DNA damage." Cell **94**: 399-409.

Lee, S. E., A. Pellicioli, M. B. Vaze, *et al.* (2003). "Yeast Rad52 and Rad51 recombination proteins define a second pathway of DNA damage assessment in response to a single double-strand break." Mol. Cell. Biol. **23**(23): 8913-23.

Lengsfeld, B. M., A. J. Rattray, V. Bhaskara, *et al.* (2007). "Sae2 is an endonuclease that processes hairpin DNA cooperatively with the Mre11/Rad50/Xrs2 complex." Mol. Cell **28**(4): 638-51.

Li, F., J. Dong, X. Pan, *et al.* (2008). "Microarray-based genetic screen defines *SAW1*, a gene required for Rad1/Rad10-dependent processing of recombination intermediates." Mol. Cell **30**(3): 325-35.

Li, W.-H., Z. Gu, H. Wang and A. Nekrutenko (2001). "Evolutionary analyses of the human genome." Nature **409**: 847-9.

Li, X. and W.-D. Heyer (2008). "RAD54 controls access to the invading 3'-OH end after RAD51-mediated DNA strand invasion in homologous recombination in *Saccharomyces cerevisiae*." Nucl. Acids Res. **37**(2): 638-46.

Liang, F., M. Han, P. J. Romanienko and M. Jasin (1998). "Homology-directed repair is a major double-strand break repair pathway in mammalian cells." Proc. Natl. Acad. Sci. USA **95**: 5172-7.

Liskay, R. M., A. Letsou and J. L. Stachelek (1987). "Homology requirement for efficient gene conversion between duplicated chromosomal sequences in mammalian cells." Genetics **115**(1): 161-7.

Lu, J., J. R. Mullen, S. J. Brill, *et al.* (1996). "Human homologues of yeast helicase." Nature **383**: 678-9.

Lynch, H. T. and A. de la Chapelle (2003). "Hereditary colorectal cancer." N. Engl. J. Med. **348**(10): 919-32.

Lyndaker, A. M. and E. Alani (2009). "A tale of tails: Insights into the coordination of 3' end processing during homologous recombination." BioEssays **31**(3).

Lyndaker, A. M., T. Goldfarb and E. Alani (2008). "Mutants defective in Rad1-Rad10-Slx4 exhibit a unique pattern of viability during mating type switching in *Saccharomyces cerevisiae*." Genetics **179**(4): 1807-21.

Marsischky, G. T., S. Lee, J. Griffith and R. D. Kolodner (1999). "*Saccharomyces cerevisiae* MSH2/6 complex interacts with Holliday junctions and facilitates their cleavage by phage resolution enzymes." J. Biol. Chem. **274**(11): 7200-6.

Mattarucchi, E., V. Guerini, A. Rambaldi*, et al.* (2008). "Microhomologies and interspersed repeat elements at genomic breakpoints in chronic myeloid leukemia." Gen. Chrom. Canc. **47**(7): 625-32.

McEachern, M. J. and J. E. Haber (2006). "Break-induced replication and recombinational telomere elongation in yeast." Annu. Rev. Biochem. **75**(1): 111-35.

McGill, C., B. Shafer and J. Strathern (1989). "Coconversion of flanking sequences with homothallic switching." Cell **57**: 459-67.

McWhir, J., J. Selfridge, D. J. Harrison*, et al.* (1993). "Mice with DNA repair gene (*ERCC-1*) deficiency have elevated levels of p53, liver nuclear abnormalities and die before weaning." Nat. Genet. **5**(3): 217-24.

Mezard, C., D. Pompon and A. Nicolas (1992). "Recombination between similar but not identical DNA sequences during yeast transformation occurs within short stretches of identity." Cell **70**(4): 659-70.

Mimitou, E. P. and L. S. Symington (2008). "Sae2, Exo1 and Sgs1 collaborate in DNA double-strand break processing." Nature **455**(7214): 770-4.

Modrich, P. and R. Lahue (1996). "Mismatch repair in replication fidelity, genetic recombination, and cancer biology." Annu. Rev. Biochem. **65**: 101-33.

Moore, J. and J. Haber (1996). "Cell cycle and genetic requirements of two pathways of nonhomologous end-joining repair of double-strand breaks in *Saccharomyces cerevisiae*." Mol. Cell. Biol. **16**(5): 2164-73.

Morozov, V., A. R. Mushegian, E. V. Koonin and P. Bork (1997). "A putative nucleic acid-binding domain in Bloom's and Werner's syndrome helicases." Trends Biochem. Sci. **22**: 417-8.

Motycka, T. A., T. Bessho, S. M. Post*, et al.* (2004). "Physical and functional interaction between the XPF/ERCC1 endonuclease and hRad52." J. Biol. Chem. **279**(14): 13634-9.

Mullen, J. R., V. Kaliraman and S. J. Brill (2000). "Bipartite structure of the *SGS1* DNA helicase in *Saccharomyces cerevisiae*." Genetics **154**: 1101-14.

Mullen, J. R., V. Kaliraman, S. S. Ibrahim and S. J. Brill (2001). "Requirement for three novel protein complexes in the absence of the Sgs1 DNA helicase in *Saccharomyces cerevisiae*." Genetics **157**: 103-18.

Myung, K., A. Datta, C. Chen and R. D. Kolodner (2001). "SGS1, the *Saccharomyces cerevisiae* homologue of BLM and WRN, suppresses genome instability and homeologous recombination." Nat. Genet. **27**: 113-6.

Nicholson, A., M. Hendrix, S. Jinks-Robertson and G. F. Crouse (2000). "Regulation of mitotic homeologous recombination in yeast: functions of mismatch repair and nucleotide excision repair genes." Genetics **154**: 133-46.

Niedernhofer, L. J., H. Odijk, M. Budzowska*, et al.* (2004). "The structure-specific endonuclease Ercc1-Xpf is required to resolve DNA interstrand cross-link-induced double-strand breaks." Mol. Cell. Biol. **24**(13): 5776-87.

Nishant, K. T., A. J. Plys and E. Alani (2008). "A mutation in the putative MLH3 endonuclease domain confers a defect in both mismatch repair and meiosis in *Saccharomyces cerevisiae*." Genetics **179**(2): 747-55.

Pannunzio, N. R., G. M. Manthey and A. M. Bailis (2008). "RAD59 is required for efficient repair of simultaneous double-strand breaks resulting in translocations in *Saccharomyces cerevisiae*." DNA Repair **7**(5): 788-800.

Pâques, F. and J. E. Haber (1997). "Two pathways for removal of nonhomologous DNA ends during double-strand break repair in *Saccharomyces cerevisiae*." Mol. Cell. Biol. **17**(11): 6765-71.

Pâques, F. and J. E. Haber (1999). "Multiple pathways of recombination induced by double-strand breaks in *Saccharomyces cerevisiae*." Microbiol. Mol. Biol. Rev. **63**(2): 349-404.

Pasero, P., K. Shimada and B. P. Duncker (2003). "Multiple roles of replication forks in S phase checkpoints." Cell Cycle **2**(6): 568-72.

Pedrazzi, G., C. Z. Bachrati, N. Selak*, et al.* (2003). "The Bloom's syndrome helicase interacts directly with the human DNA mismatch repair protein hMSH6." Biol. Chem. **384**: 1155-64.

Pedrazzi, G., C. Perrera, H. Blaser*, et al.* (2001). "Direct association of Bloom's syndrome gene product with the human mismatch repair protein MLH1." Nucl. Acids Res. **29**(21): 4378-86.

Pellicioli, A., S. E. Lee, C. Lucca*, et al.* (2001). "Regulation of *Saccharomyces* Rad53 checkpoint kinase during adaptation from DNA damage-induced G2/M arrest." Mol. Cell **7**: 293-300.

Pellicioli, A., C. Lucca, G. Liberi*, et al.* (1999). "Activation of Rad53 kinase in response to DNA damage and its effect in modulating phosphorylation of the lagging strand DNA polymerase." EMBO J. **18**: 6561-72.

Peltomaki, P. (2003). "Role of DNA mismatch repair defects in the pathogenesis of human cancer." J. Clin. Oncol. **21**(6): 1174-9.

Petit, M.-A., J. Dimpfl, M. Radman and H. Echols (1991). "Control of large chromosomal duplications in *Escherichia coli* by the mismatch repair system." Genetics **129**: 327-32.

Porter, G., J. Westmoreland, S. Priebe and M. A. Resnick (1996). "Homologous and homeologous intermolecular gene conversion are not differentially affected by mutations in the DNA damage or the mismatch repair genes *RAD1, RAD50, RAD51, RAD52, RAD54, PMS1,* and *MSH2*." Genetics **143**: 755-67.

Prakash, R., L. Krejci, S. Van Komen*, et al.* (2005). "*Saccharomyces cerevisiae MPH1* gene, required for homologous recombination-mediated mutation avoidance, encodes a 3' to 5' DNA helicase." J. Biol. Chem. **280**(9): 7854-7860.

Prakash, S. and L. Prakash (2000). "Nucleotide excision repair in yeast." Mut. Res. **451**(1-2): 13-24.

Radman, M. and R. Wagner (1993). "Mismatch recognition in chromosomal interactions and speciation." Chromosoma **102**: 369-73.

Raymond, A. C. and A. B. Burgin, Jr. (2006). "Tyrosyl-DNA phosphodiesterase (Tdp1) (3'-phosphotyrosyl DNA phosphodiesterase)." Meth. Enzymol. **409**: 511-24.

Rayssiguier, C., D. S. Thaler and M. Radman (1989). "The barrier to recombination between *Escherichia coli* and *Salmonella typhimurium* is disrupted in mismatch-repair mutants." Nature **342**: 396-401.

Roberts, T. M., M. S. Kobor, S. A. Bastin-Shanower*, et al.* (2006). "Slx4 regulates DNA damage checkpoint-dependent phosphorylation of the BRCT domain protein Rtt107/Esc4." Mol. Biol. Cell **17**(1): 539-48.

Rose, M. D., F. Winston and P. Hieter (1990). Methods in yeast genetics, Cold Spring Harbor Laboratory Press.

Rubnitz, J. and S. Subramani (1984). "The minimum amount of homology required for homologous recombination in mammalian cells." Mol. Cell. Biol. **4**(11): 2253-8.

Sandell, L. L. and V. A. Zakian (1993). "Loss of a yeast telomere: Arrest, recovery, and chromosome loss." Cell **75**: 729-39.

Saparbaev, M., L. Prakash and S. Prakash (1996). "Requirement of mismatch repair genes *MSH2* and *MSH3* in the *RAD1-RAD10* pathway of mitotic recombination in *Saccharomyces cerevisiae*." Genetics **142**(3): 727-36.

Saydam, N., R. Kanagaraj, T. Dietschy*, et al.* (2007). "Physical and functional interactions between Werner syndrome helicase and mismatch-repair initiation factors." Nucl. Acids Res. **35**(17): 5706-16.

Schofield, M. J. and P. Hsieh (2003). "DNA mismatch repair: Molecular mechanisms and biological function." Annu. Rev. Microbiol. **57**: 579-608.

Schürer, K. A., C. Rudolph, H. D. Ulrich and W. Kramer (2004). "Yeast *MPH1* gene functions in an error-free DNA damage bypass pathway that requires genes from homologous recombination, but not from postreplicative repair." Genetics **166**(4): 1673-86.

Segurado, M. and J. F. X. Diffley (2008). "Separate roles for the DNA damage checkpoint protein kinases in stabilizing DNA replication forks." Genes Dev. **22**(13): 1816-27.

Seifert, M. and J. Reichrath (2006). "The role of the human DNA mismatch repair gene *hMSH2* in DNA repair, cell cycle control and apoptosis: implications for pathogenesis, progression and therapy of cancer." J. Mol. Histol. **37**(5): 301-7.

Selva, E. M., L. New, G. F. Crouse and R. S. Lahue (1995). "Mismatch correction acts as a barrier to homeologous recombination in *Saccharomyces cerevisiae*." Genetics **139**: 1175-88.

Shen, P. and H. V. Huang (1986). "Homologous recombination in *Escherichia coli*: Dependence on substrate length and homology." Genetics **112**: 441-57.

Shen, P. and H. V. Huang (1989). "Effect of base pair mismatches on recombination via the RecBCD pathway." Mol. Gen. Genet. **218**: 358-60.

Sia, E. A., R. J. Kokoska, M. Dominska*, et al.* (1997). "Microsatellite instability in yeast: Dependence on repeat unit size and DNA mismatch repair genes." Mol. Cell. Biol. **17**(5): 2851-8.

Sinclair, D. A., K. Mills and L. Guarente (1997). "Accelerated aging and nucleolar fragmentation in yeast *sgs1* mutants." Science **277**: 1313-6.

Singer, B. S., L. Gold, P. Gauss and D. H. Doherty (1982). "Determination of the amount of homology required for recombination in bacteriophage T4." Cell **31**: 25-33.

Slean, M. M., G. B. Panigrahi, L. P. Ranum and C. E. Pearson (2008). "Mutagenic roles of DNA "repair" proteins in antibody diversity and disease-associated trinucleotide repeat instability." DNA Repair **7**(7): 1135-54.

Smolka, M. B., C. P. Albuquerque, S.-h. Chen and H. Zhou (2007). "Proteome-wide identification of *in vivo* targets of DNA damage checkpoint kinases." Proc. Natl. Acad. Sci. USA **104**(25): 10364-9.

Spell, R. M. and S. Jinks-Robertson (2003). "Role of mismatch repair in the fidelity of *RAD51*- and *RAD59*-dependent recombination in *Saccharomyces cerevisiae*." Genetics **165**: 1733-44.

Spell, R. M. and S. Jinks-Robertson (2004). "Examination of the roles of Sgs1 and Srs2 helicases in the enforcement of recombination fidelity in *Saccharomyces cerevisiae*." Genetics **168**: 1855-65.

Stenger, J. E., K. S. Lobachev, D. Gordenin*, et al.* (2001). "Biased distribution of inverted and direct *Alu*s in the human genome: Implications for insertion, exclusion, and genome stability." Genome Res. **11**(1): 12-27.

Strathern, J., J. Hicks and I. Herskowitz (1981). "Control of cell type in yeast by the mating type locus." J. Mol. Biol. **147**(3): 357-72.

Strout, M. P., G. Marcucci, C. D. Bloomfield and M. A. Caligiuri (1998). "The partial tandem duplication of ALL1 (MLL) is consistently generated by *Alu*-mediated homologous recombination in acute myeloid leukemia." Proc. Natl. Acad. Sci. USA **95**(5): 2390-5.

Studamire, B., G. Price, N. Sugawara*, et al.* (1999). "Separation-of-function mutations in *Saccharomyces cerevisiae MSH2* that confer mismatch repair defects but do not affect nonhomologous-tail removal during recombination." Mol. Cell. Biol. **19**(11): 7558-67.

Sugawara, N., T. Goldfarb, B. Studamire*, et al.* (2004). "Heteroduplex rejection during single-strand annealing requires Sgs1 helicase and mismatch repair proteins Msh2 and Msh6 but not Pms1." Proc. Natl. Acad. Sci. USA **101**(25): 9315-20.

Sugawara, N. and J. E. Haber (1992). "Characterization of double-strand break-induced recombination: Homology requirements and single-stranded DNA formation." Mol. Cell. Biol. **12**(2): 563-75.

Sugawara, N., G. Ira and J. E. Haber (2000). "DNA length dependence of the single-strand annealing pathway and the role of *Saccharomyces cerevisiae* RAD59 in double-strand break repair." Mol. Cell. Biol. **20**(14): 5300-9.

Sugawara, N., E. L. Ivanov, J. Fishman-Lobell*, et al.* (1995). "DNA structure-dependent requirements for yeast *RAD* genes in gene conversion." Nature **373**: 84-6.

Sugawara, N., F. Pâques, M. Colaiacovo and J. E. Haber (1997). "Role of *Saccharomyces cerevisiae* Msh2 and Msh3 repair proteins in double-strand break-induced recombination." Proc. Natl. Acad. Sci. USA **94**: 9214-9.

Sugawara, N., X. Wang and J. E. Haber (2003). "*In vivo* roles of Rad52, Rad54, and Rad55 proteins in Rad51-mediated recombination." Mol. Cell **12**: 209-19.

Sun, M. and M. Fasullo (2007). "Activation of the budding yeast securin Pds1 but not Rad53 correlates with double-strand break-associated G2/M cell cycle arrest in a *mec1* hypomorphic mutant." Cell Cycle **6**(15): 1896-902.

Sung, P., P. Reynolds, L. Prakash and S. Prakash (1993). "Purification and characterization of the *Saccharomyces cerevisiae* RAD1/RAD10 endonuclease." J. Biol. Chem. **268**(35): 26391-9.

Surtees, J. A. and E. Alani (2006). "Mismatch repair factor MSH2-MSH3 binds and alters the conformation of branched DNA structures predicted to form during genetic recombination." J. Mol. Biol. **360**(3): 523-6.

Surtees, J. A., J. L. Argueso and E. Alani (2004). "Mismatch repair proteins: Key regulators of genetic recombination." Cytogenet. Genome Res. **107**(3-4): 146-59.

Symington, L. S. (2002). "Role of *RAD52* epistasis group genes of homologous recombination and double-strand break repair." Microbiol. Mol. Biol. Rev. **66**(4): 630-70.

Toczyski, D. P., D. J. Galgoczy and L. H. Hartwell (1997). "*CDC5* and CKII control adaptation to the yeast DNA damage checkpoint." Cell **90**: 1097-106.

Torres-Ramos, C. A., S. Prakash and L. Prakash (2002). "Requirement of *RAD5* and *MMS2* for postreplication repair of UV-damaged DNA in *Saccharomyces cerevisiae*." Mol. Cell. Biol. **22**(7): 2419-26.

Tsaneva, I. R., B. MÃ¼ller and S. C. West (1993). "RuvA and RuvB proteins of *Escherichia coli* exhibit DNA helicase activity *in vitro*." Proc. Natl. Acad. Sci. USA **90**(4): 1315-9.

Vance, J. R. and T. E. Wilson (2002). "Yeast Tdp1 and Rad1-Rad10 function as redundant pathways for repairing Top1 replicative damage." Proc. Natl. Acad. Sci. USA **99**(21): 13669-74.

VanHulle, K., F. J. Lemoine, V. Narayanan*, et al.* (2007). "Inverted DNA repeats channel repair of distant double-strand breaks into chromatid fusions and chromosomal rearrangements." Mol. Cell. Biol. **27**(7): 2601-14.

Vaze, M. B., A. Pellicioli, S. E. Lee*, et al.* (2002). "Recovery from checkpoint-mediated arrest after repair of a double-strand break requires Srs2 helicase." Mol. Cell **10**(2): 373-85.

Vulic, M., F. Dionisio, F. Taddei and M. Radman (1997). "Molecular keys to speciation: DNA polymorphism and the control of genetic exchange in enterobacteria." Proc. Natl. Acad. Sci. USA **94**: 9763-7.

Wach, A., A. Brachat, R. Pohlmann and P. Philippsen (1994). "New heterologous modules for classical or PCR-based gene disruptions in *Saccharomyces cerevisiae*." Yeast **10**(13): 1793-808.

Waldman, A. S. (2008). "Ensuring the fidelity of recombination in mammalian chromosomes." BioEssays **30**(11-12): 1163-71.

Waldman, A. S. and R. M. Liskay (1988). "Dependence of intrachromosomal recombination in mammalian cells on uninterrupted homology." Mol. Cell. Biol. **8**(12): 5350-7.

Wang, T.-F. and W.-M. Kung (2002). "Supercomplex formation between Mlh1-Mlh3 and Sgs1-Top3 heterocomplexes in meiotic yeast cells." Biochem.Biophys. Res. Comm. **296**: 949-53.

Wang, X. and P. Baumann (2008). "Chromosome fusions following telomere loss are mediated by single-strand annealing." Mol. Cell **31**(4): 463-73.

Wang, X., G. Ira, J. A. Tercero*, et al.* (2004). "Role of DNA replication proteins in double-strand break-induced recombination in *Saccharomyces cerevisiae*." Mol. Cell. Biol. **24**(16): 6891-9.

Wang, Y. and J. Qin (2003). "MSH2 and ATR form a signaling module and regulate two branches of the damage response to DNA methylation." Proc. Natl. Acad. Sci. USA **100**(26): 15387-92.

Watt, P. M., I. D. Hickson, R. H. Borts and E. J. Louis (1996). "*SGS1*, a homologue of the Bloom's and Werner's syndrome genes, is required for maintenance of genome stability in *Saccharomyces cerevisiae*." Genetics **144**: 935-45.

Watt, P. M., E. J. Louis, R. H. Borts and I. D. Hickson (1995). "Sgs1: A eukaryotic homolog of *E. coli* RecQ that interacts with Topoisomerase II *in vivo* and is required for faithful chromosome segregation." Cell **81**: 253-60.

Watt, V. M., C. J. Ingles, M. S. Urdea and W. J. Rutter (1985). "Homology requirements for recombination in *Escherichia coli*." Proc. Natl. Acad. Sci. USA **82**: 4768-72.

Watts, F. Z. (2006). "Sumoylation of PCNA: Wrestling with recombination at stalled replication forks." DNA Repair **5**(3): 399-403.

Weeda, G., I. Donker, J. de Wit*, et al.* (1997). "Disruption of mouse *ERCC1* results in a novel repair syndrome with growth failure, nuclear abnormalities and senescence." Curr. Biol. **7**(6): 427-39.

White, C. I. and J. E. Haber (1990). "Intermediates of recombination during mating type switching in *Saccharomyces cerevisiae*." EMBO J. **9**(3): 663-73.

Wimmer, K. and J. Etzler (2008). "Constitutional mismatch repair-deficiency syndrome: have we so far seen only the tip of an iceberg?" Human Genetics **124**(2): 105-22.

Worth, L., Jr., S. Clark, M. Radman and P. Modrich (1994). "Mismatch repair proteins MutS and MutL inhibit RecA-catalyzed strand transfer between diverged DNAs." Proc. Natl. Acad. Sci. USA **91**: 3238-41.

Wu, X. and J. Haber (1995). "*MAT***a** donor preference in yeast mating-type switching: activation of a large chromosomal region for recombination." Genes Dev. **9**(15): 1922-32.

Wu, X. and J. E. Haber (1996). "A 700 bp *cis*-acting region controls mating-type dependent recombination along the entire left arm of yeast chromosome III." Cell **87**: 277-85.

Wu, X., C. Wu and J. E. Haber (1997). "Rules of donor preference in *Saccharomyces* mating-type gene switching revealed by a competition assay involving two types of recombination." Genetics **147**(2): 399-407.

Yamagata, K., J.-i. Kato, A. Shimamoto*, et al.* (1998). "Bloom's and Werner's syndrome genes suppress hyperrecombination in yeast *sgs1* mutant: Implication for genomic instability in human diseases." Proc. Natl. Acad. Sci. USA **95**: 8733-8.

Yang, D. and A. S. Waldman (1997). "Fine-resolution analysis of products of intrachromosomal homeologous recombination in mammalian cells." Mol. Cell. Biol. **17**(7): 3614-28.

Yang, Q., R. Zhang, X. W. Wang*, et al.* (2004). "The mismatch DNA repair heterodimer, hMSH2/6, regulates BLM helicase." Oncogene **23**: 3749-56.

Zawadzki, P., M. S. Roberts and F. M. Cohan (1995). "The log-linear relationship between sexual isolation and sequence divergence in *Bacillus* transformation is robust." Genetics **140**: 917-32.

Zhart, T. C. and S. Maloy (1997). "Barriers to recombination between closely related bacteria: MutS and RecBCD inhibit recombination between *Salmonella typhimurium* and *Salmonella typhi*." Proc. Natl. Acad. Sci. USA **94**: 9786-91.

Zhu, Z., W. Chung, E. Shim, *et al.* (2008). "Sgs1 helicase and two nucleases Dna2 and Exo1 resect DNA double-strand break ends." Cell **134**(6): 981-94.

http://www.biopeptide.com/PepCalc

APPENDIX

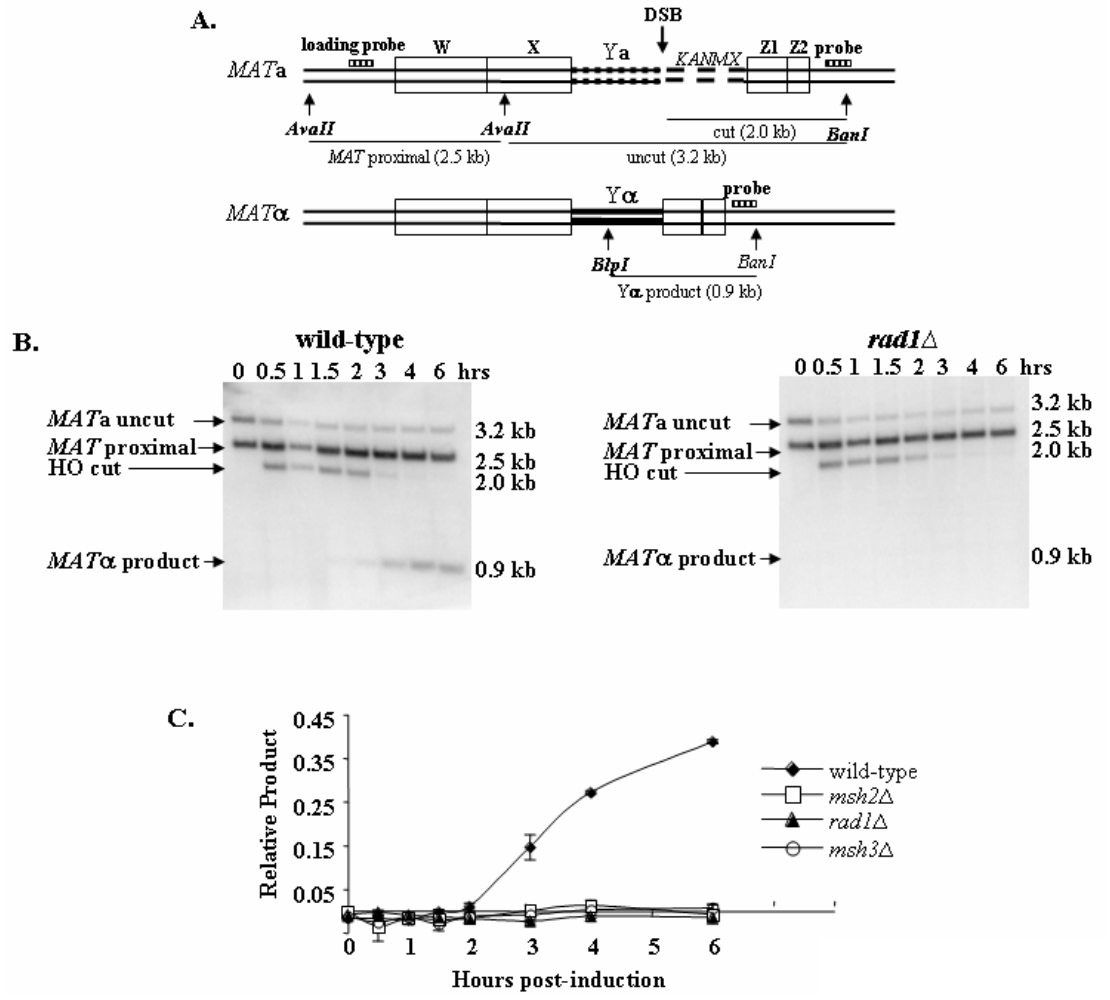

Supplementary Figure 2.6. Southern blot analysis of mating type switching in wild-type and *rad1*Δ strains containing two nonhomologous ends. A. Diagram of the *MAT* locus showing the restriction sites used for Southern blot analysis, expected fragment lengths, and location of the probes used for detection for mating type switching involving two nonhomologous ends due to insertion of *KANMX* sequence distal to the DSB. B. Southern blot analysis of digested DNA for wild-type and *rad1*Δ mutants. Experiments were performed at least three times, with representative time courses shown. C. Quantification of Y**α** product formation relative to the *MAT* proximal loading control for wild-type, *rad1*Δ, *msh2*Δ, and *msh3*Δ mutants containing the *KANMX* insertion. Data points are the mean ± SEM.

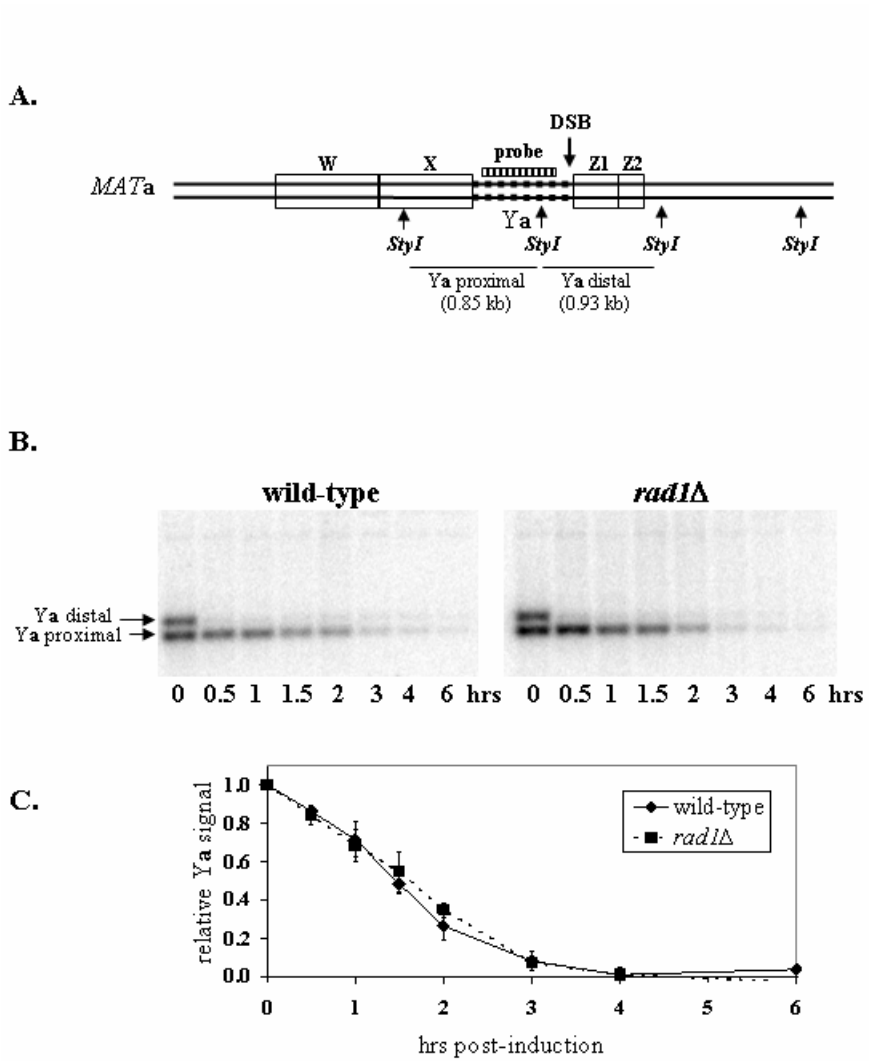

Supplementary Figure 2.7. Detection of Ya loss in wild-type and *rad1*Δ mutants. A. Location of restriction sites, expected band sizes, and double-stranded probe used for detection of Y**a**. B. Southern blot analysis of Y**a** sequence in wild-type and *rad1*Δ strains during mating type switching. C. Quantification of Y**a** signal relative to t = 0 for wild-type and *rad1*Δ (mean ± SEM for 4 individual blots).

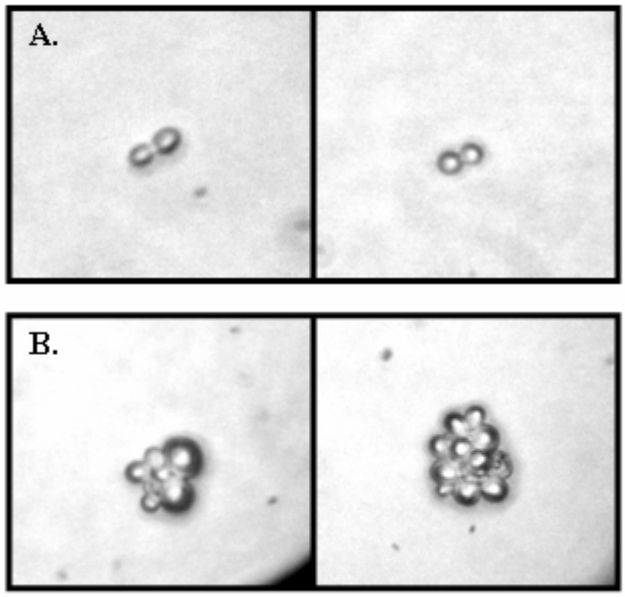

Supplementary Figure 2.8. Large-budded morphology (A) and number of cells at death (B) observed in *rad1*Δ mutants undergoing mating type switching. *rad1*Δ mutant cells induced for mating type switching were photographed under the light microscope during pedigree analysis. A. *rad1*Δ cells exhibited large-budded morphology for a prolonged period of time indicative of G2/M cell cycle delay. B. Following separation of the two daughter cells, *rad1*Δ mutants that died continued to divide several times to yield an average of 8 ± 1 cells prior to death.

Filename: Full thesis.doc
Directory: E:\Thesis
Template: C:\Documents and Settings\amh72\Application Data\Microsoft\Templates\Normal.dot
Title:
Subject:
Author: Amy Lyndaker
Keywords:
Comments:
Creation Date: 2/15/2009 9:05:00 AM
Change Number: 150
Last Saved On: 2/27/2009 11:17:00 AM
Last Saved By: Amy
Total Editing Time: 829 Minutes
Last Printed On: 2/27/2009 11:17:00 AM
As of Last Complete Printing
Number of Pages: 204
Number of Words: 85,945 (approx.)
Number of Characters: 489,892 (approx.)